



Water
Resources
Programme

WORKING MATERIALS

Origin of salinity and impacts on fresh groundwater resources: Optimisation of isotopic techniques

Results of a 2000-2004 Coordinated
Research Project

Origin of salinity and impacts on fresh groundwater resources: Optimisation of isotopic techniques

Results of a 2000-2004 Coordinated
Research Project

EDITORIAL NOTE

This publication has been prepared from the original material as submitted by the authors. The views expressed do not necessarily reflect those of the IAEA, the governments of the nominating Member States or the nominating organizations.

The use of particular designations of countries or territories does not imply any judgement by the publisher, the IAEA, as to the legal status of such countries or territories, of their authorities and institutions or of the delimitation of their boundaries.

The mention of names of specific companies or products (whether or not indicated as registered) does not imply any intention to infringe proprietary rights, nor should it be construed as an endorsement or recommendation on the part of the IAEA.

The authors are responsible for having obtained the necessary permission for the IAEA to reproduce, translate or use material from sources already protected by copyrights.

CONTENTS

Summary	1
Groundwater salinization in the South West Murray basin as a result of enhanced recharge	5
<i>F.W. Leaney and A.L. Herczeg, G.R. Walker</i>	
Origin of saline groundwater in the northeastern of Guanzhong Basin, China	15
<i>Dajun Qin</i>	
Optimization of isotopic techniques to investigate groundwater salinization in Disi Basin, Jordan	29
<i>H.M. Amro, S.F. Kilani, Z. Al-Tarawneh, M.A. Moman and A. Subeh</i>	
Environmental isotope-aided study for elucidating groundwater salinization on Cheju Island, Korea	45
<i>Sung-Jun Song, Ki-Won Koh, Won-bae Park, Avner Vengos and Yoon-Suk Park</i>	
Isotopic techniques as a tool to investigate salinization problems in the Souss Massa coastal plain (South West Morocco), Morocco	61
<i>L. Bouchaoua, M. Qurtobib, Y. Hsissoua, M. Ibn Majahb, H. Marahb</i>	
Isotopic investigation of saline water intrusion and related impacts on potable water quality in the coastal aquifer of Karachi, Pakistan	81
<i>A. Mashiatullah, R. M. Qureshi, T. Javed, M. A. Tasneem, M. Fazil, N. Ahmad, E. Ahma</i>	
List of participants	99

SUMMARY

ISOTOPE TECHNIQUES FOR CHARACTERIZING GROUNDWATER SALINIZATION

A Coordinated Research Project (CRP) on “Origin of salinity and impacts on fresh groundwater resources: Optimisation of isotopic techniques” was initiated in 2000 within the framework of the IAEA Water Programme. Research groups from Australia, China, France, Israel, Italy, Jordan, Korea, Morocco, Pakistan, Sweden, Tunisia and United Kingdom of Great Britain participated in and contributed to the project. Two Research Co-ordination meetings were held in Vienna respectively in December 2000 and June 2003. The current publication is a compilation of final reports of six individual studies carried out under the CRP.

The IAEA officer in charge of designing and coordinating all related work in this CRP and responsible for this publication was Cheikh B. Gaye of the Division of Physical and Chemical Sciences.

Salinization is a global environmental problem that affects various aspects of our life such as changing the chemical composition of natural water resources (lakes, rivers, and groundwater), degrading the quality of agricultural and domestic water supplies, contributing to loss of biodiversity, loss of fertile soil, collapse of agricultural and fishery industries, and creating severe health problems (e.g., the Aral Basin). In Australia, for example, continuous soil salinization has become a massive environmental and economic disaster requiring drastic resource management changes.

High levels of total or specific dissolved constituents associated with saline water other than sodium and chloride, may limit the use of the water for domestic, agriculture, and industrial applications. For instance, in some parts of Africa, China, and India, high fluoride content is often associated with saline groundwater and causes severe dental and skeletal fluorosis. Consequently, the “salinity” problem is only the “tip of the iceberg”. High levels of salinity often associated with high concentrations of sodium, sulphate, boron, fluoride, and bio-accumulated elements such as selenium, and arsenic. High salinity groundwater may also be associated with high radioactivity.

Water salinization is a global problem but it is more severe in water-scarce areas, such as arid and semi-arid zones, where groundwater is the primary source of water. The increasing demand of groundwater has created tremendous pressure on the use of the resources resulting in lowering of water levels and an increase in salinization. In the Middle East for example, salinity is the main factor limiting the continued use of groundwater, and future reliance on groundwater in the region is further diminished as groundwater levels decline, creating increases in salinity and in exploitation costs.

The CRP participants have addressed the following categories of salinity problems:

- River salinization (River Murray, Australia, and River Souss, Morocco).
- Salinization due to damming and base flow in the arid zone (River Souss, Morocco).

- Time of recharge/replenishment (Murray Basin, Australia, Disi aquifer, Jordan and Nubian sandstone aquifer, Israel).
- Time frames of salinization: past flushing versus modern mixing (Murray Basin, Australia, Disi aquifer, Jordan and Nubian sandstone aquifer, Israel).
- Times scale of salt accumulation (Murray Basin, Australia).
- Identifying the extent of seawater intrusion (Karachi, Pakistan, Souss coastal plain, Morocco, and Cheju Island, South Korea).
- Distinction between present and past seawater intrusion and evolution of salinity (Karachi, Pakistan, Souss coastal plain, Morocco, and Cheju Island, South Korea).
- Leaching of evaporites (Souss coastal plain, Morocco, Guanzhong Basin, China, Nubian sandstone aquifer, Israel, and Disi aquifer, Jordan).
- Mixing with formation water and/or brines (Nubian sandstone aquifer, Israel and Guanzhong Basin, China).
- Modification and salinity build-up by water-rock interactions (Souss coastal plain, Morocco, Guanzhong Basin, China, Nubian sandstone aquifer, Israel, Disi aquifer, Jordan, Murray Basin, Australia, Cheju Island, South Korea, and Karachi, Pakistan).
- Geothermal influence (demonstration study at Abano thermal basin, Italy and Cheju Island, South Korea).
- Urban environment – sewage contamination (Karachi, Pakistan).
- Agricultural environment – seepage of agricultural return flows (Souss coastal plain, Morocco, and Cheju Island, South Korea).
- Dry land salinization (Murray Basin, Australia, Nubian sandstone aquifer, Israel, Disi aquifer, Jordan, Souss coastal plain, Morocco, and Guanzhong Basin, China).
- Input salinity (all participants).

The major objective of the CRP was to explore and develop isotopic tools that can be used to determine salinity sources and processes in aquifer systems. It was based on the implementation of several coordinated regional studies and a central “flagship” study in the Souss coastal aquifer of western Morocco. The research sites represent a large variety of examples of the salinization problem. These include salt-water intrusion into coastal aquifers (Morocco, Pakistan, Cheju Island in South Korea), dry land and inland salinization (Australia, Jordan, Israel, China); salinization of fossil groundwater (Australia, Israel, Jordan), and anthropogenic salinization (Pakistan, Morocco). In addition to individual efforts of the different member countries to investigate the origin of the salinization phenomena in their own country, special efforts were given to the integration of the isotopic techniques and cross-laboratories measurements. The integration approach enabled measurements of a large suite of isotopic tools in the selected research site in Morocco that include major and minor dissolved constituents, and the isotopic compositions of oxygen ($^{18}\text{O}/^{16}\text{O}$), hydrogen ($^2\text{H}/^1\text{H}$),

tritium (^3H), sulphur ($^{34}\text{S}/^{32}\text{S}$), oxygen in the sulphate molecule ($^{18}\text{O}/^{16}\text{O}$), boron ($^{11}\text{B}/^{10}\text{B}$), strontium ($^{87}\text{Sr}/^{86}\text{Sr}$), carbon (^{14}C and $^{13}\text{C}/^{12}\text{C}$), chlorine (^{36}Cl) and iodine (^{129}I). The different case studies have indicated that aquifers can be impacted by both geogenic (natural) and anthropogenic salinity sources and often many basins are salinized by multiple sources of salinity. The CRP demonstrated that using the different isotopes and close integration with geochemical tools can provide key information on the origin and mechanisms of the multiple salinity sources.

Isotope results from the pilot site in Morocco, confirm the existence of at least 3 salinity sources in the Souss plain: marine intrusion (present day and/or Pliocene sea water); Jurassic and Cretaceous evaporites; local contribution from the unsaturated zone; anthropogenic pollution. The high SO_4/Cl ratio combined with low $\delta^{11}\text{B}$ (12-21‰), and very low $^{87}\text{Sr}/^{86}\text{Sr}$ ratios (~ 0.7076), indicate dissolution of evaporites. The water composition at Bou lbaz; (TDS=8300, mg/l) characterized by Na/Cl ratio of 0.9, a low $\delta^{11}\text{B}$ (24‰), and very high radiogenic $^{87}\text{Sr}/^{86}\text{Sr} \sim 0.711$, suggests interaction of seawater/brine with silicate rocks for obtaining a non-marine signature. The $\delta^{13}\text{C}_{\text{TDIC}}$ values ranging from -6‰ to -13‰ could be attributed to contribution of pollution to groundwater through seepage from polluted rivers and local septic tank systems/ minor sewage drains. Agriculture return flows are characterized by high nitrate contents, high $\delta^{11}\text{B}$ (45‰), and high $^{87}\text{Sr}/^{86}\text{Sr}$ ratios (~ 0.711).

Investigations carried out in Australia show that in addition to the groundwater salinization processes observed, the process of enhanced recharge following land clearing is resulting in water table rises close to the River Murray. In this area, groundwater is saline and water table rise is likely to increase the flow of the saline groundwater into the River Murray.

Isotope data from the saline groundwater lens occurring in the northeast Guanzhong basin, China, is consistent with evaporation and mixing processes.

The data from Israel shows that multiple sources of salinity affect the solute composition in the Nubian sandstone of the Negev. Based on integration of hydrochemical and isotopic data it was possible to distinguish between different water groups, to distinguish between “pristine” and “secondary” salinity sources, and identify modern versus paleo-recharge components.

In the coastal aquifer of Karachi (Pakistan), anthropogenic sources are found responsible to affect the quality of local groundwater. The shallow / phreatic aquifers are recharged by a mixture of fresh waters from the Indus and Hub rivers as well as polluted waters from Layari and Malir rivers and their feeding drains both under natural infiltration conditions and artificially induced infiltration conditions, and to a much smaller extent, from direct recharge of local precipitation.

Investigations carried out in Korea indicate clearly that seawater intrusion is the main source of groundwater salinity in Cheju Island.

Groundwater Salinisation in the South West Murray Basin as a Result of Enhanced Recharge

F. W. Leaney, A. L. Herczeg, G.R. Walker

CSIRO Land and Water, Adelaide SA, Australia

Abstract. A large reservoir of fresh groundwater underlies a large portion of the SW Murray basin of south-eastern Australia. Evidence from very low ^{14}C data, relatively depleted $\delta^{18}\text{O}$ and $\delta^2\text{H}$ values and palaeoclimatic evidence suggests this was mostly recharged >20 000 years ago. Soil water profiles throughout the area are characterized by relatively high salinity due to the predominantly semi-arid climate and very low recharge rates that have prevailed in the region over the past 20 000 years. Increasing salinity observed in many monitoring bores are due to flushing of the saline soil water to the groundwater due to land clearing, and in some cases by irrigation. The time scale of salinisation depends on the underlying salt inventory, the soil type and the intended land-use; from tens of years for sandy soils with high salinities to hundred of years for clay soils. Eventually the soil water will have the salts flushed out, but because of the very low hydraulic gradients and long flow paths in the saturated zone, the salt water will remain in the system for thousands of years.

1. Introduction

A large area of the SW Murray Basin of Australia ($\sim 3 \times 10^4 \text{ km}^2$) is underlain by fresh groundwater ($3,000 \text{ mg L}^{-1}$) (Figure 1). The fresh groundwater within the unconfined Murray Group aquifer is under the Big and Little Deserts with an unsaturated zone between 25 – 80 m. The region is characterized by sandy surface soils and semi-arid climate with rainfall $\sim 350 \text{ mm yr}^{-1}$ and potential evapo-transpiration of $2,000 \text{ mm yr}^{-1}$. Soil water throughout most of the SW Murray basin has much higher salinities than that of groundwater – often up to seawater concentration of 35 g/L.

Groundwater salinity is slowly increasing in approximately half of the observation bores that are regularly monitored within the fresh groundwater resource. It is thought that downward displacement of saline soil water as a result of increased recharge due to land clearing might be responsible for the observed trends. However, there is insufficient information on salinity of soil profiles in the studied area. Furthermore, a significant increase in the use of groundwater for irrigation since the 1970's in the area has raised concerns that groundwater salinity problems may be exacerbated.

The three objectives for this study area as follows:

- i) Determine the origin of the fresh groundwater in the SW Murray Basin.
- ii) Determine the origin of the salt in the unsaturated zone.
- iii) Develop a model to predict changes in groundwater salinity as a result of changes in land-use.

Soil types in the SW Murray basin range from heavy textured soils in the low-lying flat areas and interdunal swales, to areas of deep, sandy soil profiles (indicated by shaded areas in Figure 1). These deep sandy soils are associated with the Big and Little deserts which closely correspond to the areas of fresh groundwater. Three main hypotheses to explain the existence of the fresh groundwater is that either i) it was recharged at the basin margins where recharge rates are generally higher, and has traveled northwards to reach its current location, ii) recharge has occurred episodically during times of vegetation removal due to fires over the past several hundred years, or iii) recharge has occurred through the light textures soils during a time of wetter climate in the past.

Recharge rates estimated from Cl^- mass balance are <1 mm/yr [1][2][3]. However, recharge rates increase by up to two orders of magnitude once the native high water use *mallee* vegetation is removed for dryland agriculture [4]. Irrigation development using local groundwater also greatly increases recharge depending on the soil type and type of crop grown. This project applies a number of natural environmental tracers such as $\delta^2\text{H}$ and $\delta^{18}\text{O}$ and ^{14}C and $\delta^{13}\text{C}$ to assist with determination of timing and mechanism of recharge processes. Analysis of soil water profiles for water content, chloride content, soilwater potential and clay content provides information on the salt and water inventory of the unsaturated zone. A one-dimensional numerical model is used to predict the timing and extent of groundwater salinisation resulting from vertical displacement of soilwater in the unsaturated zone into the groundwater after clearing (unsaturated zone model) and irrigation (combined unsaturated/saturated zone model).

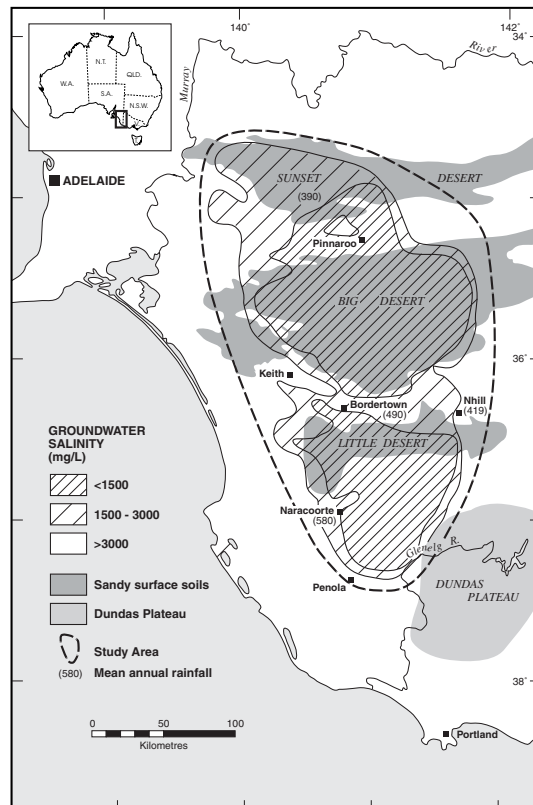


FIG. 1. Location map of the study area. Note that the fresh groundwater is located primarily beneath the Big and Little Sandy Deserts.

2. Results and Discussion

2.1. ^{14}C data

Groundwater samples were collected and analysed for chemistry and isotopic composition from 50 existing boreholes in the S-W Murray Basin. ^{14}C results for these samples range from 0 to 26 pMC for the shallow boreholes and 0–20 pMC for the deep boreholes (Figure 2). $\delta^{13}\text{C}$ results range from -4.4 to -15.6 ‰ and -0.8 to -9.2 ‰ for the shallow and deep boreholes respectively. A further 16 samples were collected from 5 boreholes (A5–A9) drilled specifically for this project. These boreholes remained uncased to a depth of up to 35 m below the water table allowing groundwater to be sampled from discrete 2 m depth intervals using a pump-packer system.

Based on the hydraulic gradient and measured values of aquifer transmissivity, estimates of groundwater flow in the S-W Murray Basin are of the order of 1 m/yr. If the initial ^{14}C concentration

of recharging water is 100 ‰MC and radioactive decay is the only process that reduces the ^{14}C concentration, it would not be possible to measure detectable levels (>2 ‰MC) of ^{14}C beyond 30 km of the basin margin if that were the only source of recharge. In fact, there are several ways in which ^{14}C can be diluted in the unsaturated and saturated zone apart from radioactive decay, therefore detectable levels of ^{14}C would be unlikely well before the 30 km zone. There clearly must be another process that results in measurable amounts of ^{14}C being observed in groundwater samples throughout most of the study area.

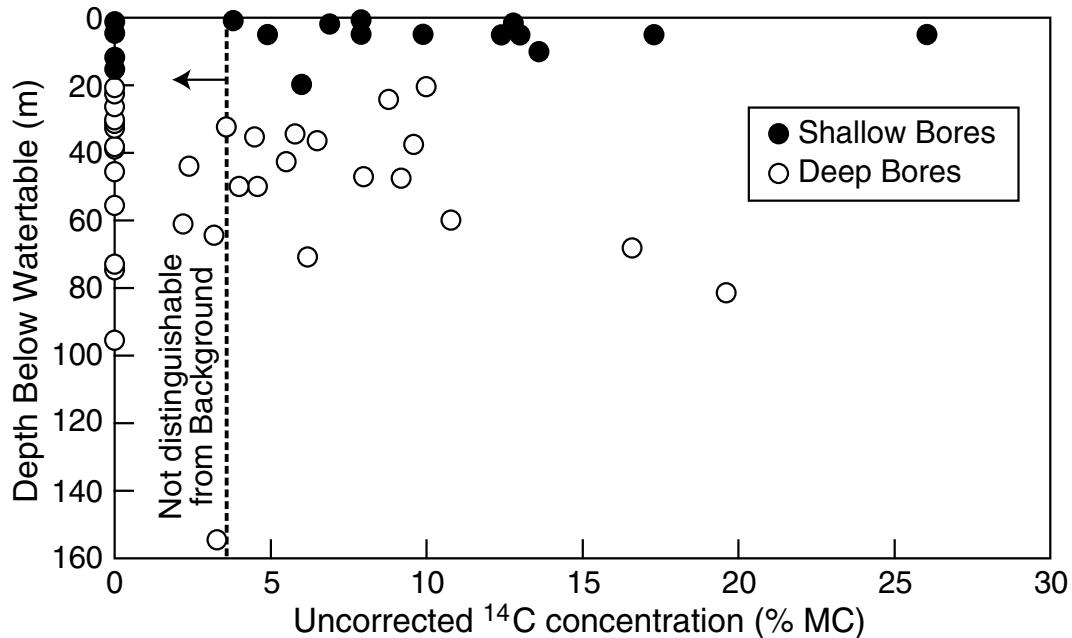


FIG. 2. ^{14}C activity (uncorrected) vs depth for groundwater in the SW Murray basin.

Any ^{14}C present in groundwater beyond 30 km of the basin margin must be the result of water recharging at, or just up-gradient of the point of sampling. Using the ^{14}C concentration of groundwater and the depth below the water table at which the sample was collected, recharge at any site can be estimated if the rate of water movement over that depth interval is assumed to be constant [5][6]. The corrected ^{14}C data presented here (Figure 3) follows that of Wigley et al. [7] and assumes dissolution of a high Mg-calcite and reprecipitation of a Mg-poor calcite.

^{14}C data for the study area, corrected using the approach [7], ranges from 0–50 pMC. Dogramaci (1998) suggested that this data can be interpreted to represent long term recharge rates ranging from less than 0.1 to greater than 20 mm/yr. He also noted that higher values for corrected ^{14}C concentration (attributed to higher overall recharge rates) were found to the southern half of the study area. This area includes all of the Little Desert and most of the Big Desert.

We suggest that rather than consistently and slightly higher overall mean recharge rates for the southern half of the study area, that the recharge can be divided into two distinct temporal periods. Much higher recharge rates in this area occurred during wetter periods >20 000 years ago (predominantly in sandy areas) and, since then, very low recharge has prevailed during the semi-arid climatic conditions experienced in the SW Murray Basin. Rather than use the approach by Wigley et al., [7] we have chosen to consider a range of ages for the groundwater assuming radiometric decay as the only process by which the ^{14}C activity can change for water within the saturated zone. Depending on the value chosen for the ^{14}C activity of input water (50–100 pMC), ages for the groundwater could range from 5000 (based on the maximum observed ^{14}C activity and $A_0 = 50$ pMC) to $>30,000$ years.

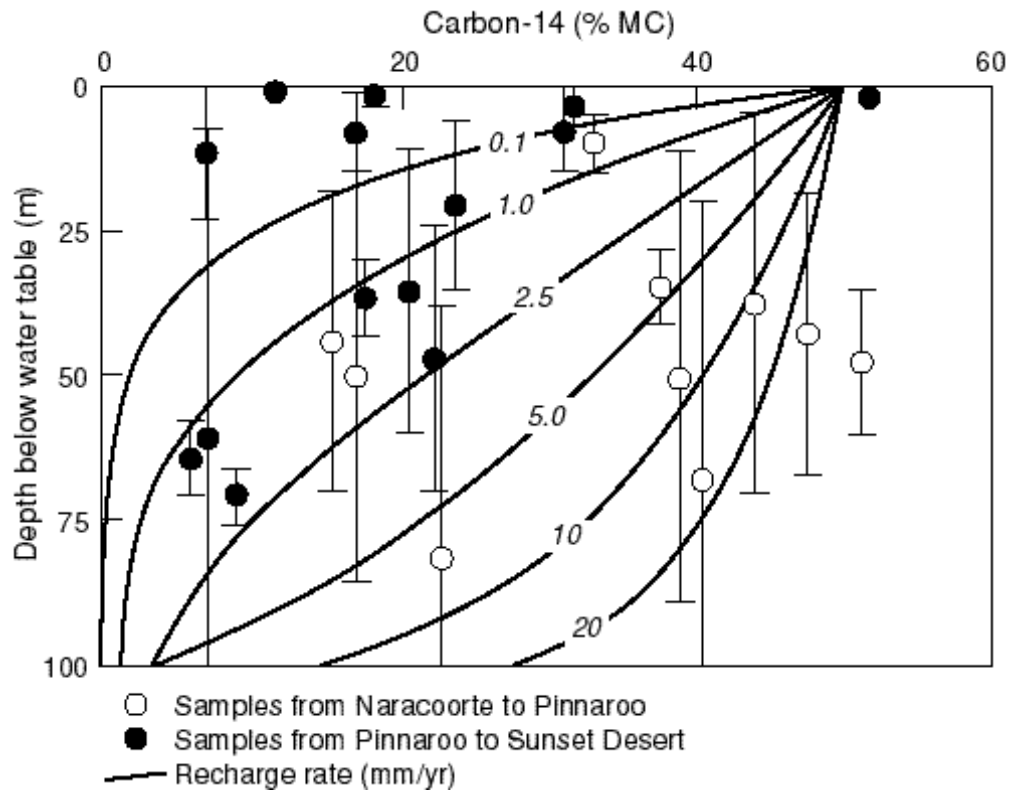


FIG. 3. Carbon-14 data for the SW Murray basin with screen intervals and modeled recharge rates (Figure reproduced from Dogramaci, 1998).

If groundwater is ~5000 years old, then it is probable that the fresher groundwater would be located within a few kilometres of where it recharged. Alternatively, if the groundwater is closer to 30 000 years (and/or deeper in the aquifer), then, as a result of lateral flow, the fresher groundwater could be 30 km or more from the area of recharge. Because of this, it may be difficult on a small spatial scale to correlate higher recharge areas (as indicated by higher ^{14}C concentrations) with specific areas and soil/rainfall conditions under which recharge took place. However, there is reassurance from the general observation that higher corrected ^{14}C concentrations are associated with factors known to enhance recharge such as sandy surface soil and higher rainfall seen in the southern half of the study area.

2.2. $\delta^{18}\text{O}$ and $\delta^2\text{H}$ data

Results of stable isotope analyses of water from the groundwater range from -24 to -43 ‰ for $\delta^2\text{H}$ and -3.5 to -6.5 ‰ for $\delta^{18}\text{O}$ (Figure 4). The isotopic composition of groundwater for most of the samples straddle the Global Meteoric Water Line (GMWL). There is no significant difference in the isotopic composition of the groundwater from the shallow bores (mean \pm 1 s.d. = -38.2 ± 3.3 ‰, -5.74 ± 0.49 ‰ for $\delta^2\text{H}$ and $\delta^{18}\text{O}$ respectively) and the deep bores (-36.2 ± 4.1 ‰, -5.54 ± 0.61 ‰). Most of the groundwater is depleted compared to that of the precipitation weighted mean rainfall for Melbourne and Adelaide ($\delta^2\text{H}$, $\delta^{18}\text{O}$ = -28.3, -4.8 ‰ and -24, -4.6 ‰ respectively). The most probable explanation for this is that the groundwater recharged during a previous wetter and/or cooler period, when the climate was much cooler than today [8].

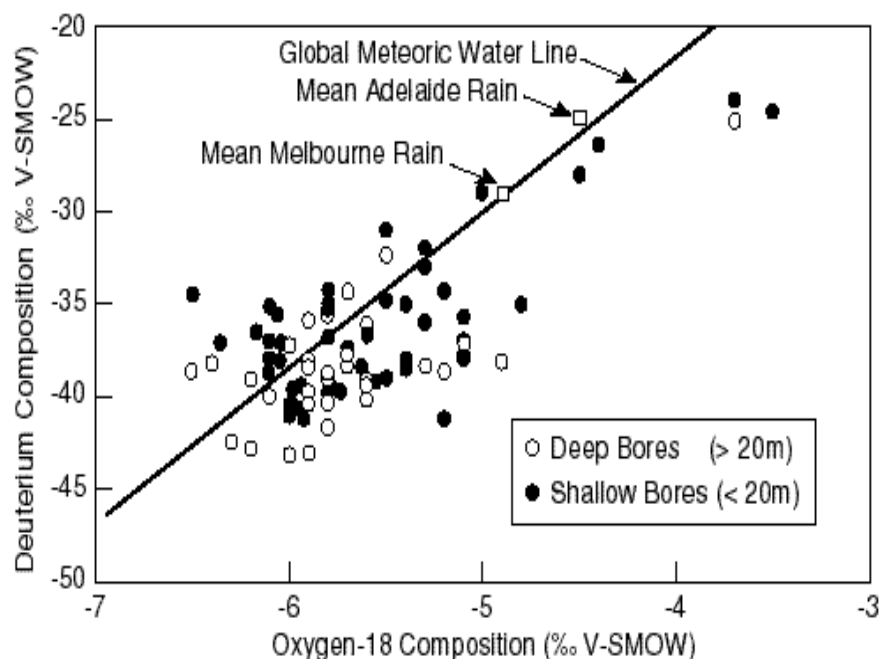


FIG. 4. Deuterium versus oxygen-18 composition of deep and shallow groundwaters of the study area. There is considerable scatter about the MWL, but most samples are more negative than current mean annual rainfall.

Analyses for the $\delta^2\text{H}$ and $\delta^{18}\text{O}$ composition of soil-water are available from 4 sites (Figure 5). At these sites, core samples were collected using drilling procedures that ensured the samples were not evaporated during drilling. Most of the samples for sites U1, U4 and U5 plot to the right the Global Meteoric Water Line (GMWL) in the range -5 to -6 ‰ and -30 to -40 ‰ for $\delta^{18}\text{O}$ and $\delta^2\text{H}$ respectively. Samples from site 2 tend to be more considerably enriched and are displaced on a slope close to 5 from the GMWL.

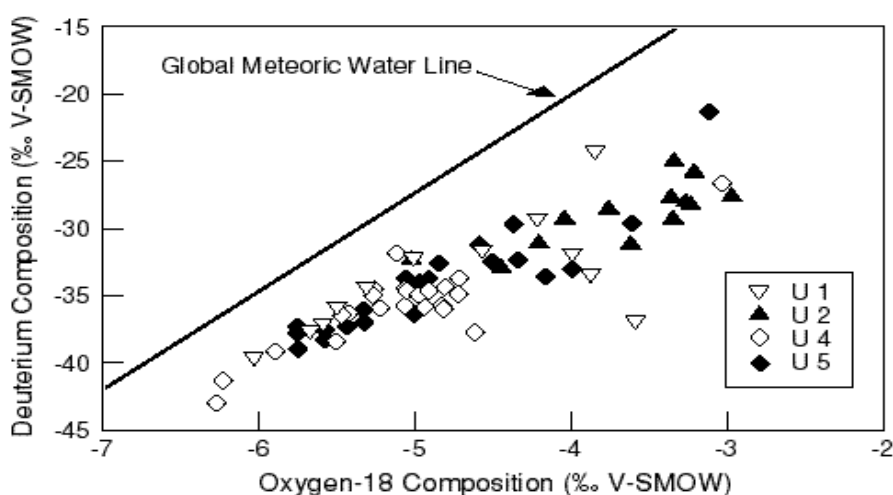


FIG. 5. Deuterium versus oxygen-18 composition of four soil water profiles for the study area. All data lie to the right of the MWL and are very different to that of the underlying fresh groundwater (see Figure 4). Extrapolation of the trend to the GMWL intersects at a value more negative than current mean annual rainfall.

When soil-water isotopic compositions plots on or near to the GMWL, it is indicative that rainfall at these sites has experienced relatively less evaporation during infiltration than at sites where the soil-water isotopic composition is displaced to the right of the GMWL. Hence, the data presented here suggest that evaporation has been less at sites U1, U4 and U5 compared to that at site U2 which will possibly result in higher recharge rates for these 3 sites. However, this is not always the case because water passing beyond the zone of evaporation may still be removed from the soil by transpiration, a process which does not alter the isotopic composition of the water. The interpretation of soil-water chloride analyses (seen above) at these sites suggests higher recharge at sites U1 and U5 and for some of the time at site U4, which is consistent with the interpretation from the isotopic data.

2.3. Soil water chloride inventories

Several studies involving analysis of soil water chloride inventories have revealed that large stores of saline soil water have accumulated in the SW Murray Basin during the predominantly semi-arid climate experienced in South Eastern Australia [9][10]. The saline soil water accumulates because of high rates of evaporation and transpiration, concentrating the salt present in rainfall to values near that of seawater. Recharge in the area has increased by 2-3 orders of magnitude as a result of the removal of deep-rooted native vegetation (*mallee*) and replacement with shallow rooted crops and pastures. This clearing occurred ~ 100 years ago.

Data presented here is in the form of cumulative water CW (mm) against cumulative chloride CC (g/dm^2) for each site (Figure 6). Cumulative water represents a parameter closely related to the total amount of recharge (to a particular depth) and provides a way of comparing profiles with differing structural composition [11][12]. At each site, the value zero for cumulative water is taken at the surface of the core and the bottom value measured is taken at the water table. Hence, for example, there is ~6 m of water in the unsaturated zone at site U5 ~11 m of soil in the unsaturated zone at site U4.

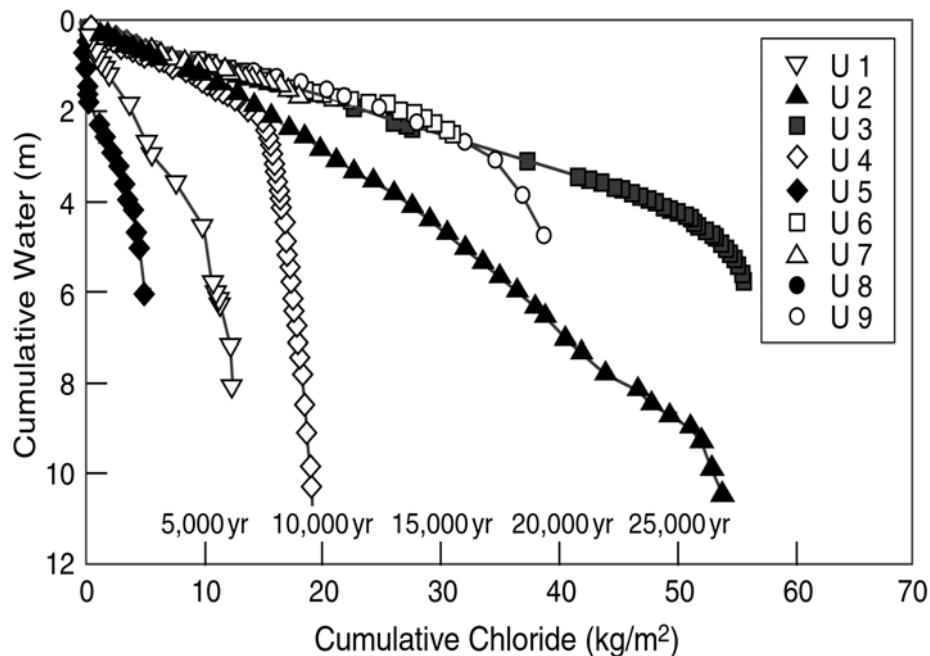


FIG. 6. Cumulative water versus cumulative chloride for nine soil water profiles in the SW Murray Basin.

Cumulative chloride may be considered as an approximate proxy for time if one assumes a constant chloride flux in precipitation over time. Hence, steeper slopes for cumulative water plotted against cumulative chloride are indicative of high recharge while lower slopes represent periods when recharge rates were low. If climate changes resulted in changes to recharge, the slopes of cumulative water to cumulative recharge would also change. For all sites except site U1, U5 and the bottom of site U4, cumulative water vs cumulative chloride profile display similar slopes with no break of slope to the water table. However, at sites U1 and U5, the slope is much steeper and at site U4, there is a distinct break of slope at a cumulative water value of 2 m.

Estimates of recharge rate can be made at each site by multiplying the slope of the CW vs CC profile ($\text{mm.dm}^2/\text{g}_{(\text{Cl})}$) by the mean chloride fallout ($\text{g}_{(\text{Cl})}/\text{dm}^2/\text{yr}$). Where there is a change in slope, estimates of recharge rate can be made for different CW intervals corresponding to different time periods and inferring different climatic conditions. As no data is available for temporal changes in chloride, we have used present day values for chloride fallout. Blackburn and McLeod [12] estimated chloride concentrations in rainfall in the Little Desert to be $\sim 4.5 \text{ mg/L}$ and, as the other sites are a similar distance from the coast, this value is probably a reasonable approximation for all of the sites. Multiplying this value by annual rainfall suggests estimates of chloride accession ranging from $0.016\text{--}0.024 \text{ g/dm}^2/\text{yr}$. Using this estimate for chloride flux, current recharge rate estimates for the S-W Murray Basin are $<0.3 \text{ mm/yr}$ for most sites except sites U1 and U5 where higher precipitation and sandy surface soil have increased this at least 5 fold.

Near vertical slope at the surface for U1 and U5 are indicative of the high rates of recharge expected following the clearing of native vegetation. A significant increase in recharge following clearing is not evident for the other sites indicating that either there has not been enough time since the area was cleared for these changes to occur or that the soil type and/or rainfall at these sites are not favourable to recharge (see next section) The recharge rate at site U4 was as high as at sites U1 and U5 at some time in the past but a change to the current climate has reduced recharge to values close to those at the other clay sites ($<0.3 \text{ mm/yr}$).

The chloride mass balance method of recharge estimation cannot be applied quantitatively where there is substantial change in recharge rate during the development of the soil-water profile. Salt concentration builds up in the unsaturated zone during a period of low recharge and is then leached to greater depths in the profile when higher recharge prevails during wetter climatic regimes. It is necessary to flush several pore volume of water through the soil before the chloride concentration of the soil-water is an accurate proxy for recharge. Any estimate for recharge using a chloride mass balance approach will be too low if chloride from a previous recharge regime has not been flushed out [13]. For this reason it is not possible to assign precise quantitative estimates of palaeo-recharge where slopes are high (sites U1, U5 and bottom of site U4) even though we can unequivocally state that recharge is much higher during these times.

2.4. Predicting change to groundwater salinity as a result of land-use change

The conceptual model describing the process for increasing groundwater salinity due to land-use change is shown schematically in Figure 7. Enhanced recharge following land clearing and even greater enhanced recharge from irrigation returns to the aquifer provides the mechanism for displacement of the saline soil water into the fresh groundwater and hence the observed increase in groundwater salinisation.

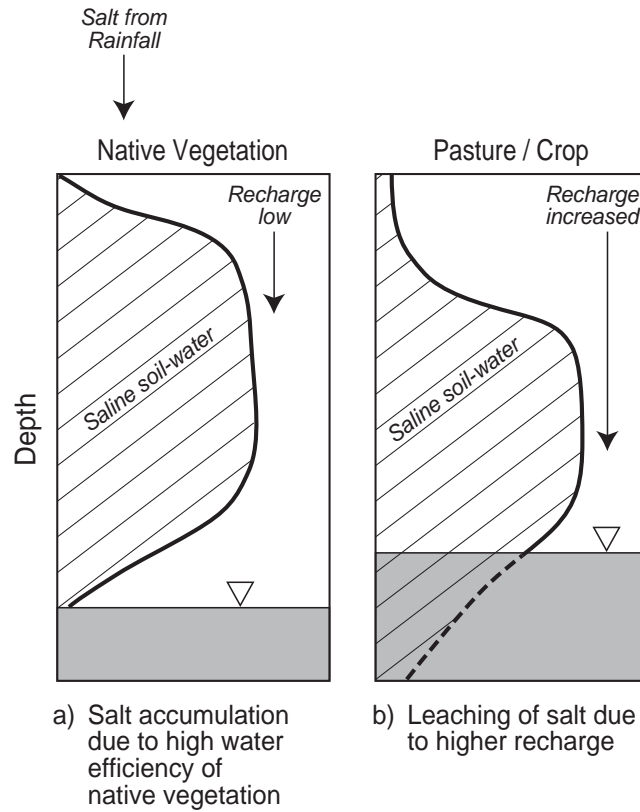


FIG. 7. Conceptual model showing a) the process of accumulation of saline soil water above the water table, and b) displacement of the saline soil water and increase in water table as a result of land clearing.

Cook et al. [14] developed a distributed parameter recharge model to calculate projected changes in groundwater salinity over a 200-year time frame as a result of land-clearing for two sites in the SW Murray Basin. Input data for their calculations at the two sites was recharge (estimated using chloride peak displacement techniques), soil-water salinity (estimated from chloride data from cores taken at the sites), water content of the unsaturated zone (pre and post clearing) and depth to groundwater.

The model calculates the time taken for the pressure front to reach the water table by considering the drainage flux, the depth to water and the difference in mean volumetric water content above (θ_1) and below (θ_0) the pressure front. It also accounts for the water table rising as a result of the increased recharge rate following clearing and includes a log normal distribution of drainage rate as found by Cook et al. [15]. As no better data is available for this study, we have used the same values for (θ_1) and (θ_0) and for the log normal distribution of drainage rate and used new input data derived from our work for post-clearing recharge rates and for soil-water salinity.

Predicted changes to groundwater salinity are calculated from three monitored boreholes where soil-water salinity data and recharge estimates and soil-water salinity data are available. Figure 8 shows the starting point is present day groundwater salinity levels and depths for each area (Figure 8). For these calculations, three scenarios are presented by assuming that complete mixing between displaced saline soil-water and groundwater occurs to a depth of 5 m, 10 m and 20m.

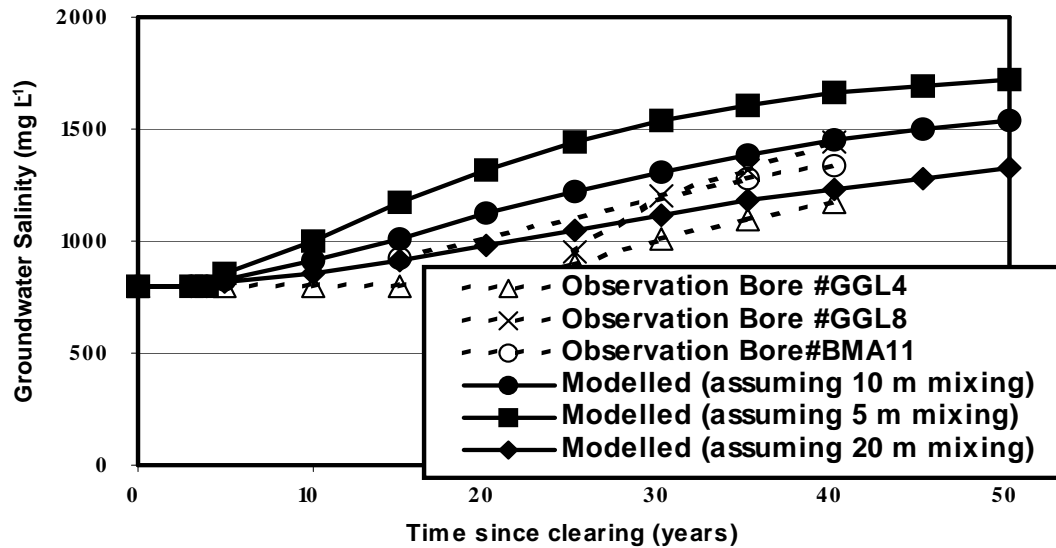


FIG. 8. Comparison of measured and modeled groundwater salinity for three observations boreholes. The model was run assuming depths of mixing of displaced saline soil water to 5m, 10m and 20 m respectively.

3. Conclusions

Fresh groundwater in the semi-arid SW Murray basin of Australia was derived from vertically driven palaeo-recharge through sandy subsoils below the Big and Little Deserts during wet climatic periods > 20,000 years ago. Saline soilwater is present throughout most of the unsaturated zone as a result of concentrating the salt present in rainfall by evapo-transpiration during the predominantly semi-arid climate for the last 20,000 years. There is a lag time of 50-200 years following clearing before groundwater salinities increase as a result of enhanced recharge following land clearing. Because clearing took place ~100 years ago, the effect of land clearing on groundwater salinisation is now being seen in many areas. Increases in groundwater salinity are likely to continue for many decades. Irrigation development will exacerbate the rate of groundwater salinisation by a factor of 5-10. Groundwater salinity levels will increase most rapidly in areas of surface soils and shallower (<30 m) water tables and least rapidly where surface soils are clay and the water table is deeper (~50 m).

REFERENCES

- [1] ALLISON, G.B. and HUGHES, M.W. (1983) The use of natural tracers as indicators of soil-water movement in a temperate semi-arid region. *J. Hydrol.* 60:157–173.
- [2] KENNETT-SMITH A.K., COOK, P.G. and THORNE, R. (1992) Comparisons of recharge under native vegetation and dryland agriculture in the Big Desert region of Victoria. CGS report # 46, Flinders University of South Australia.
- [3] KENNETT-SMITH A.K., THORNE, R. and WALKER, G.R. (1993) Comparison of recharge under native vegetation and dryland agriculture near Gorokey, Victoria. Centre for Groundwater Studies Report # 49. Flinders University of SA.
- [4] KENNETT-SMITH, A.K., COOK, P.G. and WALKER, G.R. (1994) Factors affecting groundwater recharge following clearing in the south western Murray Basin. *J. Hydrol.* 154:85–105.

- [5] VOGEL, J. (1966). Investigations of groundwater flow with radiocarbon. Proceedings of Symp. on Isotope Hydrology. 1966. IAEA Vienna, pp. 355-367.
- [6] LEANEY, F.W. and ALLISON, G.B. (1986) Carbon-14 and stable isotope data for an area in the Murray Basin: its use in estimating recharge. *J. Hydrol.*, 88: 129–145.
- [7] WIGLEY, T. M. L., PLUMMER, L.N. and PEARSON, F. J. (1978) Mass transfer and carbon isotope evolution in natural water systems. *Geochim. Cosmochim. Acta*, 42: 1117–1139.
- [8] CLARK, I. D. and FRITZ, P. (1997) Environmental isotopes in Hydrogeology. Lewis, Boca Raton, 328pp.
- [9] ALLISON, G.B., COOK, P.G., BARNETT, S.R., WALKER, G.R., JOLLY, I.D. and HUGHES, M.W. (1990) Land clearance and river salinisation in the Western Murray Basin, Australia. *J. Hydrol.*, 119:1–20.
- [10] BARNETT, S.R. (1989) The effect of land clearance in the Mallee region on River Murray salinity and land salinisation. *B.M.R. J. Aust. Geol. Geophys.*, 11:205–208.
- [11] STONE, W.J. (1994) Paleohydrologic implications of some deep soil-water chloride profiles, Murray Basin, South Australia. *J. Hydrol.* 132:201–223.
- [12] BLACKBURN, G. and MCLEOD, S. (1983) Salinity of atmospheric precipitation in the Murray-Darling drainage division, Australia. *Aust. J. Soil Res.* 21:411–434.
- [13] COOK, P.G., EDMUNDS, W.M. and GAYE, C.B. 1992. Estimating palaeorecharge and palaeoclimate from unsaturated zone profiles. *Water Resour. Res.* 28(10): 2721–2731.
- [14] COOK, P.G., TELFER, A.L. and WALKER, G.R. (1993) Potential for salinisation of the groundwater beneath mallee areas of the Murray Basin. Centre for Groundwater Studies, Report # 42 Flinders University of South Australia.
- [15] COOK, P.G., WALKER, G.R. and JOLLY, I.D. (1989) Spatial variability of groundwater recharge in a semi-arid region. *J. Hydrol.*, 111:195–212.
- [16] ALLISON, G.B., STONE, W.J. and HUGHES, M.W. (1985) Recharge in karst and dune elements of a semi-arid landscape as indicated by natural isotopes and chloride. *J. Hydrol.*, 176:1–25.
- [17] BARNETT, S.R. (1994) The hydrogeology of the Murray Basin in South Australia. Dept Mines & Energy Sth Aust Rep.
- [18] DOGRAMACI, S.S. (1998) Isotopes of Sr, S, O and C as tracers of mixing and geochemical processes in groundwater, SW Murray Basin. PhD Dissertation, U of Adelaide, South Australia.
- [19] JOLLY, I.D., COOK, P.G., ALLISON, G.B. and HUGHES, M.W. (1989) Simultaneous water and solute movement through an unsaturated soil following an increase in recharge. *J. Hydrol.*, 111:391–396.
- [20] LEANEY, F.W. and HERCZEG, A.L. (1999) The origin of fresh groundwater in the SW Murray Basin and Potential for Salinisation. CSIRO Land and Water Tech. Rpt. 7/99., Feb 1999., 78 pp.
- [21] LEANEY, F.W., HERCZEG, A.L. and WALKER, G.R. 2003. Salinisation of a fresh palaeo-ground water resource by enhanced recharge. *Ground Water* 41(1),84-93.
- [22] WALKER, G.R., JOLLY, I.D. and COOK, P.G. (1991) A new chloride leaching approach to the estimation of diffuse recharge following a change in land use. *J. Hydrol.*, 128:49–67.

Origin of saline groundwater in the northeastern of Guanzhong Basin, China

Dajun Qin

Institute of Geology and Geophysics, CAS, China, People's Republic of

Abstract. A saline groundwater lens occurs in river-lake sediments overlain by loess in the north-eastern Guanzhong basin, Shaanxi Province, China. The groundwater is classified into two groups: (1) freshwater, TDS < 1 g/L and (2) salinewater, TDS from 1 to 10 g/L. Saline water is mostly encountered between the foreland alluvial pan and north of Wei River. Saline groundwaters are supersaturated with respect to carbonate, aragonite and dolomite and undersaturated with respect to gypsum and anhydrite. $\delta^{18}\text{O}$ and $\delta^2\text{H}$ values plot fairly well along the local and global meteoric water lines, but show no correlation with salinity. $\delta^{13}\text{C}_{\text{DIC}}$ values range from -11 to -15‰, indicating dissolved inorganic carbon in groundwater is similar to soil CO_2 . The $\delta^{34}\text{S}$ values suggest sulphate in groundwater may derive from dissolution of gypsum, anhydrite in lacustrine sediment and rivers.

Key words: Hydrochemistry; isotopes; saline groundwater; shallow circulation

1. Introduction

Saline groundwaters in the north-eastern of China have been investigated by the Geological Survey of China since 1990s. Hydrochemical data have been obtained, including spatial distribution of major ions (Figure 1). The data are used to evaluate whether the occurrences of saline groundwater is attributed to the remnant of an ancient salt lake or other processes.

In order to decrease the salinity of groundwater, water table was lowered through drainage. However this method was later abandoned. Water supply pipe lines have now been built to transport ground water pumped from wells near the north side of Wei River and the North Mountain front (mainly karstic groundwater) in order to increase the supply of water for drinking, irrigation and industrial uses.

Generally, the saline groundwater overlaps the karstic groundwater. Increasing use of deep karstic groundwater has lowered its water level. Due to this situation, local hydraulic conditions can be changed. Two possibilities can be predicted: (1) saline groundwater intrusion into the karstic groundwater system; (2) promotion of shallow water circulation and solute transportation. Saline groundwater may usually relate to particular hydrologic and chemical fluxes in the development and reflects a dynamic equilibrium between the surface of the groundwater table and eolian processes [1][2]. The objective of this study to identify the sources and processes involved in the formation of saline groundwater in the northeast of the Guanzhong basin.

2. Geological settings

The Guanzhong basin is located in northwest of China, with an annual mean precipitation of 648 mm, and annual average atmospheric temperature of 13.6°. Wei River passes through the basin from west to east and it joins the Yellow River. The Guanzhong Basin is bounded by the Qinling Mountain to the south, by the North Mountain to the north and the Yellow River to the east (Figure 1). Bedrock in the northeast of the Guanzhong basin is Ordovician-Cambrian limestone. The bedrock is overlain by the late Pliocene Red Formation (5 Ma) in the North Mountain front and subsequent fluvio-lacustrine

sediments (3.08 to 1.9 Ma) [3]. Until the early Pleistocene, the graben lake disappeared and loess accumulated on the river-lake sequence. Currently, loess has covered most of the basin except the central Wei River channel. Flat and extensive terraces have developed in the north side of the Wei River. Relatively high and limited terraces with elevated loess platforms developed in its south side due to the faster tectonic uplift rate in the south side of the Wei River than in north.

Tertiary fluvio-lacustrine sediments consist of sandy, fine sandy and argillaceous sediments. Quaternary friable deposits consist predominately of gravel, sand, fine sand and clay sediments, which lie close to river channel. Saline groundwater is mainly hosted in fluvio-lacustrine sediments, consisting of alternating fine sandy layers and argillaceous layer in the northeast of the Guanzhong basin.

Recharge by infiltrating rainfall takes place at the North Mountain front and rivers, forming unconfined freshwater fringe, or saline groundwater lenses. Freshwater recharge may displace saline water near recharge region. Vertical infiltration in the center of the basin, especially in the areas covered by loess, is quite limited.

In the foreland of the North Mountain, the groundwater flow rate is relatively higher than in the plain, where the shallow groundwater table is close to the water level of the Wei River (Figure 2).

3. Paleoclimatic history of the basin

Pliocene-Pleistocene change has been documented in fluvio-lacustrine sediments in the Shijiawan profile, Guanzhong Basin, China [4]. The dominant lithologic facies, characterized by coarse channel sand and poorly sorted flood material (sand-mixed loam or salty clay) suggest that they consist mainly of fluvial deposition with little of lacustrine origin.

From 3.0 to 2.7 Ma, palaeoclimate (warm and dry) was a stable and relatively dry climate, and higher pollen concentrations in the Tertiary Red Clay formation suggest that steppe flora was persistently dense. Elephant fossils were found in the upper part of the interval, indicating that the climate was remarkably warmer and drier than at present.

From 2.7 to 2.47 Ma, a typical dry climate (cool and dry) has been recognized. The first thick loess-like layer in the river-lake sequence at 2.6 Ma is consistent with the beginning of loess deposition, reflecting cooling of the regional climate.

From 2.47 to 1.9 Ma, fluctuation of climate between cold-dry and warm-wet states has occurred at least three and half cycles [4]. There are 37 climatic cycles in the last 2.5 Ma [5]. The cold-dry climate in loess accumulation periods can be demonstrated by dry steppe flora and warm-wet period by developed palaeosols.

Climate changes, such as cold-dry and warm-wet suggest salts accumulation during cold-dry and dissolution during warm-wet may provide important mechanism for formation of saline groundwater.

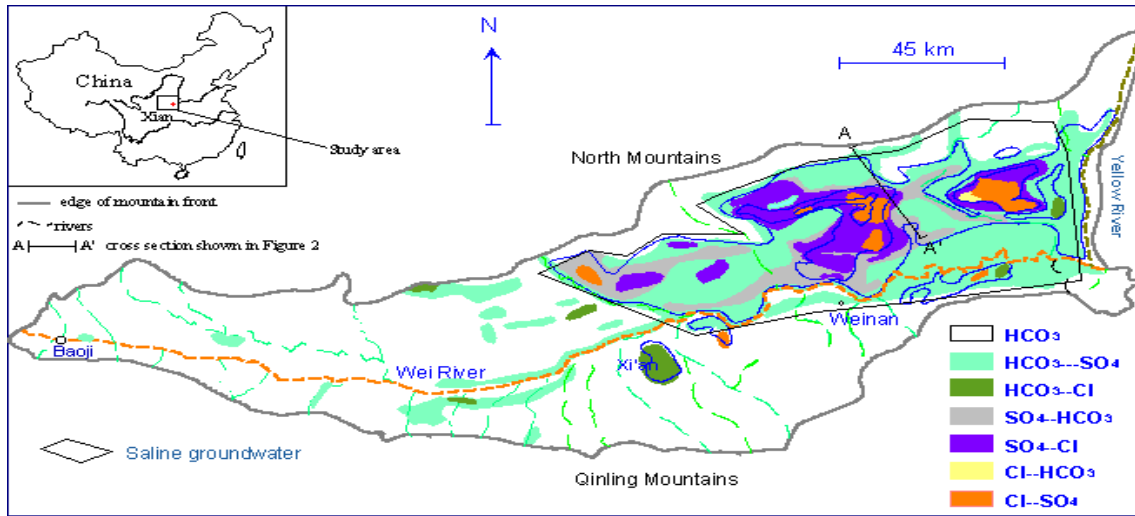


FIG. 1. Map of the distribution of saline groundwater in the northeast of the Guanzhong Basin. Inset shows the study area in China

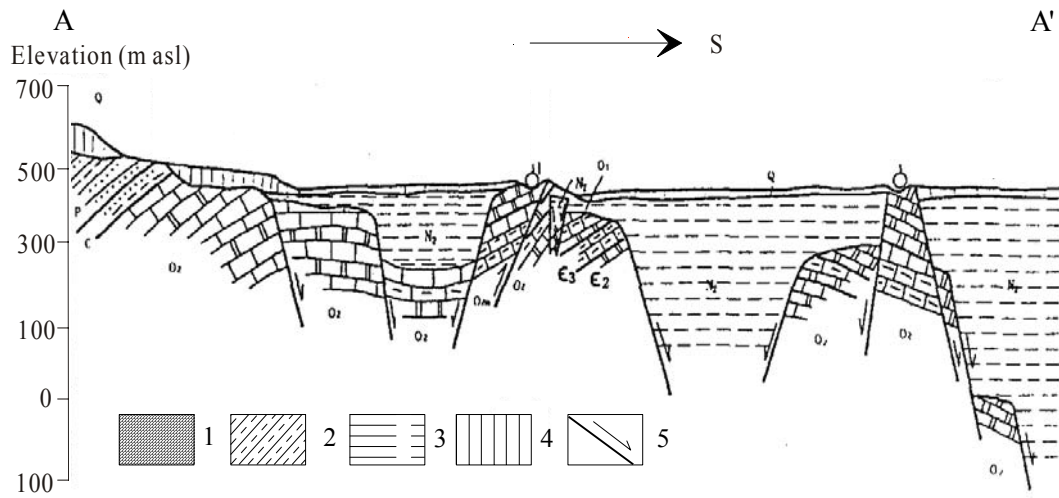


FIG. 2. Figure 2 Cross section from A-A' in the figure 1 showing double layer structure consisting of the river-lake sediments and the Ordovician-Cambrian carbonate. 1: Ordovician-cambrian carbonate; 2: Permian-Carboferious sandstone; 3: Tertiary sand and silt clay; 4: Quaternary loess; 5: Faults

4. Methods

We selected various hydrogeological settings for obtaining representative water samples. Sample sites are reported in Figure 3. Cations (Na, K, Ca, Mg, Si) were analyzed by atomic absorption spectrometry (AAS) and the anions (F, Cl, SO₄) by ion chromatography and HCO₃, CO₃ and pH by alkalinity titration at the Huadong Geology University, China, reported as the mg/L. The stable isotopes $\delta^{18}\text{O}$ and deuterium were measured by mass spectrometry, reported relative to Standard Mean Ocean Water (SMOW). $\delta^{13}\text{C}$ (in PDB) for water samples and $\delta^{34}\text{S}$ values (reported as the Canyon Diablo meteorite) were measured in the Institute of Geology and Geophysics, Chinese Academy of Sciences.

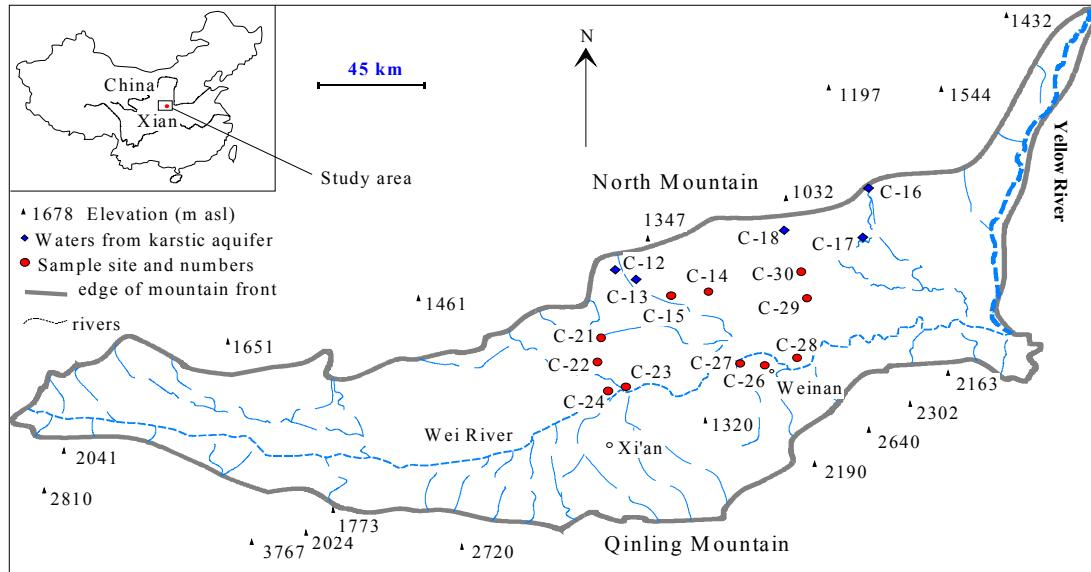


FIG. 3. Sample locations in the northeast of Guanzhong basin, Cina

5. Hydrochemistry

Table 1 reports the temperature and chemical data for 10 groundwaters from wells at depths ranging from 15 to 200 m. The total dissolved solids in the waters from the Weibei area ranges from 774.8 to 6160.4 mg/L. These waters show slightly alkaline pH values from 7.2 to 8.2. The order of abundance of cations and anions in the waters is Na>Ca>Mg, and HCO₃>Cl and SO₄ for low TDS groundwater and Na>Mg> Ca and Cl and SO₄>HCO₃ for high TDS groundwaters. Low TDS groundwater is mainly located near the Wei River and its tributaries, and high TDS groundwater principally lies in the center plain between Wei River and North Mountain (Figure 4). The water samples could be classified into two groups (Figure 5). The first group has low salinity (0-10 equivalents per million Cl-[meq]) and is generally located near the Wei river and the North Mountain foreland fan, indicating the fresh water in the study area. The second group is of medium salinity (10-60 meq Cl), located in the middle part of the investigated area. High salinity (>60 meq Cl) groundwater has not been encountered through this investigation.

Table 1. Physical and chemical composition of groundwater from the Weibei area, China (concentrations in mg/L).

Sample No.	Well depth (m)	T (°C)	pH	EC (ms/cm)	Na	K	Ca	Mg	Sr	B	SO ₄ ²⁻	Cl ⁻	HCO ₃	SiO ₂	F ⁻	TDS	B/Cl (×10 ⁻³) molar	Na/Cl molar
GZC-12	300	21.8	7.68	1	85.24	3.51	105.3	38.01	1.39	0.2	173	89.3	355.4	16.69	0.59	1199.19	7.35	1.47
GZC-13	70	17.5	7.68	7.08	1298	1.8	107.9	471.3	6.27	1.21	2008	1548	547.8	14.07	0.88	6107.61	2.57	1.29
GZC-14	100	21.4	7.64	0.64	84.08	1.29	50	24.3	0.56	0.2	64	17.9	386.8	15.53	0.38	774.79	36.69	7.25
GZC-15	100	16.6	7.75	0.86	70.01	1.38	89.94	41.22	0.83	0.1	115	47.62	436.2	16.64	0.3	944.47	6.90	2.27
GZC-16	600	25.1	7.4	1.12	125.7	6.4	88.88	39.3	2.85	0.31	221	125	331.5	19.52	0.77	1594.94	8.14	1.55
GZC-17	600	37.1	7.15	1.47	188.6	10.28	98.41	40.54	3.26	0.45	265	232.1	304.9	22.77	0.92	1813.07	6.37	1.25
GZC-18	1000	31.7	7.2	1.03	104.2	6.18	89.68	36.57	2.71	0.24	200	107.1	316.3	18.97	—	1921.94	7.36	1.50
GZC-21	300	28.0	7.7	2.9	398	2.08	88.09	135.2	4.64	0.53	485	675.2	286.8	14.45	0.65	2429.24	2.58	0.91
GZC-22	160	27.9	7.8	1.24	182.1	1.64	30.69	69.13	1.74	0.66	201	113.1	507.8	12.55	1.13	1318.48	19.16	2.49
GZC-23	130	27.8	7.73	1.5	270.1	1.11	45.08	40.32	1.03	0.71	336	172.6	404.9	13.49	1.24	1453.61	13.51	2.42
GZC-24	210	27.4	8.18	0.41	76.19	0.09	26.98	4.04	0.24	0.18	33	17.9	237.2	14.16	1.13	657.1	33.02	6.57
GZC-27	18	19.5	7.78	0.9	109.1	1.92	70.95	32.43	0.55	0.33	123	95.2	363.9	11.66	0.74	855.96	11.38	1.77
GZC-28	65	27.5	7.23	1.18	130.4	2.39	104.5	61.27	1.19	0.29	122	101.2	564.9	15.97	0.37	1205.39	9.41	1.99
GZC-29	15	27.3	7.53	7.86	1563	2.14	88.49	299.3	6.11	3.01	1844	1676	607.8	11.32	1.5	6160.36	5.90	1.44
GZC-30	6	26.8	7.88	3.74	880	1.54	29.76	61.11	1.19	4.4	1172	440.5	618.3	16.79	3.22	3273.32	32.80	3.08
Sea water										4.6		19000					0.7	0.86

Notes: —, undetected.

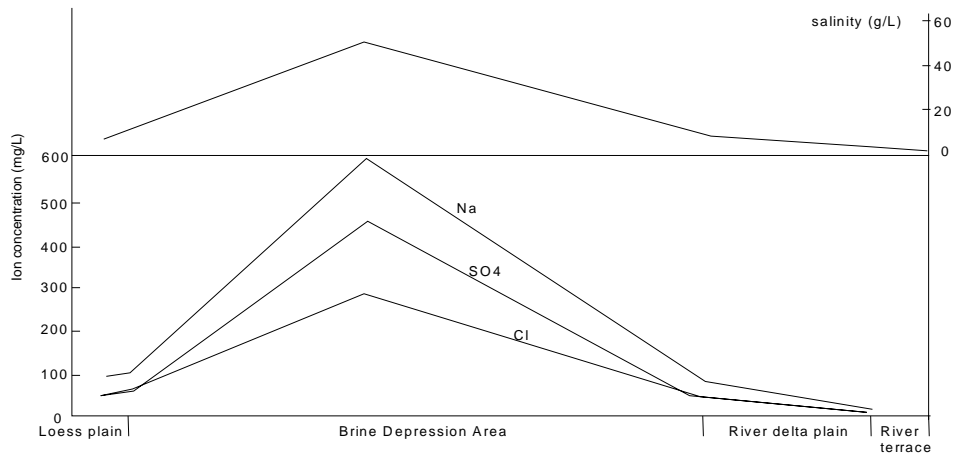


FIG. 4. Plot of major ions along north-south profile in the northeast Guanzhong basin

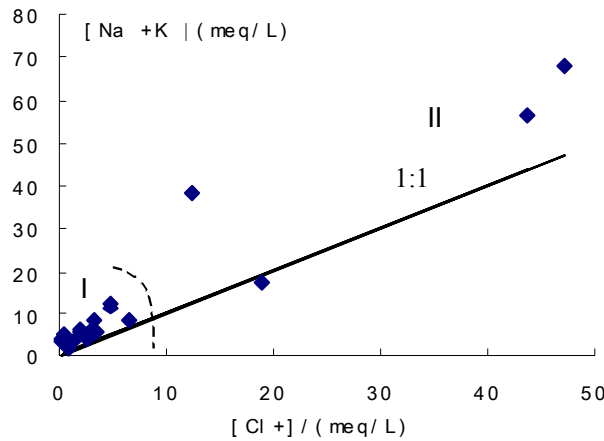


FIG. 5. Relation between $[Na^+ + K^+]$ and $[Cl^-]$ in saline groundwater: I) fresh water, II) medium salinity groundwater

Na versus Cl and Mg versus SO_4 show good linear correlation (Figure 6). Na, Mg, Cl, and SO_4 versus TDS also show good linear correlation (Figure 7). The enriched SO_4 and Cl concentrations in saline groundwaters (Table 1) is possibly the result of the dissolution of gypsum and halite. Gypsum and dolomite dissolution are reflected in the SO_4^{2-} and Mg^{2+} concentrations.

These waters have similar chemical composition and evolutionary characteristics with increasing salinity (Figure 8). This suggests the existence of common hydrogeochemical processes (mixing and/or chemical reactions).

The saturation indices (SI) were used to describe the extent to which a particular solution is supersaturated or undersaturated with a particular solid phase. The theoretical saturation states of calcite, dolomite, gypsum etc were calculated for the water samples using the computer program NETPATH [6]. The SI values (Table 2) indicate that calcite, dolomite and aragonite are supersaturated, $SI > 0$, except sample GZC-12. Gypsum and anhydrate are undersaturated, $SI < 0$. The increased Mg concentrations with salinity may indicate the dissolution of gypsum.

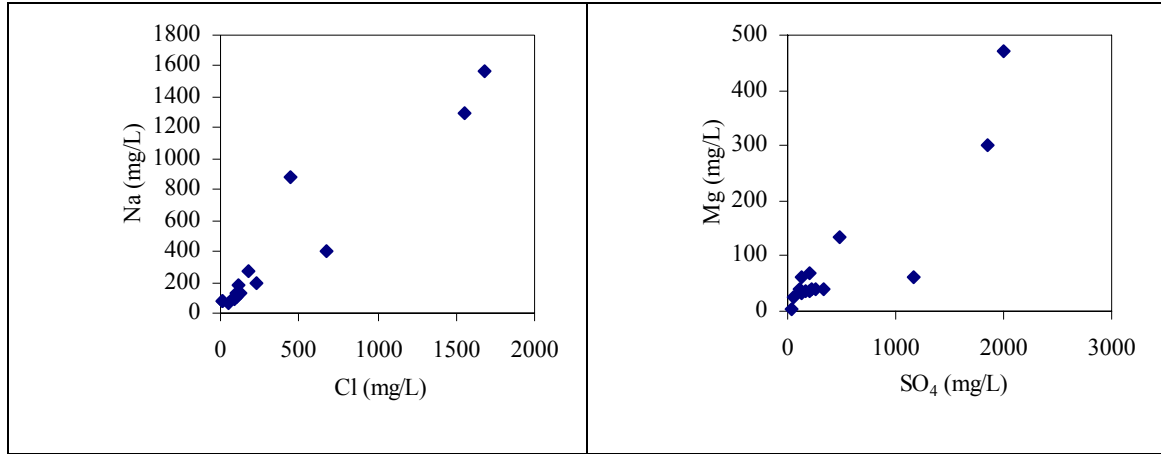


FIG. 6. Na vs Cl and Mg vs SO₄

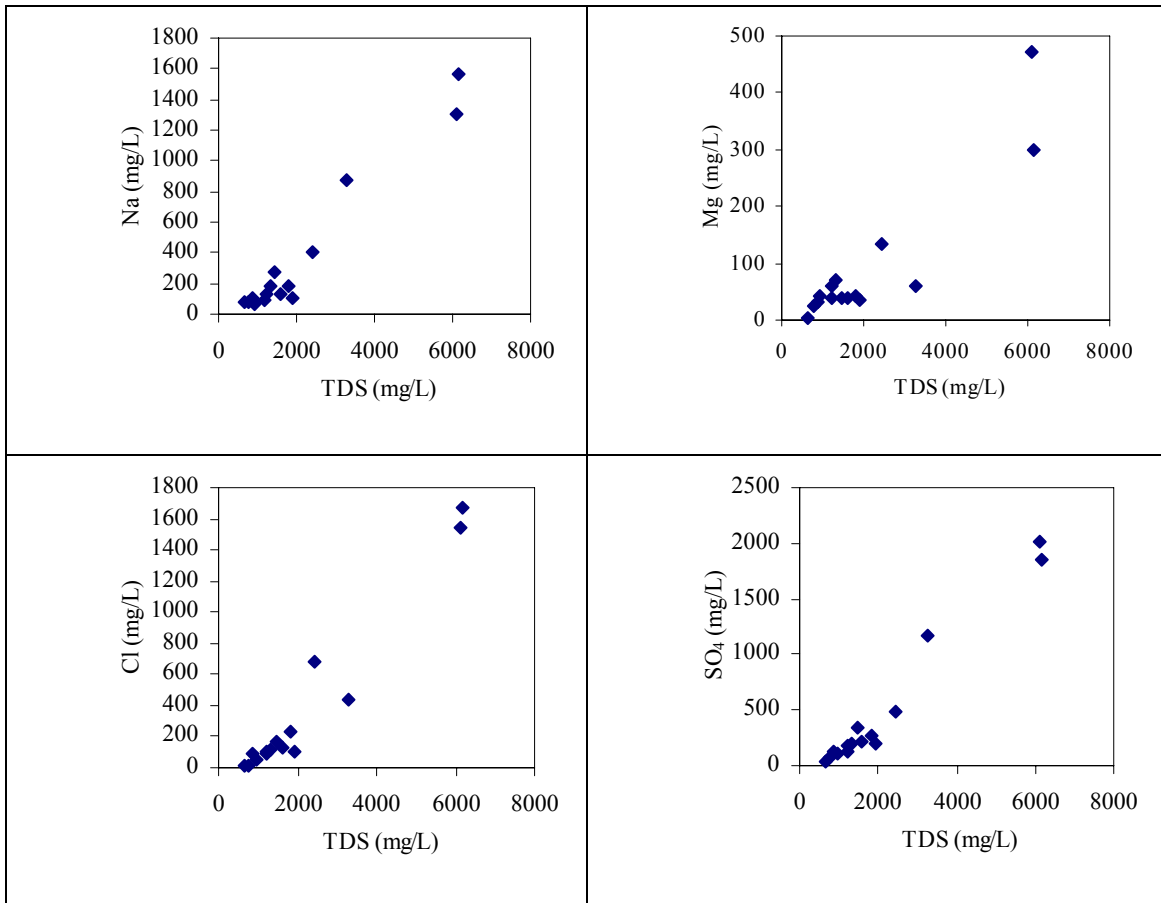


FIG. 7. TDS versus Na, Mg, Cl and SO₄

Table 2. Calculated P_{CO_2} and saturation indices (SI) values of groundwater from the Weibei area for various minerals using Netpath program.

Sample No.	Calcite	Aragonite	Dolomite	Gypsum	Anhydrite	log P_{CO_2}
GZC-12	-0.06	-0.21	-0.26	-1.34	-1.57	-1.50
GZC-13	0.31	0.17	1.54	-0.85	-1.09	-2.00
GZC-14	0.28	0.13	0.54	-1.97	-2.20	-2.08
GZC-15	0.50	0.35	0.90	-1.54	-1.79	-2.05
GZC-16	0.27	0.13	0.54		-1.55	
GZC-17	0.21	0.08	0.48		-1.42	
GZC-18	0.16	0.02	0.34		-1.55	
GZC-21	0.41	0.27	1.38	-1.22	-1.43	-2.31
GZC-22	0.41	0.27	1.55	-1.86	-2.07	-2.13
GZC-23	0.37	0.23	1.07	-1.49	-1.69	-2.17
GZC-24	0.54	0.40	0.64	-2.42	-2.63	-2.81
GZC-27	0.54	0.40	1.03	-1.61	-1.85	-2.30
GZC-28	0.39	0.25	0.92	-1.54	-1.76	-1.52
GZC-29	0.31	0.17	1.51	-0.96	-1.17	-1.81
GZC-30	0.23	0.09	1.12	-1.39	-1.61	-2.08

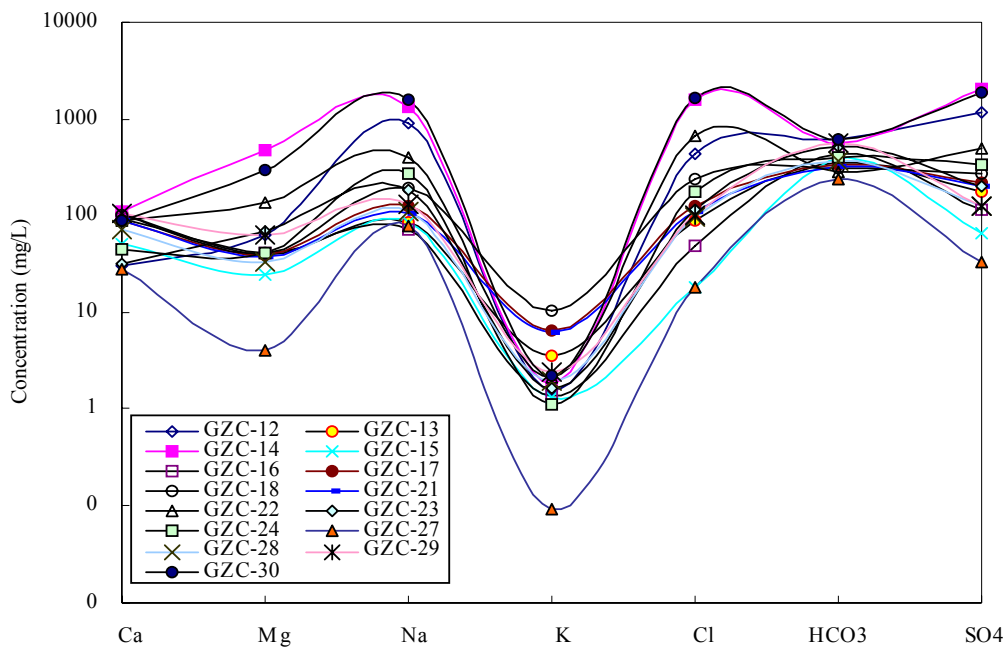


FIG. 8. Chemical analysis of major ions in the saline groundwater, displayed on Schoeller semilogarithmic diagram. Data from Table 1

5.1. Chemistry of the saline alkali soil

Figure 9 shows that soluble compositions increase at depth of 150 to 200 m. Saline alkali soil is mainly distributed in the area close to saline groundwater. The surface soil contains high Na, SO₄ and Cl, but low HCO₃, Ca and Mg, resulting in the presence of sulphate soil (Table 3).

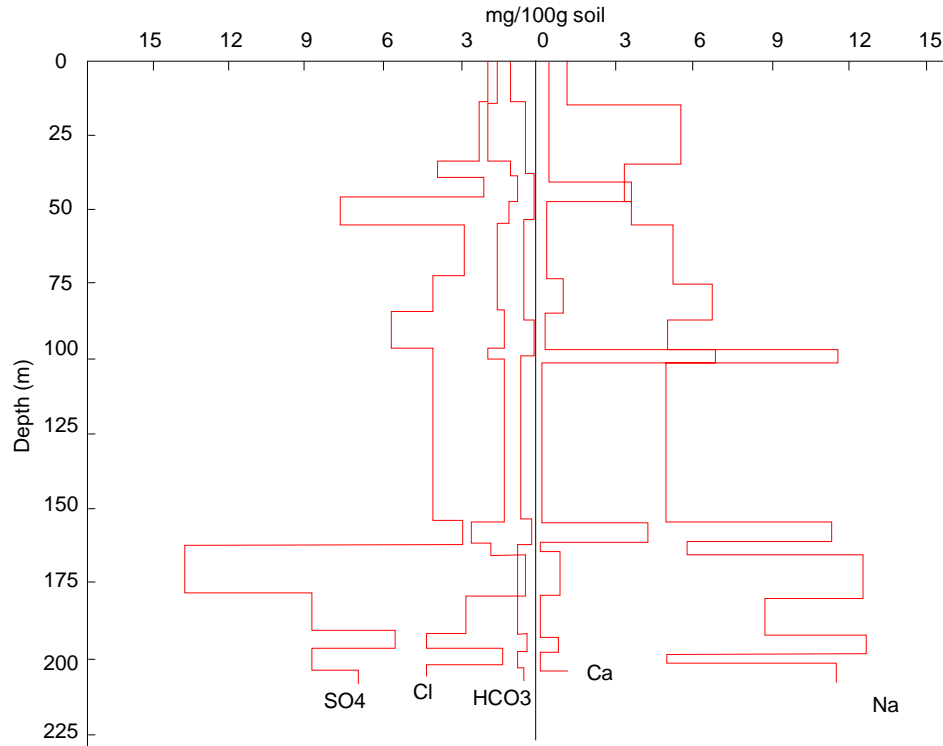


FIG. 9. Soluble composition of soil from a well profile [7]

Table 3. Soluble compositions (%) in Saline alkali soil (0-1.0 m deep) [7].

Location	Sample No.	K+Na	Ca	Mg	Cl	SO ₄	HCO ₃	TDS (%)
River terrace	G1	0.007	0.02	0.003	0.001	0.011	0.066	0.108
	G2	0.011	0.019	0.004	0.003	0.017	0.081	0.135
River delta plain	G3	0.021	0.012	0.004	0.007	0.015	0.077	0.136
	G4	0.024	0.081	0.006	0.027	0.180	0.057	0.375
	G5	0.028	0.021	0.004	0.023	0.048	0.056	0.18
Loess plain	G6	0.083	0.006	0.001	0.022	0.073	0.101	0.286
Brine Depression	G7	0.14	0.005	0.002	0.086	0.113	0.096	0.442
	G8	0.173	0.139	0.037	0.124	0.646	0.034	1.153

6. Stable isotopes

Deuterium and oxygen-18 were measured in both saline and karstic groundwaters (Table 3). The isotopic contents of the water samples are plotted on the $\delta^{18}\text{O}$ - δD diagram (Figure 10). The deuterium and $\delta^{18}\text{O}$ values are in the range from -60‰ to -90‰ and -7‰ to -12‰ , respectively.

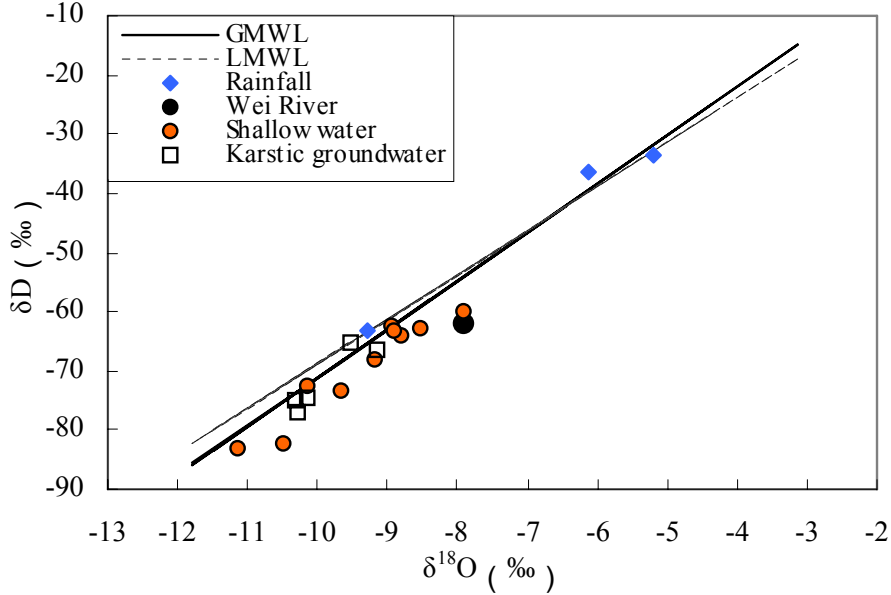


FIG. 10. Relation between δD and $\delta^{18}\text{O}$ for the saline groundwater

6.1. Carbon isotopes

$\delta^{13}\text{C}$ values range from -11.1 to -15.6‰ (Table 4). Soil samples for the ^{13}C values from a depth of 0 to 16 m range from -8.0‰ to -3.0‰ in Tianshuogou, -7.8‰ to -2.8 in Yuanlei.

Possible sources of carbon in the saline groundwater are: (1) atmospheric CO_2 , (2) soil CO_2 , and (3) dissolution of carbonate minerals.

Rain water $\delta^{13}\text{C}$: $\delta^{13}\text{C}$ in DIC of rain water depends on the atmospheric CO_2 and the fractionation of carbon isotopes between gaseous and aqueous phases. $\delta^{13}\text{C}$ of atmospheric CO_2 is assumed to be between -6 to -8‰ PDB [8] and has an average value of -7‰ [9] and -7.6‰ [10]. The atmospheric CO_2 dissolves in rainwater to form DIC and is included in groundwater recharge. Usual range of riverine $\delta^{13}\text{C}_{\text{DIC}}$ values that equilibrate with the atmospheric CO_2 ranges between -6.0 and -9.0‰ [11] and -8.8‰ in unaltered rainwater [12]. Concentrations (3.88-10.13 mmole/L) of DIC are found in the saline groundwater. These concentrations are far higher than those of rainwater. In addition $\delta^{13}\text{C}$ values are much depleted compared to the rain water. This suggests that rainwater is not the direct source of DIC of saline groundwater.

Table 3. Water types and isotopic data for groundwaters.

Sample No.	Water type	$\delta^{18}\text{O}$ (‰)	δD (‰)	$\delta^{13}\text{C}$ (‰)	$\delta^{34}\text{S}$ (‰)
GZC-12	Na-SO ₄ -Cl-HCO ₃	-9.54	-65.4		15.24
GZC-13	Ca-Na-Mg-HCO ₃	-9.65	-73.3	-12.35	
GZC-14	Na-Mg-Cl-SO ₄	-9.16	-66.4	-12.39	11.21
GZC-15	Na-Ca-Mg-HCO ₃	-8.79	-64.0	-11.12	
GZC-16	Ca-Mg-Na-HCO ₃	-10.27	-77.1		13.93
GZC-17	Na-Ca-Mg-HCO ₃	-10.14	-74.5	-12.06	
GZC-18	Na-Ca-Cl-SO ₄	-10.33	-74.9	-13.47	
GZC-21	Na-Ca-Mg-HCO ₃	-11.14	-83.0	-12.81	
GZC-22	Na-Mg-Cl-SO ₄	-9.19	-68.0	-12.77	10.25
GZC-23	Na-Mg-HCO ₃ -SO ₄	-10.48	-82.3	-11.40	9.81
GZC-24	Na-SO ₄ -HCO ₃	-10.15	-72.5	-11.33	7.6
GZC-27	Na-Ca-HCO ₃	-8.94	-62.3	-12.49	
GZC-28	Na-Ca-Mg-HCO ₃	-8.54	-62.7	-14.78	14.00
GZC-29	Na-Ca-Mg-HCO ₃	-8.91	-63.4	-15.61	20.98
GZC-30	Na-Mg-Cl-SO ₄	-7.91	-59.8	-13.54	11.66

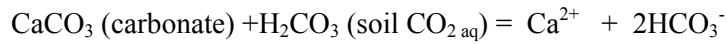
Soil water $\delta^{13}\text{C}$: In regions with well developed soils, biogenic CO₂ constitutes the largest pool of DIC. The isotopic composition of CO₂ is similar to that of the decaying organics that, in turn, depends on the type of vegetation, which has a value of -24 to -34‰, with an average of -28‰ [9]. No fractionation occurs when this material is respired to produce CO₂ gas. The difference between the diffusion coefficients of ¹²CO₂ and ¹³CO₂ cause soil gases to be enriched in ¹³CO₂ by up to 4.4‰ [8], relative to the organic source material. Soil gas has $\delta^{13}\text{C}$ of -30 to -19‰, with an average of -23‰, and the dissolution of this gas in soil water gives the average soil water a $\delta^{13}\text{C}$ of -23 to -13‰ [13].

Groundwater $\delta^{13}\text{C}$ values: Stable carbon isotope study of the modern vegetation and related soils in the Guanzhong Basin indicates $\delta^{13}\text{C}$ values of organic matter to be around -22‰ to -27.5‰ [4], with an average of -24.7‰. Therefore, the soil gas has a $\delta^{13}\text{C}$ of about -18 to -23‰ due to the enrichment caused by the difference in the diffusion coefficients of ¹²CO₂ and ¹³CO₂. The dissolution of this gas may produce soil water with a $\delta^{13}\text{C}$ of about -9 to -15‰. This is consistent with the measured $\delta^{13}\text{C}$ values from groundwater samples. The groundwater $\delta^{13}\text{C}$ of -11.12 to -15.61‰ implies that over 80% of the $\delta^{13}\text{C}_{\text{DIC}}$ has a soil CO₂ source. Figure shows $\delta^{13}\text{C}$ is in reverse proportional to pCO₂, indicating that soil CO₂ must have been in equilibrium with soil water to produce the observed carbon isotope

characteristics of groundwater and changes of groundwater $\delta^{13}\text{C}$ is mainly controlled by soil CO_2 partial pressure.

$\delta^{13}\text{C}$ from dissolution of carbonate: Dissolution of carbonate minerals can take place by carbonic acid as well as sulfuric acid, the latter derived from oxidation of sulfide minerals. Dissolution of gypsum and /or anhydrite can provide sulfate. In groundwater, the $\text{SO}_4^{2-}/\text{HCO}_3^-$ equivalent ratio of the samples ranges between 0.04 and 1.16, with an average of 0.32. This implies that CO_2 remains the largest source of acidity. Overlain loess can provide a soil cover to produce and sustain pCO_2 levels several orders of magnitude higher than the atmosphere.

Soil gas has $\delta^{13}\text{C}$ values ranging from -18 to -23‰ as discussed above, with an average of -20.5‰ . Carbonates in the carbonate nodule in the red clay layers have $\delta^{13}\text{C}$ of -9.6 to -5.3‰ [14], with an average of -7.45‰ . The dissolution of carbonate by carbonic acid is as follows:



Then a carbonate with a $\delta^{13}\text{C}$ of -7.45‰ and a soil CO_2 with a $\delta^{13}\text{C}$ of -20.5‰ yields $\delta^{13}\text{C}$ of -14‰ for carbon of carbonate dissolution end member.

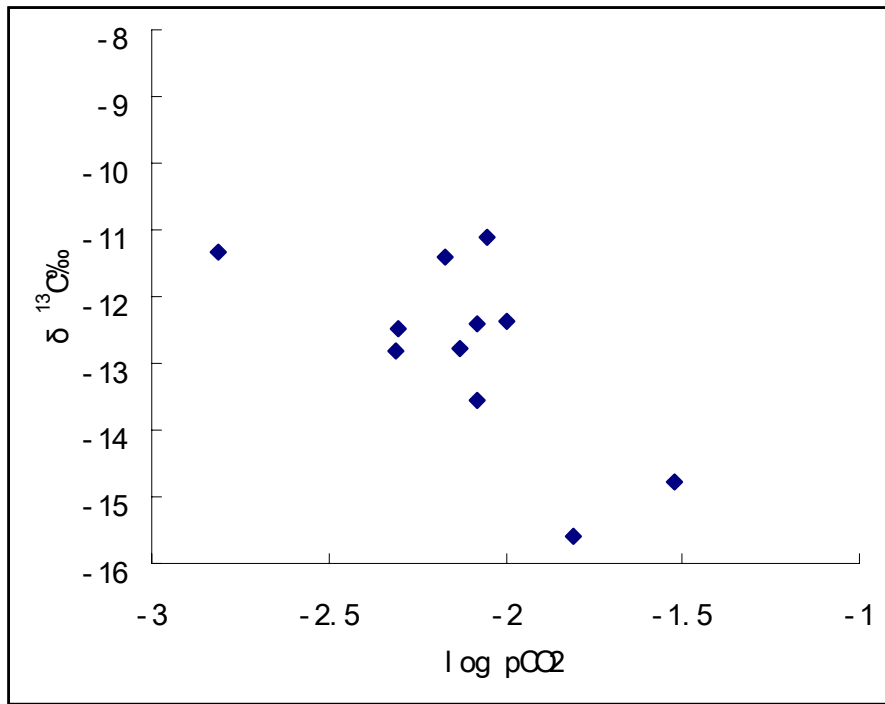


FIG. 11. $\delta^{13}\text{C}$ versus pCO_2 for groundwater from northeast Wei River

6.2. Sulphur isotopes

The $\delta^{34}\text{S}$ values of the thermal waters are in the range from $+7.60$ to $+20.98\text{‰}$. The mean values for atmospheric $\delta^{34}\text{S}$ sulphate for southern Germany and Austria range from $+2.1$ to $+3.5$ [15]. The sulphur isotopic composition of modern dissolved seawater sulphate is $+20\text{‰}$ to $+20.5\text{‰}$ (CDT) distributed homogeneously throughout the world ocean [16]. $\delta^{34}\text{S}$ values of marine sulphate is around $+30\text{‰}$ to $+35\text{‰}$ [17][18]. The average of dissolved sulphate in modern rivers has been averaged globally at $+8\text{‰}$ [19]. The $\delta^{34}\text{S}$ value data suggest sulphate in groundwater may derive from dissolution of gypsum, anhydrite in lacustrine sediment and rivers.

7. Conclusion

The chemical and isotopic composition of saline groundwater indicate that its salinity is closely related to the dissolution of salts in the lacustrine sediments and stagnant hydrogeological conditions. The similarity in the chemical composition between saline groundwater and saline alkaline soil suggests that water has been transported and accumulated salt leading to the salinization of soil in surface. The chemical variations between groundwater and soil provide a reliable monitoring tool that enable to reveal water-soil interaction.

ACKNOWLEDGEMENTS

This paper was financially supported by the IAEA Research Contract project (Number: CPR/11730).

REFERENCES

- [1] STOKES, W.L., Eolian varving in the Colorado Plateau. *Journal of Sedimentary Petrology* 34, 429–432 (1964).
- [2] STOKES, W.L., Multiple parallel-truncation bedding planes—a feature of wind-deposited sandstone formations. *Journal of Sedimentary Petrology* 38 (1968) 510–515.
- [3] ZHENG H. B., AN Z. S., SHAW J., LIU T. S., A detailed terrestrial geomagnetic record for the interval 0–5.0 Ma. In *Loess, Environment and Global Change* (eds. T.S. Liu, Z.L. Ding, and Z.T. Guo), (1991) 147–156. Science Press, Beijing.
- [4] HAN, J. FYFE, W.S., LONGSTAFFE, F.J., PALMER, F. H., YAN, F.H., MAI, X.S., Pliocene-Pleistocene climatic change recorded in river-lake sediments in central China. *Palaeogeography, Palaeoclimatology, Palaeoecology*. (1997) 135: 27–39.
- [5] DING, Z.L., LIU, T.S., LIU, X.M., CHEN, M.Y., AN, Z.S., Thirty-seven climatic cycles in the last 2.5 Ma. *Chin. Sci. Bull.* 35 (1990) 667–671.
- [6] PLUMMER, N. L., PRESTEMON, E.C., PARKHURST, D.L., An interactive code (NETPATH) for modelling net geochemical reactions along a flow path, version 2.0. U.S. Geological Survey Water Resources Investigations Report 94-4169, (1994) U.S.G.S., Reston, VA.
- [7] TIAN SHENGCHUN, ET AL., The environmental hydrogeological problems of Guanzhong Basin, Shaanxi Science and Technology Press (1995).
- [8] CERLING, T.E., SOLOMON, D.K., QUADE, J., BROWMAN, J.R., On the isotopic composition of carbon in soil carbon dioxide. *Geochim. Cosmochim. Acta* 55, 3403–3455 (1991).
- [9] FAURE, G., *Principles of Isotope Geology*. Wiley, Toronto, (1986) 492–493.
- [10] ZHANG, J., QUARY, P.D., WILBOUR, D.O., Carbon isotope fractionation during gas-water exchange and dissolution of CO₂. *Geochim. Cosmochim. Acta* 59, (1995) 107–114.
- [11] ANDERSON, T.F., ARTHUR, M.A., Stable isotopes of oxygen and carbon and their application to sedimentologic and paleoenvironmental problems. In Arthur, M.A., Anderson, T.F., Kaplan, I.R., Veizer, J., Land, L.S. (Eds.), *Stable Isotopes in Sedimentary Geology*. Society of Economic Paleontologist and mineralogists, (1983) 1.1–1.151 Short Course Notes No. 10.
- [12] KARIM A., VEIZER, J., Weathering processes in the Indus River Basin: implications from riverine carbon, sulphur, oxygen, and strontium isotopes. *Chemical Geology*, (2000) 170, 153–177.
- [13] KEVIN, T., VEIZER, J., Carbon fluxes, pCO and substrate weathering in a large northern river basin, Canada: carbon isotope perspectives. *Chemical Geology*, (1999) 159, 61–86.
- [14] DING, Z.L. YANG, S.L., C₃/C₄ vegetation evolution over the last 7.0 Myr in the Chinese Loess Plateau: evidence from pedogenic carbonate $\delta^{13}\text{C}$. *Palaeogeography, Palaeoclimatology, Palaeoecology*, (2000) 160, 291–299.
- [15] MAYER B., Potential and limitations of using sulphur isotope, abundance ratios as an indicator for natural and anthropogenic environmental, change. In *Isotope Techniques in the Study of Environmental Change*, (1998) 423–435. International Atomic Energy Agency, Vienna.

Dajun Qin

- [16] LONGINELLI, A., Oxygen-18 and sulphur-34 in dissolved oceanic sulphate and phosphate. In: Fritz, P., Frontes, J.Ch. (Eds.), *Handb. Environ. Isot. Geochem.* Vol. 3. Elsevier, Amsterdam, (1989) 219-255.
- [17] CLAYPOOL, G.E., HOLSER, W.T., KAPLAN, I.R., SAKAI, H., ZAK, I., The age curves of sulphur and oxygen isotopes in marine sulphate and their mutual interpretation. *Chem. Geol.* 28, (1980) 190-260.
- [18] SOLOMON, M., RAFTER, T.A., DUNHAM, K.C., Sulphur and oxygen isotope studies in the northern Pennines in relation to ore genesis. *Trans. Inst. Min. Metall., B*, (1971) 259-275
- [19] GRINENKO, V.A., KROUSE, H.R., Isotope data on the nature of riverine sulphates. *Mitt. Geol.Palaeontol. Inst. Univ. Hamburg* (1992) 72, 9-18.
- [20] HOUGHTON, M.L., *Geochemistry of the Proterozoic Hormuz Evaporites, Southern Iran*. MSc thesis, University of Oregon (1980).

Optimization of isotopic techniques to investigate groundwater salinization in Disi Basin, Jordan

H. M. Amro, S. F. Kilani, Z. Al-Tarawneh, M. A. Momani, A. Subeh

Ministry of Water and Irrigation, Water Authority of Jordan, Jordan, Hashemite Kingdom of

Abstract. The Disi sandstone aquifer crops out in southern Jordan and extends to the northern part of Saudi Arabia. The water bearing strata consist of two groups; the saline Khraim group of Ordovician-Silurian age and the fresh waters Ram group of Cambro-Ordovician age. Environmental isotopes showed that present day recharge in the region is negligible and that groundwater is not being replenished. Aquifer recharge took place in different pluvial periods in the Pleistocene and early Holocene. Recent recharge is limited and localized in areas suitable to indirect recharge from Wadis. The Disi groundwater residence time and velocity were estimated both, by the conventional hydrological approach and environmental isotopes. Results are in a good agreement. Investigations using advanced tools like strontium and boron isotopes were used to distinguish the different sources and origins of ground water salinities, as well as for studying water origin and water dynamics within the aquifer. Using Sr and B relationship we were able to distinguish between sources and origins of different salinities such as those of marine origins, anthropogenic origins, dissolution of gypsum, halite and other matrix minerals. It was also possible to distinguish the origin of salinities of different water bodies and aquifer formations.

Introduction

The Disi sandstone aquifer is of regional importance as it extends over a wide area from southern Jordan to several parts of Saudi Arabia. The Disi sandstone group forms part of the most extensive aquifer system in the Arabian Peninsula, and was first recognized as a potential source of groundwater by UNDP/FAO, based on the work of J.W. Lloyds during their investigations in the late 1960's.

The recent isotopic dating of the groundwater in the Disi aquifer indicates that the aquifer contains fossil groundwater of more than 30000 years in age. Modern recharge constitutes a small fraction of total inflows, which means that abstracted ground water will be derived from the aquifer storage. Groundwater has been abstracted since 1950, and the pumping rate increased rapidly in the 1980s. The extracted water is mainly used for irrigation purposes, but increasing concern and demand for water encouraged projects to make the best use of this good but limited water resource [1].

Study objectives

Monitoring and identifying the source and origin of the groundwater salinity, particularly during the early stage of salinization are important steps for both better management of the aquifers and future possible remediation.

The main objective of the current study is to predict, determine and understand the salinity origin(s) and transport mechanisms using an integrated approach of advanced isotopic tools such as the $^{87}\text{Sr}/^{86}\text{Sr}$ ratio, $\delta^{11}\text{B}$ together with the conventional environmental isotopes of hydrogen, oxygen and carbon and other geo-chemical methods.

The study is aimed to formulate isotopic criteria that characterize water-rock interaction and distinguish it from other sources of water salinity, such as anthropogenic contamination and marine sources of salinization.

Study Area

The sandstone aquifer in Jordan covers an area of 3000 km² across the southern desert, The main extension of the aquifer is in Saudi Arabia. The outcrop extends over a distance of 1500 km and is 91000 km² in size. Larger area of the sandstone sinks beneath overlying sediments to the east of the outcrop [1].

The study area at Disi & Mudawara in Jordan is illustrated in Figure 1.

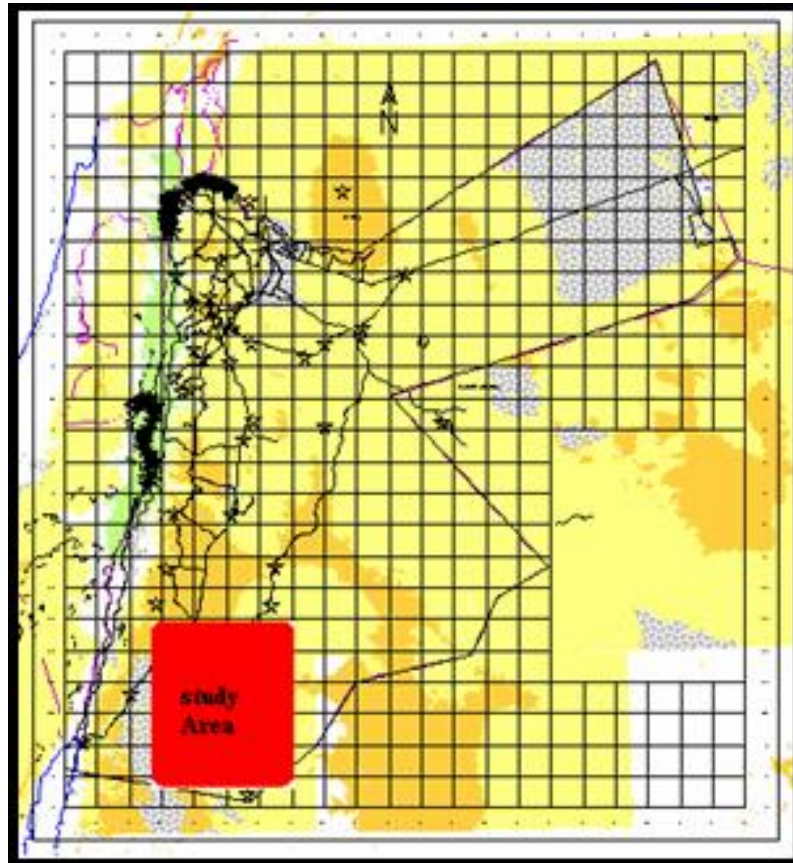


FIG. 1. Location of study area in south Jordan.

Geology and Hydrogeology

The geological map of the study area and locations of the sampled wells are shown in Figure 2. These wells are distributed to cover the unconfined part of the aquifer at Disi area and the confined part at Mudawara, near the Saudi border.

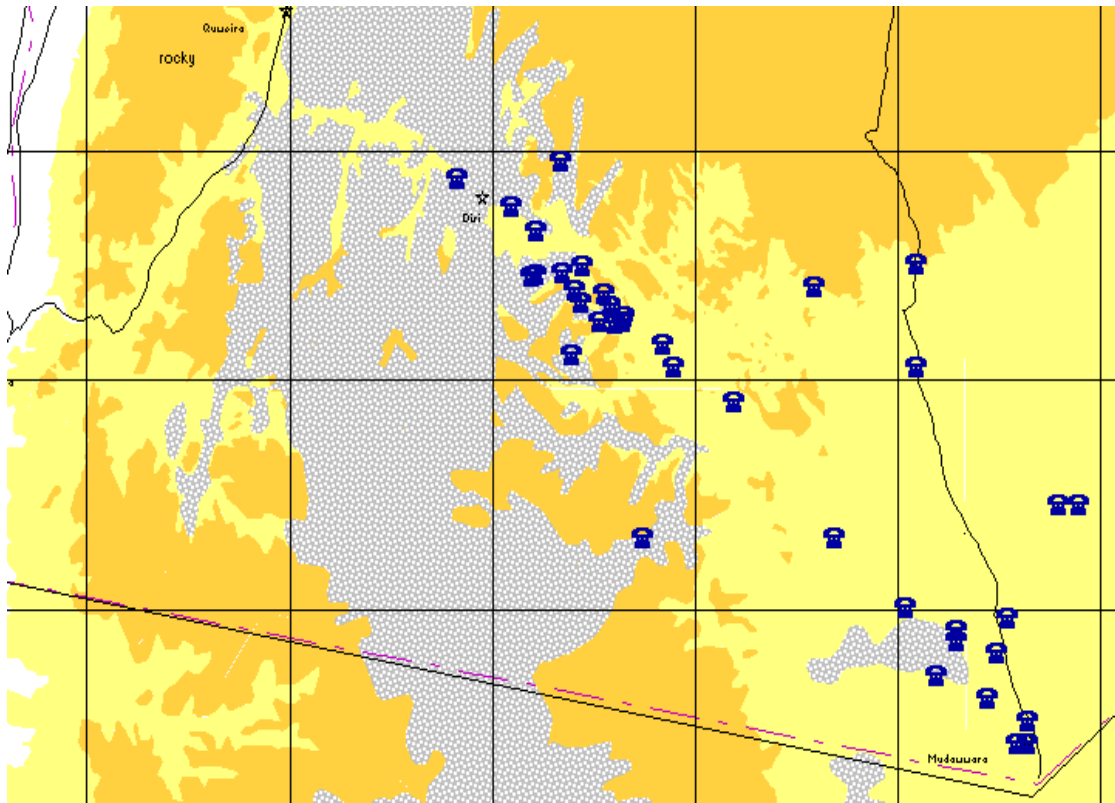


FIG. 2. Location of sampled wells in the study area.

Topography and climate

In general, the climate from west to east is transitional from Mediterranean climate to that of hot dry desert. The climate of Jordan is characterized as arid to semi-arid with average rainfall rangy from 500 mm/y over the western highs, to less than 50 mm/y in desert areas. The average rainfall in the study area is about 65 mm/y.

The topography is determined by the Al Quwayra Fault, which has an easterly downthrown. The crystalline basement east of the fault has been downthrown and does not crop out.

The lowest elevation in the study area is 560 meters above sea level (masl) and the maximum elevation is 1546 m asl on Jabal al Naqab.

Geology and Structure

The lithology of the basin under study is illustrated in Table 1.

The main formations in the area are the Cambro-Ordovician sandstone of the Ram Group (Table 2).

Table 1: Lithology of the basin under study

ERA	PERIOD	GROUP	FORMATION	SYMBOL	AQUIFER	AQUICLUDE
	Lower Cretaceous	Kurnub	Subeihi	K	Sandstone Dolomite	
			Aarada	K	Sandstone Dolomite	
	Jurassic Trias	Zerqa	Azab	Z	Sandstone Dolomite	
			Main	Z	Sandstone Dolomite	
Paleozoic	Permian to Silurian	Khreim		Kh	Sdst.Siltst.	Shale
	Ordovician Cambrian	Ram	Disi	D	Sdst., Quartzite	
Pre Cambrian		Basement Complex		G		Granite

In Jordan the Precambrian crystalline granitic basement exposed east and northeast of Aqaba, is overlain by a thick sequence of Paleozoic fluvial, littoral, and estuarine and later fully marine silicate sediment extending east into Jordan, and southeast into Saudi Arabia. The Ram group, which forms the major aquifer in southern Jordan, is the lower part of this thick sequence [2] and presented in Table 2.

Table 2. Lithology and thickness of the different formations [1][2]

Formation Saudi Arabia	Formation Jordan	Lithology	Thickness
Tabuk	Khreim (the confining strata to the Ram group)	Paleozoic rock, varicolored, marine fine grained, interbedded shale and sandstone.	650 m
Upper Saq	Sahm (Ram group)	Brownish, hard, close jointed, tabular bedded sandstone.	250 m
	Disi (Ram group)	Moderately cemented to unconsolidated, thick bedded, quartzitic sandstone.	350 m
Saq Wajid (south)	Ishrin (Ram group)	Medium grained brown sandstone, moderately cemented, quartz, lower feldspathic bands, fractured at outcrop	350 m
	Saleb (Ram group)	Yellow –brown fine-medium grained, poorly sorted, well bedded feldspathic sandstone, basal arkosic pebbly conglomerate	60 m

Sources and Areas of Recharge

The aquifer is believed to contain groundwater derived from ancient recharge i.e. from 7,000 to more than 30,000 years old.

The area has experienced a number of climatic fluctuations in the Pleistocene and Holocene. Table 3 illustrates the pluvial phases that prevailed in the region and their isotopic signatures.

Table 3: Pluvial phases that prevailed in the region [3]

Period	Age before present (ka)	Deuterium excess	Slope of regression line
Pleistocene Period	70-11	0.5-10	
Early Pleistocene Period	70-40	0.5 - 6	9.3
Middle Pleistocene Period	32-22	8- 10	8.1
Late Pleistocene Period	22-11	No groundwater recharge	
Holocene	7-4.5	13-18	6.4
Present precipitation	Recent	≈22	6.2

Ground Water Flow Pattern

The ground water flow pattern of the study area is shown in Figure 3.

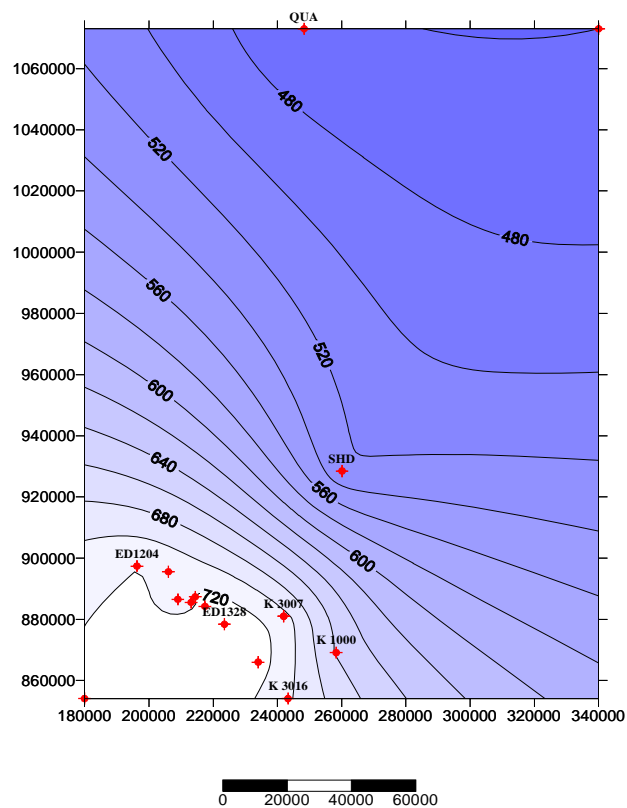


FIG. 3. Ground water flow pattern in the study area.

The regional flow pattern for the Ram formation was established starting from Disi area in the south to the drainage area in the Dead Sea. The aquifer changes from unconfined beneath the outcrop, to confined beneath the east shale cover of the Khraim sandstone group.

Sample Collection and Analysis

During the period 2001 to 2003 about 45 groundwater samples were collected from different wells representing Ram and Khraim formations in the study area. These samples were analyzed for hydrochemical and isotopic parameters at the Laboratories and Quality Department of the Water Authority of Jordan (WAJ). Stable isotopes were measured using a Finnigan Mat Delta-E ratio mass spectrometer. Eight water samples representing the aquifer under investigation were collected in 2003 for advanced isotopic parameters (Sr & B stable isotopes). Major and trace elements were analyzed at USGS Strontium isotopes were analyzed through Dr. Avner Vengosh in the US Geological Survey (USGS) laboratories using MAT-261 solid-source mass spectrometer. Boron isotopes were measured by negative thermal ionization mass spectrometry technique [4]. Isotope ratios of boron are reported as $\delta^{11}\text{B}$ values, where

$$\delta^{11}\text{B} \text{ ‰} = [((^{11}\text{B}/^{10}\text{B})_{\text{sample}} / (^{11}\text{B}/^{10}\text{B})_{\text{NBS951}}) - 1] * 1000$$

This part of the study is mainly concentrated on the interpretation of the obtained analytical results of these eight wells as these wells are representing the different water types and ground water bodies in the study area.

Results and Discussion

Hydrochemistry

The analytical results of water samples collected from the eight wells within the study area are shown in Table 4. Seven samples represent water from the Ordovician to Cambrian sandstone formation which is locally known as the Ram formation. The water wells ED1302, ED3028 and SS4 are located in the unconfined part of the Ram aquifer in Disi area, while the water wells BH11S1-Ram, K3028, and Wafa-5 are located in the confined part of the aquifer in Mudawara area. The Qatrana well taps the Ram formation in the midway along the ground water flow line that terminates at the discharge area in the Jordan valley. One sample is taken from BH11 (Khraim well) - taps the overlying Permian Silurian sandstone formation. This formation is locally known as the “Khraim” and consists of sandstone with silt.

Table 4. Analytical results in mg/L (pH in pH units)

Source	pH	TDS	Ca	Mg	Na	K	Cl	SO4	HCO3	NO3
SS4	3.1	232.9	40.14	7.2	18.4	1.4	35.1	17.7	0	12.5
Qatr.	6.5	524.6	58.4	22.5	71	11	187	69.2	104.1	0.1
BH11 S1 (Ram)	7.7	270.0	39.8	6.2	29.7	1.4	53.2	31.1	102.9	5.3
BH11 Khraim	7.8	2549.9	21.4	20.9	784	43.4	1136	249	293.1	0.2
K3023	7.5	247.8	34.6	6.2	27	1.3	49.1	28.1	96.2	5.0
Wafa 5	7.6	237.2	35.9	6.1	20.2	1.2	35.7	19.2	114.1	4.5
ED 1302	7.7	644.8	82.9	16	83.9	1.8	106	221.2	120	11.9
ED 3028	7.8	242.7	36.3	6.1	19.4	1.2	33.2	17.7	117.4	11.1

The ground water of the Ram formation in both Disi and Mudawara areas is of good quality with low dissolved solids content (200 to 300 mg/L) with the exception of well ED1302. In this case, the total

dissolved solids (TDS) increased from 236 mg/L in 1994 to 645 mg/L in 2004. One of the study objectives is to investigate the source(s) and origin(s) of the salinity of this well.

At the unconfined part of the aquifer where some groundwater recharge occurs, groundwater is fresh and dissolved oxygen is about 6 mg/L and nitrate is around 10 mg/L. As water moves towards the confined part of the aquifer at Mudawara area, the water salinity slightly increases and the dissolved oxygen becomes 4 to 5 mg/L. At further distances along the groundwater flow line, the TDS increases and DO decreases. A Qatrana site, the TDS reaches 525 mg/L and groundwater turns to reducing water as shown by the absence of dissolved oxygen (negative Eh). The upper confining Khraim formation hosts saline water with TDS ranging from 900 to 9,000 mg/l [5].

For the purpose of this study, four ground water groups can be distinguished according to salinity and well locations. These water groups are shown in Table 5.

Table 5. Ground water groups in the study area

Water Groups	TDS (mg/L)	Well Names
Group I	232 - 269	ED3028, SS4, Wafa 5, K3028 & BH11Ram
Group II	645	ED1302
Group III	525	Qatrana
Group IV	2250	BH11Khraim

Group I: Includes samples representing the fresh water of the Ram formation at both, unconfined part of the aquifer in the Disi area and the adjacent confined part in Mudawara area. This group represents fresh groundwater of the Ram formation. The TDS is low, ranging from 230 to 270 mg/L. It is characterized by intermediate, close to marine Na/Cl ratio (0.88), $\text{Br/Cl} = 1.2 \times 10^{-3}$ and $\text{SO}_4/\text{Cl} = 0.2$. The slight increase of salinity along the ground water flow line is the result of normal interaction between water and the aquifer host rocks during groundwater flow.

Group II: This group is represented by ED1302 well, which is located in the unconfined part of the aquifer. The TDS of the water increased from 325 mg/L in 1980, to 645 mg/L in 2002. The well is located in the Mnesheer village. The increase of water salinity when related to the presence of 10 mg/L of nitrate might lead to the belief that the well was affected by an anthropogenic source of contamination. This water type is characterized by high Na/Cl ratio (1.22), low Br/Cl ratio (0.7×10^{-3}), and a very high SO_4/Cl ratio (0.77) ratio. Such ionic ratios enforces the hypothesis of dissolution of evaporites, mainly gypsum dissolution rather than an anthropogenic effect.

Group III: This group represents the groundwater of the Ram formation with long residence time, and represented by Qatrana well in central Jordan. This well is lying on the groundwater flow line closer to the discharge area in the Dead Sea. This water has intermediate salinity range with total dissolved solids of 625 mg/L. The ionic ratios of this type of water are characterized by a low Na/Cl ratio (0.59), low Br/Cl ratio (1.1×10^{-3}), low SO_4/Cl ratio (0.14), and very high Ca/ SO_4 ratio (2). These ratios reflect the natural dissolution process of the matrix minerals, such as halite and dolomite, as a result of long groundwater residence time in the aquifer.

Group IV: This group represents the saline water of the Khraim formation (sample BH11-Khraim) with TDS reaching 2,550 mg/L. The Khraim formation (the confining layer to the Ram group) holds saline water of marine origin with TDS ranging of 900 to 9000 mg/L [3][5]. This type of water has a high Na/Cl ratio (1.06), low Br/Cl ratio (0.5×10^{-3}), very low SO_4/Cl ratio (0.08), and very low Ca/Cl ratio (0.02). The depleted stable isotopic content of this water ($\delta^{18}\text{O} = -6.58\text{‰}$ and $\delta\text{D} = -44.5\text{‰}$) with deuterium excess around 8‰ indicates that this water has a very old origin and it was not affected by evaporation or dilution with evaporated brines. The high Na/Cl ratio together with low Br/Cl and SO_4/Cl ratios suggests that the water gained its salinity from halite dissolution.

The Piper diagram (Figure 4) illustrates the types of water in the both the Ram and the Khraim formations. Khraim formation water is represented by wells 1 & 8 in the Piper diagram. This type of water is shifted towards the NaCl type as compared to the cluster of the Ram group waters. Water of wells in the confined and unconfined parts of the aquifer at Disi and Modawara areas shows calcium bicarbonate type.

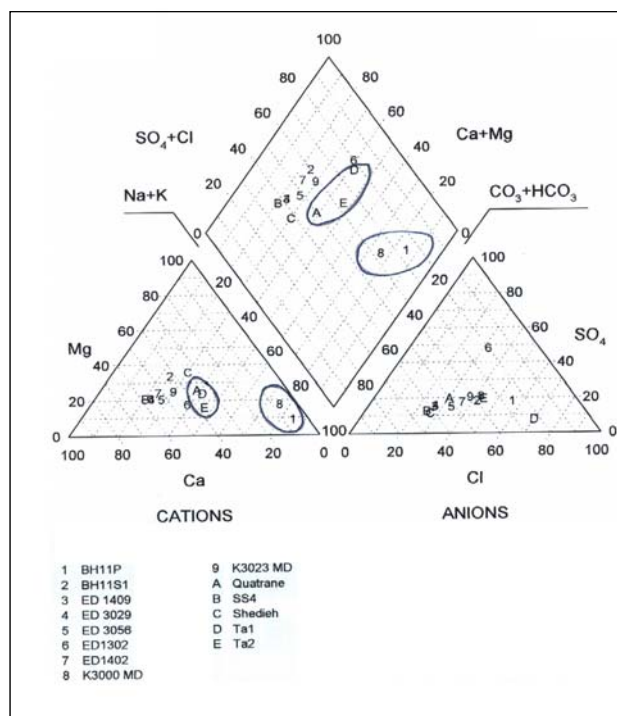


FIG. 4. Piper diagram of waters in the study area.

Previous work at this area showed that water is stable in the $\text{Fe}(\text{OH})_3$ field with pH range from 6 - 8 and Eh +0.1 to +0.5, indicating high corrosivity of this water, and therefore the presence of potential well encrustation and the possibility of corrosion [1].

Isotope indicators of ground water origin and recharge regime

Carbon-14 (^{14}C) Tritium (T) and stable isotopes of Oxygen-18 ($\text{O}-18$) and Deuterium (D) were used to provide information about the water origin, residence time, and its recharge history. The isotope results of samples collected from the water wells are shown in Table 6.

Table 6. Analytical results of stable and radioactive environmental isotopes

Source	Tritium	$\delta^{18}\text{O}$	$\delta^2\text{H}$	d-excess	^{14}C (pMC)	$\delta^{13}\text{C}$
SS4	<0.7	-6.20	-39.1	10.5		
Qatr	<0.8	-7.27	-50.3	7.9	<1.45	-3.56
BH11 S1 (Ram)	<0.7	-5.74	-33.2	12.7	4.49	-5.10
BH11 (Khraim)	<0.7	-6.58	-44.5	8.1	<1.73	-8.45
K3023	<1	-5.70	-33.8	11.8	<5.46	-5.79
Wafa 5	<1	-6.54	-38.0	14.3		
ED 1302	<0.9	-6.26	-38.6	11.5	34.4	-5.32
ED 3028	<1	-6.66	-40.2	13.1	26.3	-5.56

The age of water can be determined using the radioactive isotopes according the law of radioactive decay:

$$A_t = A_0 * e^{-\lambda t}$$

Where A_t is the measured activity at time t , A_0 is the initial activity, $\lambda = \ln 2 / T_{1/2}$ is the decay constant t of the nuclide, and t is the age.

In all sampled wells, the tritium content is below the detection limit of 1 Tritium Unit (TU). This indicates that the ground water among the whole aquifer is older than 50 years.

For time periods up to 30,000 years, C-14 was used to determinate the ground water age. The ^{14}C initial activity at recharge area (A_0) was taken as 61 Percent Modern Carbon (pMC) to compensate for carbonate dissolution [3]. C-14 results of the unconfined part of the aquifer vary from 26 to 33 pMC. This indicates that this part of the aquifer either receives a component of recent recharge, or the last aquifer recharge happened during the past 5 to 10 thousand years (late Pleistocene- early Holocene). In both cases, this means that this part of the aquifer has the most recent water. In the confined part of the aquifer ^{14}C was not detected, indicating water age is more than 30,000 years.

Stable isotope contents of all water groups range between -5.7‰ and -7.2‰ for oxygen-18 and between -33‰ to -50.3‰ for deuterium. The deuterium excess vary between 8 and 14.3‰ .

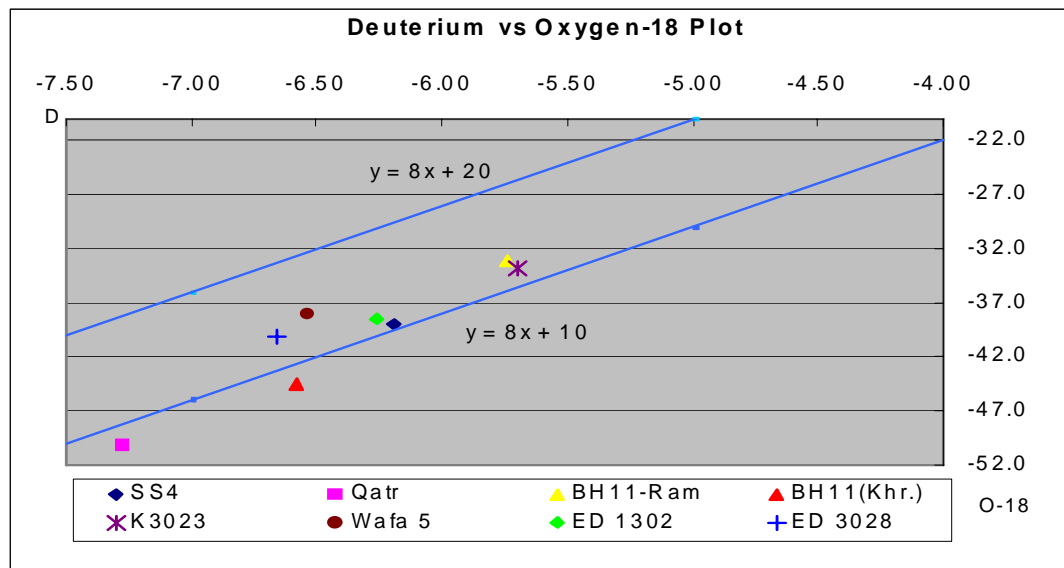


FIG. 5. Deuterium - Oxygen 18 relationship.

The relationship between deuterium and ^{18}O of all water groups is shown in Figure 5. All samples fall close to the Global Meteoric Water Line (GMWL), which reflect the paleo origin of the aquifer water. The depleted stable isotope contents with low d-excess around 10‰ , indicates that the main aquifer recharge most likely took place during the middle Pleistocene pluvial period.

Along the ground water flow line, the stable isotope content became more depleted with remarkable decrease in deuterium excess. Qatrana well (group III), which most likely fall on the ground water flow line to the discharge area, has a very depleted isotopic content. These are of -7.29‰ for O-18 and -50.5‰ for deuterium and 8.1 of the deuterium excess. This depletion of the stable isotope content, and the associated very low deuterium excess, and the absence of ^{14}C is supporting the hypothesis that

this water was recharged around 60 to 70 thousand years ago, probably during the Early Pleistocene pluvial period. These results are supported by conventional hydrological calculations of the ground water flow pattern. The initial estimation of regional flow velocity of the water based on hydrological parameters (average $K=1\text{m/d}$ and effective porosity n_e of 0.1) and following Darcy's law in calculating Darcy's velocity ($q = (K \cdot i) / n_e$) showed a range of q values of 0.015 to 0.03 meters per day with an average residence time of 55,000 years until Qatrana well and about 68,000 years until discharge area in Jordan valley [6].

ED1302 groundwater sample, which represents group II of the increased salinity, has also depleted isotope content, with deuterium excess of 10.5‰. The depletion of stable isotopes in conjunction with deuterium excess around 10‰ means that this water was neither effected by evaporation nor mixed with evaporated water. Therefore, the salinity of this water group might be the result of dissolution of matrix minerals, but not as a result of mixing with surface waters such as agriculture return flows or sewage effluents.

Strontium and boron isotopes in aquifer investigation

Strontium (Sr) and Boron (B) isotopes have been used to investigate the source of salinity of groundwater, as well as to apply as source of dating of groundwater along the ground water flow path.

Boron in ground water might be derived from leaching of rocks, infiltration of meteoric salts, mixing with other boron-rich waters, and contamination by anthropogenic sources.

Boron has two naturally occurring stable isotopes, B-10 (80.1%) and B-11 (19.9%). The mass difference between the two isotopes results in a wide range of Delta Boron-11 ($\delta^{11}\text{B}$) values in natural waters, ranging from -16 to +59‰ [7].

The isotopic ratios of boron have been used to trace the origin of water masses, to track the evolution of brines, to determine the origin of evaporates, and to examine hydrothermal flow systems [8].

The analytical results of boron and strontium isotopes are shown in Table 7.

Table 7. Analytical results of boron and strontium isotopes

Source	Cl (mg/L)	B (mg/L)	Sr (mg/L)	Br (mg/L)	$^{11}\text{B}/^{10}\text{B}$	$^{87}\text{S}/^{86}\text{S}$
SS4	3 .1	0.065	0.33	0	3 .2	0.7084
Qat .	18	0.10	0.77	0.4	4 .2	0.7091
BH11 S1 (Ram)	5 .2	0.034	0.21	0.1	4 .9	0.7084
BH11 Khraim	113	0.342	0.3	1.3	5 .6	0.711
K3023	4 .1	0.038	0.18	0.1	4 .4	0.7086
Wafa 5	3 .7	0.032	0.17	0.1	4 .4	0.708
ED 1302	10	0.318	0.66	0.1	5 .6	0.7082
ED 3028	3 .2	0.043	0.23	0.0	4 .9	0.708

The $\delta^{11}\text{B}$ values of fresh water of Ram formation (water group I) are ranging between +34 and +45‰. The highest boron concentrations and highest $\delta^{11}\text{B}$ values are obtained for samples ED1302 and BH11-Khraim, which are representing water groups II and IV respectively. The $\delta^{11}\text{B}$ average value is around +57‰. This value is much higher than the reported $\delta^{11}\text{B}$ for seawater, which is around 39 to 40‰ [7].

As shown in Figure 6, there is a linear relationship observed between the boron concentration and groundwater salinity. From boron versus chloride plot (Figure 6a) it is observed that boron concentration is directly proportional to the chloride concentration. The exception to that trend is sample ED1320 (Figure 6b) representing water group II, which has high boron content compared to its

chloride content, associated with high sulfate concentration. The additional boron source might have come either from aquifer boron-containing minerals, or from an anthropogenic source of contamination, such as mixing with wastewater effluents.

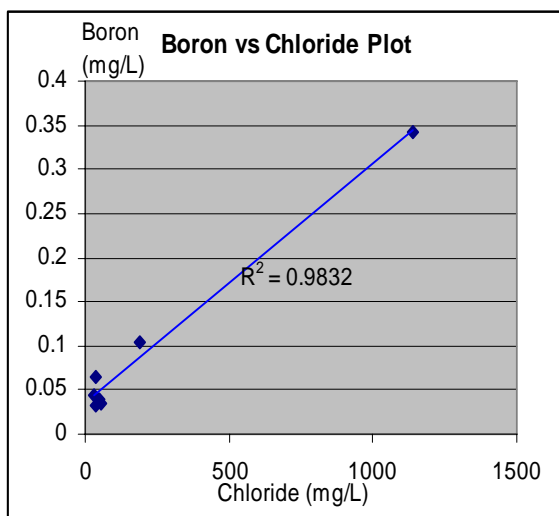


FIG. 6a. Boron versus chloride without ED1302.

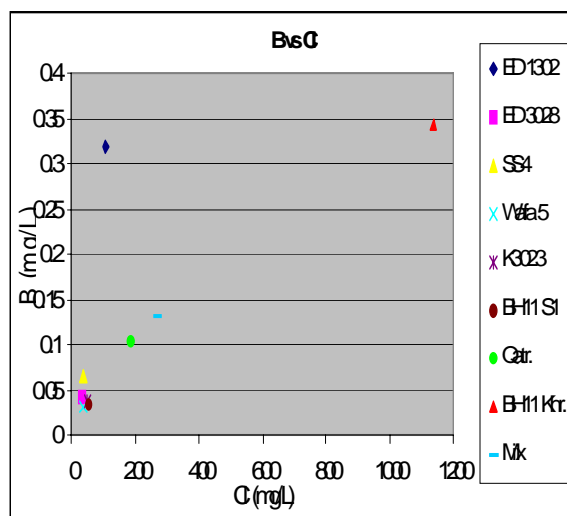


FIG. 6b. Boron versus chloride for all samples.

Figure 7 shows the relationship between $\delta^{11}\text{B}$ values and the chloride concentration of collected water samples. There is no clear correlation observed between $\delta^{11}\text{B}$ and the chloride content of all water groups, while $\delta^{11}\text{B}$ values for ground waters within Ram sandstone formation mostly remains constant along the ground water flow line (samples of groups I and III in Figure 7), with some deviations in $\delta^{11}\text{B}$ values observed for samples ED1302 and SS4.

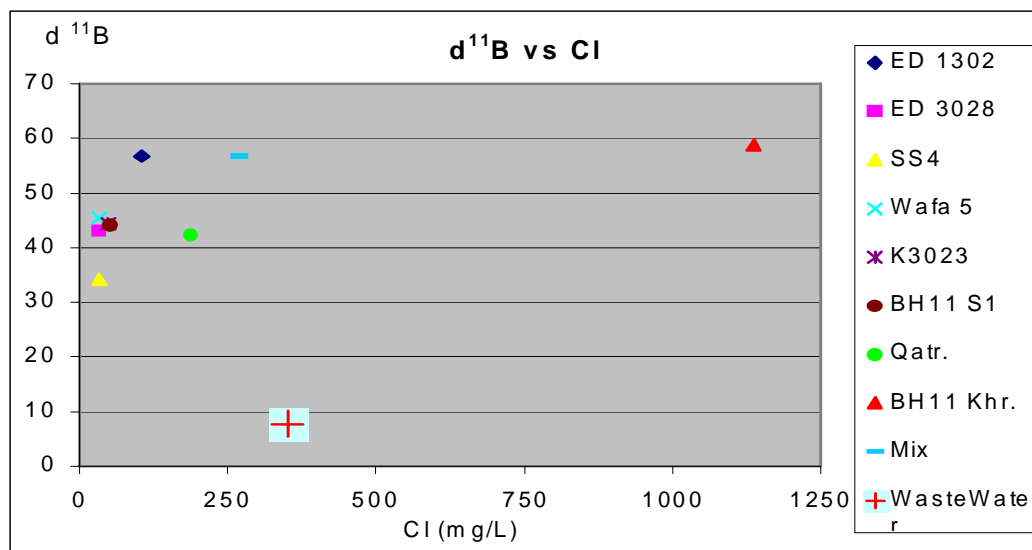


FIG. 7. The relation between $\delta^{11}\text{B}$ and the chloride content.

These wells are located in the unconfined part of the aquifer, and the $\delta^{11}\text{B}$ variations can be explained as a result of enhanced dissolution processes of different minerals within the matrix as a result of the variation of the water table and the associated weathering of the matrix. Using $\delta^{11}\text{B}$ versus chloride plot (Figure 7); one can distinguish between water salinities of different origins. Salinities originated from anthropogenic sources of contamination. Domestic wastewater has very low $\delta^{11}\text{B}$ values, ranging from 0 and 10‰ [9].

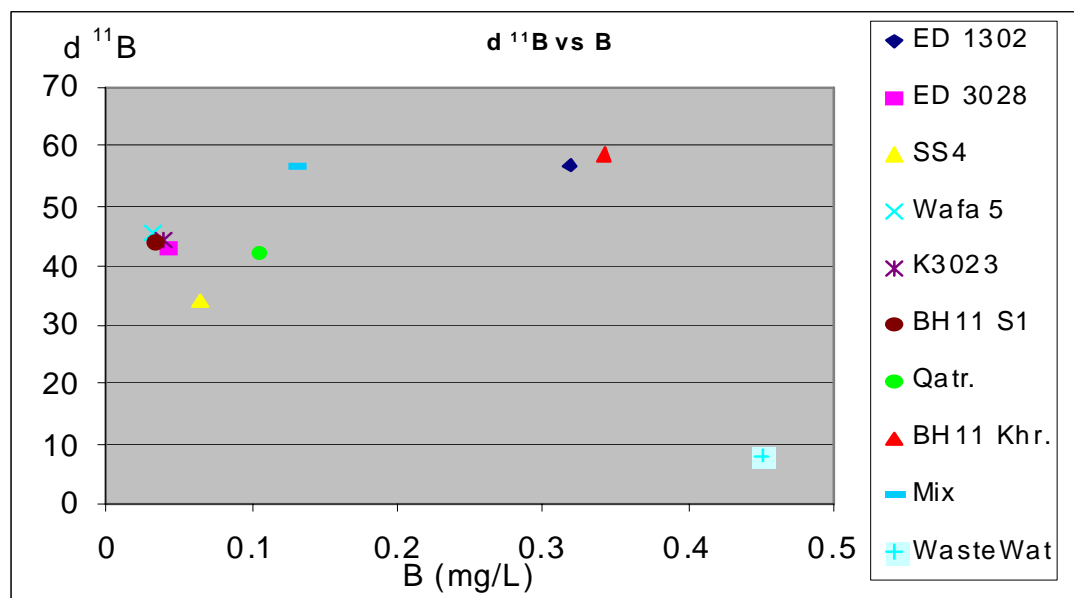


FIG. 8. Relation between $\delta^{11}\text{B}$ and boron concentration.

This type of water is plotted in the lower side of the graph, while waters with natural origin salinities as for water groups II and IV, are plotted in the upper part of the graph. Consequently, we can conclude that the source of salinity for water group II (sample ED1302) is not anthropogenic, but it can be related to the dissolution of gypsum and evaporites from the aquifer matrix during the water rock interaction. Other indicator, which can be used to distinguish salinities of different origins, is the relation between $\delta^{11}\text{B}$ values and the boron concentration, as shown in Figure 8. Water groups II and IV (sample ED1302 and sample BH11-Khram) are clustered in the upper right corner of the graph, while domestic wastewaters with $\delta^{11}\text{B}$ less than 10‰ are clustered at the lower part of the figure. Salinities of such origin can be easily distinguished, from salining induced by gypsum or halite dissolution (samples BH11Khr and ED1302). It is also possible to distinguished salinities coming from dissolution of other aquifer minerals like carbonates represented by the rest of the samples in Figure 8.

Strontium isotopes ratio ($^{87}\text{Sr}/^{86}\text{Sr}$) have proven to be a useful indicator for water-rock interaction, a good indicator for salinity origin(s) and a tracer for ground water movement. Strontium is divalent cation that readily substitutes for calcium in carbonates, sulfates, feldspars, and other rock-forming minerals.

Rubidium-87, decays with half-life of 4,88 billion years to strontium-87. The ratio of strontium-87 to the stable isotope of strontium-86 increases over time as more rubidium-87 turns to strontium-87. Rubidium has a larger atomic diameter than strontium, so rubidium does not fit into the crystal structure of most minerals. Therefore, some of the minerals in the rock have higher rubidium/strontium ratio than others. The older rocks such as the granites, which have higher initial

concentrations of rubidium-87, have higher $^{87}\text{Sr}/^{86}\text{Sr}$ ratios than younger volcanic rocks derived from the earth's mantle. Sedimentary rocks generally have intermediate values. The late Cenozoic marine sediments experienced a dramatic increase in ^{87}Sr due to climate cooling and increased rates of continental weathering of glaciations. This rapid and steady increase through the Pliocene and Pleistocene provides a high-resolution dating tool for sedimentary rocks.

Modern seawater has a $^{87}\text{Sr}/^{86}\text{Sr}$ ratio = 0.709, which is intermediate between ^{87}Sr depleted value for ocean basalts with $^{87}\text{Sr}/^{86}\text{Sr} \approx 0.703$ and the ^{87}Sr enriched values from continental rocks with $^{87}\text{Sr}/^{86}\text{Sr} = 0.710$ to 0.740.

The analytical results of strontium isotopes are shown in Table 7. The relationship between the strontium concentration and the water salinity for both Ram and Khraim formations is shown in Figures 9 and 10. Within Ram formation (water groups I, II, and III), strontium concentration generally increases with increasing TDS contents, while there is no such relationship between Sr concentration and water salinity when comparing waters of different formations. Saline Khraim formation water (water group IV) has low Sr concentration compared to Ram formation fresh water.

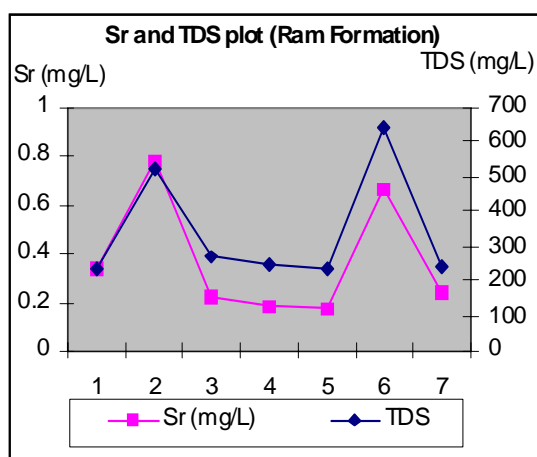


FIG. 9. Sr and TDS plot (Ram).

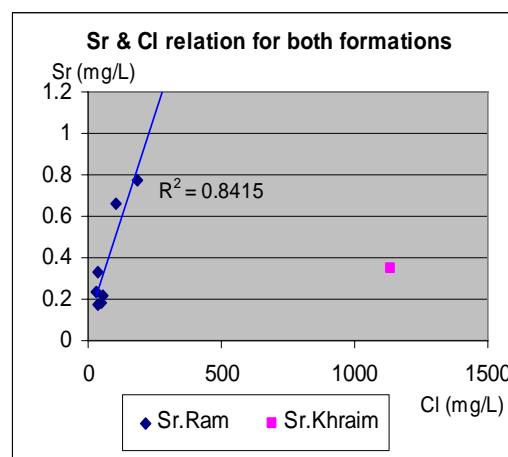


FIG. 10. Relation between Sr and Cl.

$^{87}\text{Sr}/^{86}\text{Sr}$ ratio in the Precambrian Ram sandstone formation varies between 0.7083 and 0.7092, while the $^{87}\text{Sr}/^{86}\text{Sr}$ ratio of Khraim formation is much higher (0.7114), which is even higher than the modern seawater ratio.

There is no clear correlation observed between $^{87}\text{Sr}/^{86}\text{Sr}$ ratio and strontium concentration (Figure 12), while $^{87}\text{Sr}/^{86}\text{Sr}$ ratio versus chloride concentration shows a linear correlation for all water types from both Ram and Khraim formations (Figure 11).

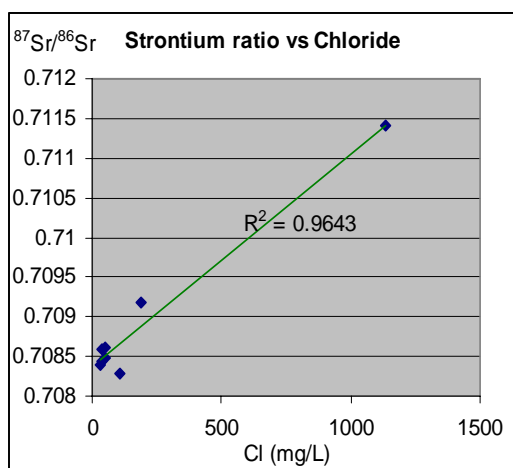


FIG. 11. Relation between the strontium isotope ratio and the chloride content

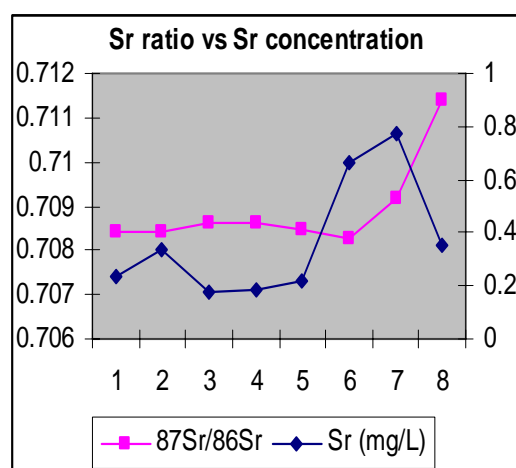


FIG. 12. Relation ship between $^{87}\text{Sr}/^{86}\text{Sr}$ ratio and the Sr concentration

The increase of the $^{87}\text{Sr}/^{86}\text{Sr}$ ratio with increasing chloride concentration could be mainly related to the increase of potassium (K) along the ground water flow line (Figures 13 and 14), as the abundance of ^{87}Sr is directly linked to the geochemistry of potassium, for which rubidium (Rb) readily substitutes. K-rich rocks will have high ^{87}Rb and ^{87}Sr contents, and this is reflected in the $^{87}\text{Sr}/^{86}\text{Sr}$ ratio of water with which they have equilibrated. The increase of $^{87}\text{Sr}/^{86}\text{Sr}$ with increasing chloride concentration along the groundwater flow line can be used as a good tool for investigating groundwater movement and groundwater residence time.

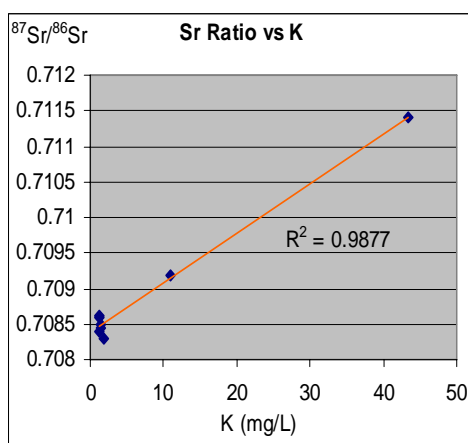


FIG. 13: Relation between the Sr isotope ratio and the K content

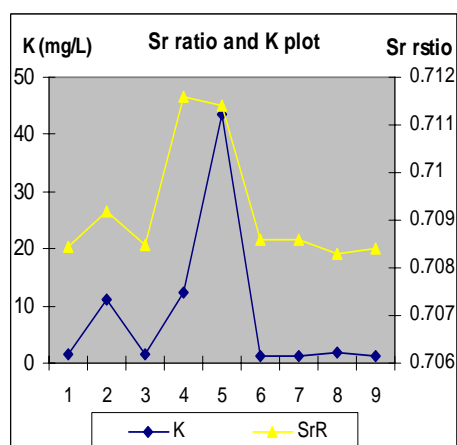


FIG. 14: Sr isotope ratio and K plot in the study area

The relationship between $\delta^{11}\text{B}$ and $^{87}\text{Sr}/^{86}\text{Sr}$ ratio for all water groups in the study area is shown in Figure 15. Fresh ground waters are clustered mainly in one group and can be clearly distinguished from other waters like wastewater and saline water of Khraim formation. Groundwater salinities gained by high residence time along the groundwater flow line group III can be distinguished by the increased $^{87}\text{Sr}/^{86}\text{Sr}$ ratio with constant $\delta^{11}\text{B}$ values. Groundwater salinities gained by dissolution of gypsum such as group II, can be distinguished from other sources of salinity and characterized by high $\delta^{11}\text{B}$ values with low $^{87}\text{Sr}/^{86}\text{Sr}$ ratios.

From the plot of $\delta^{11}\text{B}$ versus $^{87}\text{Sr}/^{86}\text{Sr}$ ratio (Figure 15), it is possible to distinguish between the clusters of each water type. Wastewater effluents are clustered at the bottom of the figure, while freshwaters are clustered in the middle to the left and moves to the right direction as groundwater moves along its flow line. Groundwater with increased salinity, due to gypsum dissolution or/ and dissolution of other boron -containing minerals, is shifted to the upper part of the figure to the region of high strontium isotopic ratios.

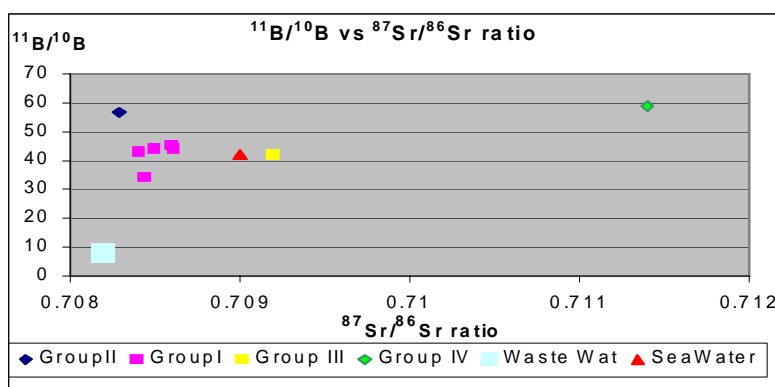


FIG. 15. Relationship between $\delta^{11}\text{B}$ and the $^{87}\text{Sr}/^{86}\text{Sr}$ ratio.

The saline water of Khraim formation of marine origin is different from all other water types and it is characterized by a very high (0.7114) $^{87}\text{Sr}/^{86}\text{Sr}$ ratio. Thus, the relationship between strontium and boron isotopes proven to be useful as a tool to discriminate between water salinities originating from anthropogenic sources as sewage effluents, and salinities derived from the dissolution of the aquifer matrix along the ground water flow path.

Conclusions

1. Strontium and boron isotopes can be used as useful tool is in distinguishing the different sources and origins of groundwater salinities, as well as for studying water origin and water dynamics within the aquifer.
2. The study of the Cambro-Ordovician sandstone aquifer in the South of Jordan shows that $^{87}\text{Sr}/^{86}\text{Sr}$ ratio steadily increase along the groundwater flow line while $\delta^{11}\text{B}$ values remains in the same range within the same formation. Waters of saline formations have remarkable increase in $^{87}\text{Sr}/^{86}\text{Sr}$ ratio with generally medium to high $\delta^{11}\text{B}$ values, depending on the type of dissolved minerals.
3. Groundwater salinities of anthropogenic origins is distinguished from other natural sources of contamination by its low $\delta^{11}\text{B}$ values and very low $^{87}\text{Sr}/^{86}\text{Sr}$ ratios.
4. Stable isotopes indicated that the salinity observed in ED1302 is not due to mixing with wastewater effluents but due to water rock interaction. This was further confirmed by the boron and strontium isotopes.

5. $^{87}\text{Sr}/^{86}\text{Sr}$ ratios increases along the groundwater flow line within the Ram formation. This relation can be used as a valuable tool in studying groundwater residence time and water dynamics within the hydro-geological formation.

ACKNOWLEDGEMENTS

The authors wish to thank Dr. Cheikh Gaye at Isotope Hydrology Section, IAEA, Vienna for his efforts in making a successful outcomes of this research project. The authors are thankful to Dr. Avner Vengosh for his fruitful cooperation and support in sample analysis. Special thanks to the Ministry of Water and Irrigation and Water Authority of Jordan management for providing all the logistic requirements to carry out the mission. Also thanked the director and staff of WAJ Laboratory in Jordan for performing the isotopic and chemical analyses.

REFERENCES

- [1] LLOYD, J.W. and PIM, R.H., The Hydrology and Groundwater Resources Development of the Campro-Ordovician Sandstone Aquifer in Saudi Arabia and Jordan. *Journal of Hydrology*. (1990) Vol.121, 1-20.
- [2] BUCKLE, D.J.E., Borehole Geophysical Investigation and Hydraulic Parameter Determination of the Sandstone Aquifer System in the Southern Desert of Jordan, Submitted in Partial Fulfillment of M.Sc. in Hydrogeology at UCL (September 1993).
- [3] BAJJALI, W., ABU-JABER, N., Climatological Signals of the Paleo-groundwater in Jordan. *Journal of Hydrology* 243. (2001) 133-147.
- [4] VENGOSH, A., CHIVAS, R., and McCULLOCH, M.T., Direct Determination of Boron and Chlorine Isotopes in Geological Materials by Negative Thermal-Ionisation mass spectrometry. *Chem. Geol., Isotope Geosci. Sec.*, (1989) 333- 343.
- [5] EL-NASER H., GEDEON, R., Hydrochemistry and Isotopic Composition of the Nubian Sandstone Aquifers of Disi-Mudawwara Area, South Jordan. Proceedings of the final co-ordination meeting of a regional technical co-operation project held in Ankara, Turkey, 21-25 November 1994. 61.
- [6] KILANI S. Investigation of the Present Recharge Rate and Recharge Origins in the Disi Sandstone Aquifer in Southern Jordan. 6th Arab Conference on the Peaceful Uses of Atomic Energy, Cairo, 2002.
- [7] VENGOSH, A., HEUMANN K.G., JURASKE S., and KASHER R., Boron Isotope Application for Tracing Sources of Contamination in Groundwater. *Env.Sci and Technology* (1994).
- [8] USGS Web Site: http://wwwrcamnl.wr.usgs.gov/isoig/period/b_iig.html
- [9] VENGOSH, A., KOLODNY Y., and SPIVACK A. J. (1989). Ground water Pollution Determined by Boron Isotopes Systematics. IAEA CRP TECDOC-1046, 1998. Vienna.

Environmental Isotope-aided study for elucidating groundwater salinization on Cheju Island, Korea

Sung-Jun Song^a, Ki-Won Koh^b, Won-Bae Park^c, Avner Vengosh^d, Yoon-Suk Park^b

^a Applied Radiological Science Research Institute, Cheju National University, Jeju, Korea, Republic of

^b Jeju Provincial Water Resources Management Office, Jeju, Korea, Republic of

^c Jeju Development Institute, Jeju, Korea, Republic of

^d Department of Geological and Environmental Sciences, Ben Gurion University, Beer Sheva, Israel, State of

Abstract. The salinization of groundwater in the eastern part of Jeju-do was not due to the over-exploitation of groundwater resources or the dissolution of salts in the strata but due to the simple mixing with the diffused seawater resulted from the hydrogeological structure. It is considered that the mixing process with the sea water does not happen in a short period but in a certain period enough to reach an equilibrium of Na-Ca ion exchange in the aquifer. The thin layer of fresh water in the aquifer was also attributed to the natural hydrogeological structure. The mixing ratio of the fresh water with the sea water range from 0.03 to 2.37 %, having higher values in the wells near seashore. Especially, the analysis of $\delta^{18}\text{O}$, δD , $\delta^{11}\text{B}$, $^{87}\text{Sr}/^{86}\text{Sr}$, $\delta^{34}\text{S}_{\text{SO}_4}$ and $\delta^{18}\text{O}_{\text{SO}_4}$ gave the direct answer on the cause of the salinization of groundwater in the study area. $\delta^{18}\text{O}$ and δD showed the mixing of fresh ground water with sea water. $\delta^{11}\text{B}$ values explain the origin of saline water from the sea water. $\delta^{34}\text{S}_{\text{SO}_4}$ and $\delta^{18}\text{O}_{\text{SO}_4}$ gave the evidence of intrusion of modern sea water into the groundwater. In addition, the value of $^{87}\text{Sr}/^{86}\text{Sr}$ indicates that the salinization was not from the dissolution of rock salts but from the mixing with seawater.

1. Introduction

It is expected that the water shortage with the increase of population and the development of industry will be more serious worldwide and Korea will be one of the water-lacking countries in the 21 century. The efforts of securing water resources may be important but the conservation for the sustainable use of the secured water resources to the future be more essential. In particular, since it is very difficult and costly to remove the contaminants once groundwater is contaminated, more scientific and systematic efforts to the prevention of groundwater contamination are required. In fact, through chemical analysis we can know the degree of contamination but can not discriminate the origin. Therefore, the use of isotope technique is indispensable to delineating the origin of contamination. In the recent years the additional isotope signatures, ^{11}B and $^{87}\text{Sr}/^{86}\text{Sr}$ besides ^2H , ^{18}O , ^{15}N and ^{34}S are being actively used for the more precise discrimination of the composite contamination of groundwater [2][3][9][17][21][22][23][28][30][32].

Jeju in Korea is a volcanic island and the water supply to the island relies on groundwater. Until now many research progresses on the hydrogeological characteristics, the occurrence and geochemical properties of Jeju groundwater, etc. have been made to some extent but more detailed studies on flow paths, the salinization process and the contamination origin are still needed. In particular, in the eastern part of Jeju the salinization of groundwater has been serious and has been a big constraint to local development. Understanding the salinization process of groundwater in this area has become one of the most important issues for the sustainable use of the fresh groundwater. In fact, there has been a

repeated controversy on the salinization of groundwater in the eastern part of Jeju whether it is due to the sea intrusion [7][8][14] or the salt dissolution from the bedrock [34]. Therefore, the purposes of the study are to investigate the salinization of groundwater in Jeju island as a case study and to establish the multi-isotope fingerprinting technique to search for the impacts of groundwater salinization in the volcanic island.

2. General hydrogeology of Jeju Island

Jeju Island is the biggest island in Korea and is located 90 km off the south coast of Korean peninsula. Its area is 1,825 km² and there is a central cone-crater, Mount Halla (1950m). It has the population of 550,000 and subtropical climate. The volcanic activities in this island have been dormant for the past 310 years after having continued active for 1 million years and the last eruption occurred on November 15, 1690. The island has about 360 parasitic cones along the long axis of the elliptically shaped island. In general, the geology of this island is mainly composed of olivine basalt flows with some trachyte, trachyandesite, tuff and pyroclastics, etc. [13]. As rain water percolates easily into underground due to highly permeable strata, about 60 dry rivers have the temporary flows only for rainy period and thus, very little surface water can be obtained. Two common hydrogeological factors to govern groundwater replenishment are permeable and impermeable elements. The permeable elements are primary porosity, secondary fracture, pyroclastics, clinker and various voids and the impermeable ones are dense rocks, paleosols and old pyroclastics [5]. Basal, para-basal groundwater and perched water exist in the island [13][14]. Aquifers near seashore in study area in the eastern part of Jeju show the property of basal groundwater and those in the western part para-basal groundwater. Jeju has the highest precipitation in Korea. The average precipitation is 2,027 mm/y in the northern, 2,339 mm/y in the southern, 1,299 mm/y in the western and 2,077 mm/y in the eastern regions. The total precipitation of Jeju is estimated at 33.9 billion m³/year. 19 billion m³/year is shared by run off along the dry river rapidly or evaporate. Other 14.9 billion m³/year penetrates to the underground to become groundwater [14]. The current exploitation is 1.3 billion m³/year and the possible exploitation in the future 6.2 billion m³/year. ¹³⁾

3. Methodology

Twenty samples of groundwater (S1, S2, S3, S4, S5, S8, S9, S10, S11, S12), one spring water (S6) and one sea water (S13) located in the different elevations were taken on April, August and November of 2001 in Kujwa in the eastern part of Jeju (Figure 1, Table 1). The groundwater samples, S4 and S5 and the seawater, S13, were taken from two different depths. The basement groundwater samples, S7 was also sampled on January of 2002. Additionally, water samples were taken on June of 2003 from the five depths of wells at the four different elevations in the two areas (Kujwa and Susan) using water sampler as shown in Figure 2. All samples were collected in separate Nalgene bottles rinsed several times with the same water samples for chemical, B, Sr, S, N, and oxygen and hydrogen isotopic analyses, respectively, transferred to laboratory and were filtered with 0.45 µm membrane filter with 48 h after sampling except ones for oxygen and hydrogen isotopic analyses. The filtered samples were stored at 4 °C.

Temperature, pH and electrical conductivity of water samples were measured in the field. Na⁺ and K⁺ ions were measured by atomic absorption spectrophotometry (AAS), Ca²⁺, Mg²⁺, Sr²⁺ ions and boron by inductively coupled plasma-atomic emission spectrometer, Cl⁻, SO₄²⁻, Br⁻ and NO₃⁻ by ion chromatography, and HCO₃⁻ by titration.

The isotopic composition of hydrogen, oxygen, carbon, nitrogen, sulfur and oxygen in sulfate were analyzed in the Pakistan Institute of Nuclear Science Technology (PINSTEC). For measurement of sulfur and oxygen isotopes in sulfate, BaCl_2 solution was added in the acidified ($\text{pH} < 2$) and boiled water samples in order to obtain BaSO_4 precipitation and BaSO_4 ppt was dried in the dry oven [1] and was sent to the PINSTEC. The analytical reproducibility for δD , $\delta^{18}\text{O}$, $\delta^{15}\text{N}$, $\delta^{13}\text{C}$, $\delta^{34}\text{S}_{\text{SO}_4}$ and $\delta^{18}\text{O}_{\text{SO}_4}$ were $\pm 1 \text{ ‰}$, $\pm 0.1 \text{ ‰}$, $\pm 0.2 \text{ ‰}$, $\pm 0.1 \text{ ‰}$, $\pm 0.15 \text{ ‰}$, $\pm 0.2 \text{ ‰}$, respectively. $^{11}\text{B}/^{10}\text{B}$ isotope ratios were measured by negative thermal ionization mass spectrometry at the U.S. Geological Survey, Menlo Park, California, USA. The measured $^{11}\text{B}/^{10}\text{B}$ ratios were normalized to the N.I.S.T. 951 boric acid standard. At the Menlo Park laboratory $\delta^{11}\text{B}$ of seawater is $+39.2 \text{ ‰}$ relative to this standard [30]. External analytical reproducibility of boron isotope ratios is 1 ‰ , based on replicate analyses of the N.I.S.T. 951 and seawater standards, and duplicate measurements of individual samples. Sr isotope ratios were determined by thermal ionization mass spectrometry at Korea Basic Science Institute, Dajeon, Republic of Korea. NBS987 standard gave $^{87}\text{Sr}/^{86}\text{Sr}$ of 0.710228 ± 0.000015 ($N=22$, 2s standard error) during the analysis [17][31]. Total chemical blank level was less than 60 pg of Sr. Sr isotope ratios in some water samples were cross-analyzed at the U.S. Geological Survey to obtain the reliability of those measured in Korea.

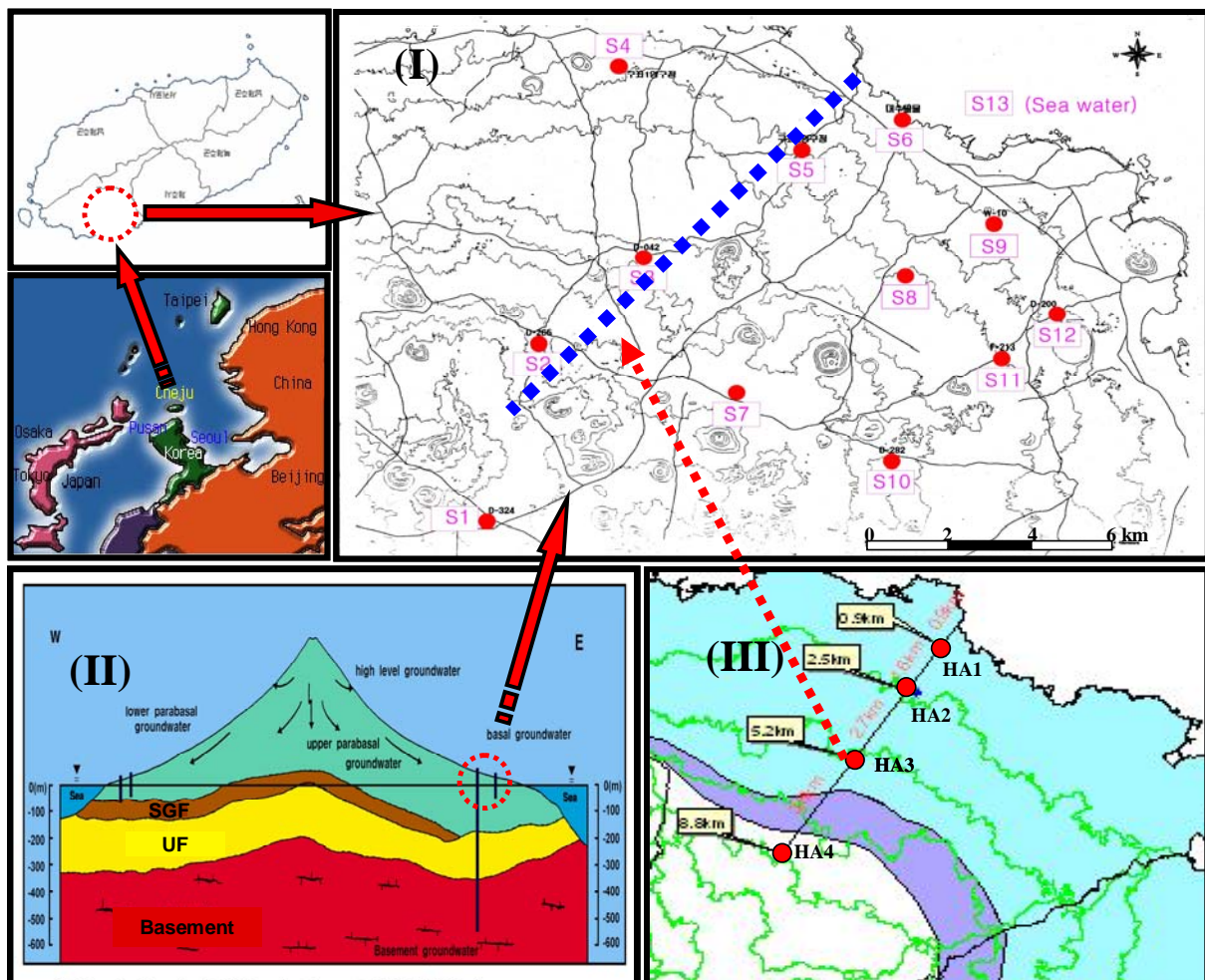


Fig. 1. (I) Sampling locations in the study area in the eastern part of Jeju Island. (II) A schematic geological cross section and occurrence of groundwater (after Koh, 1997) [19]. SGF and UF stand for Soguipo formation and UF, respectively. (III) Sampling locations of studying the aquifer profile at the different altitude and hydrogeological implications in the study area

4. Results and discussion

4.1. Hydrogeology of study area

Kujwa area is located some 40 km away from Jeju city in the the eastern part of Jeju island. Cinder cones and lava tubes are often found throughout the area. Due to highly permeable surface –geological structure and shallow layer of volcanic ash soil, the rain water can be infiltrated very rapidly into the groundwater [11]. Typical geological structure in the study area was investigated by the core interpretation of observation wells drilled recently the Jeju province. As shown in Figure 2, the geological cross-section of well HA-1, 0.9 km away from the seashore, consists of acicular feldspar olivine basalt (AFOB), augite olivine basalt (AOB), gravel and unconsolidated marine sediment followed by U formation [19]. Well HA-2, 2.5 km away from the seashore, has the same profile as the one of HA-1, except a gravel layer. In particular, pillow lava is often observed in the AOB layer just above the marine sediments. On the other hand, well HA-3, 5.8 km away from the seashore has a more complicated geological profile, consisting of AOB, AFOB, volcanic ash, AFOB, AOB, marine sediment, AFOB, marine sediment and then U formation. Well HA-4, over 8 km distant from the seashore, has much more complicated cross-section than HA-1, 2 and 3 and its U formation is found at deeper levels. In general AFOB consists of a few or a dozen of porous lava flow units and partially vertical joints. These units are thought to facilitate the infiltration of precipitation into the aquifer. In the case of HA-1, 2 and 3 wells, 10 – 15 cm long glassy -broken rocks are found in the whole(HA-1) or a part of the AOB (HA-2 and 3) layer and are regarded as a pillow lava formed by the rapid cooling process of the lava flow when contacted with seawater.

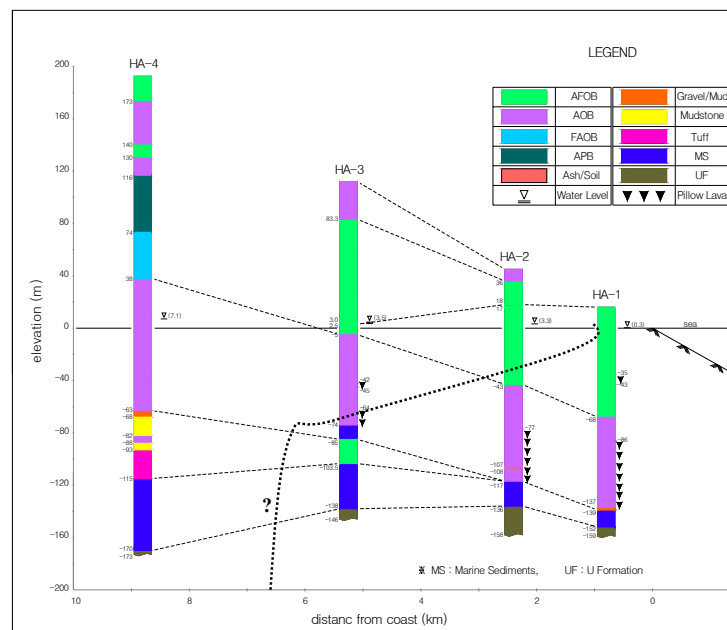


Fig. 2. Typical hydrogeological cross-section and putative aquifer formation.

Figure 2 shows the hydrogeological cross-sections and aquifer layers of observation wells. This data supports the occurrence of basal groundwater in the eastern part. However, HA-1 well has no fresh water and HA-2 and 3 wells have 37 m and 70 m thick layer of fresh water, respectively. When Ghyben-Herzberg relation is applied [35] the actual depths to the interface are much less than the theoretical depth (HA-2=135 m, HA-3=143m) in those wells. This means that groundwater in the study area forms a relatively thin layer of fresh water. It can be possibly explained by the following reasons; 1) amount of groundwater recharge 2) over-pumping 3) the presence of confined bed or

aquiclude 4) hydrogeological characteristics of aquifer [12][20]. But as the annual average of the precipitation in the study area amounts to 1,900- 2,000 mm, and its recharge rate of groundwater is the highest in the island, due to good permeable bedrock, a possibility of limited recharge of groundwater may be ruled out. When comparing the present chemical results of groundwaters with the previous ones in the area no remarkable increase in the chemical composition and EC could be found. This stability indicates that over-pumping in the area is not happening. Therefore, the explanations 3) or 4) may be persuasive to explain the smaller thickness lens formation of fresh water. From the geological sections of the drilled wells the most plausible layers able to play the role of a confined bed or aquiclude, may be the marine sediments or the U formation but they lie deeper, being less impermeable and thus it will be difficult to control the fresh groundwater flow. In addition, the broken layer of pillow lava placed on marine sediments, as a permeable strata, the occurrence of saline groundwater mixed with seawater.

4.2. Chemical composition

Temperature, pH, electrical conductivity and the chemical composition of groundwater samples are shown in Table 1. The temperature range was between 15 and 16 °C. The pH ranged from 7.4 to 7.9. Based on the electrical conductivity (EC), Na and Cl concentrations at the pumping positions (almost averaged seawater table), groundwater samples can be divided in the three groups; group I (S1, S2, S3, S10) where EC is less than 150 $\mu\text{S}/\text{cm}$ (Na = 10 mg/L and Cl < 12 mg/L), group II (S4, S5, S8, S11, S12) where EC is between 300 and 600 $\mu\text{S}/\text{cm}$ (Na = 20 ~80 mg/L, Cl = 70 ~150 mg/L) and group III (S6, S9) that EC ranges between 1200 and 1700 $\mu\text{S}/\text{cm}$ (Na = 200 ~ 250 mg/L, Cl = 400 ~ 450 mg/L). In particular, the chemical composition of groundwater for wells S1, S2 and S3 more than 4.6 km away from the seashore, were almost the same as that of the natural mineral water ‘Samdasoo’ produced in Jeju island (Na= ~5 mg/L, K = ~ 2.2 mg/L, Mg = ~ 2.4 mg/L, Ca= ~ 3.0 mg/L, Cl = ~ 5.6 mg/L, SO_4 = ~ 0.8 mg/L, <http://jpdco.kr/samdasoo>) and represented the lower end member of groundwater in this island.

Table 1. Chemical composition of water samples collected in the study area.

Sample No.	Descrip- tion	Elevat- ion(m)	Depth (m)	Water level(m)	Temp. °C	pH	EC $\mu\text{S}/\text{cm}$	Na mg/L	K mg/L	Ca mg/L	Mg mg/L	Sr ug/L	Cl mg/L	Br mg/L	SO_4 mg/L	NO_3 mg/L	B ug/L	HCO_3 mg/L
S1	GW	305	320	234	16	7.7	90	7	3	5	4	28	7	*	2	2.5	14	40
S2	GW	240	270	204	15	7.5	75	7	2	4	3	18	7	*	2	3.8	13	30
S3	GW	132	171	131	15	7.5	81	7	2	4	3	21	8	*	2	4.7	13	31
S4-1	UGW	46	105	44	16	7.6	607	87	5	10	13	89	149	0.5	25	5.4	56	33
S4-2	LGW				16	7.5	24000	5200	209	276	736	4140	9744	34.5	1609	1.8	1723	105
S5-1	UGW	44	120	43	16	7.6	420	63	5	11	14	95	120	0.4	20	18.7	43	37
S5-2	LGW				16	7.4	18800	3845	165	162	483	2420	6451	24.5	1139	6.9	1740	66
S6	SW	0	20	30	17	7.7	1787	239	13	40	37	333	445	1.5	74	59.2	111	67
S7	BGW	165	380	102	28	7.9	2700	630	8	52	17	922	632	1.6	196	*	662	631
S8	GW	85	120	96	16	8.0	324	25	4	26	9	66	78	0.3	10	6.3	12	46
S9	GW	30	20	30	16	7.6	1285	209	11	23	34	226	404	1.3	60	15.7	77	47
S10	GW	155	170	147	16	7.7	127	10	3	7	6	39	13	0.1	3	5.3	10	58
S11	GW	77	100	72	16	7.8	350	33	4	12	12	105	72	0.3	14	12.5	14	43
S12	GW	55	75	51	16	7.9	603	84	6	6	17	133	152	0.5	26	14.5	40	42
S13-1	SEW	0	0	0	16	8.2	43300	10100	455	415	1259	6660	19000	72.0	2936	0.5	3950	143
S13-2	SEW	0	-60	0	16	8.2	43300	9750	428	419	1241	6330	17952	64.0	2801	0.5	3990	143

* GW: Groundwater, UGW: Upper layer of sea water, LGW: Lower layer of groundwater, SW: Springwater, BGW: Basement groundwater, USEW: Upper layer of sea water, LSEW: Lower layer of sea water.

In general, as in our previous studies, [26], the contents of cations and anions, as well as the electrical conductivity of ground water below 100 m altitude, were 5 – 20 fold higher than those of fresh groundwater in the upper 100 m altitude (Table 1). The chemical composition of groundwater near the seashore suggested the possibility of sea water intrusion. Also, the value of EC data-logged according

to the depth in the observation wells and the change of EC and the evaluation of the water table coincided with the tide regime, supported the possibility of sea water intrusion.

However, the present chemical compositions of groundwater samples S9, S11 and S12 which we collected in 1986 and 1991 were very similar to those measured in the past [26][27] suggesting that there has been little or no seawater intrusion in those wells due to over-pumping.

The contents of cations and anions of groundwater and springwater in the rainy season (August) were lower than those in dry season (April or November). Their seasonal changes were attributed to the dilution with the torrential rain in summer. In addition, a basement groundwater sample S7, should high bicarbonate (631 mg/L) in the leaching process when fresh groundwater passed through the U formation layer, including shellfish etc.

On the other hand, nitrate concentrations in groundwater varied from 2.5 to 59 mg/L on April. The S6 spring water in the lower altitude had the highest concentration of nitrate.

Table 2. Ionic molar ratios of groundwater samples collected in the study area.

Sample No.	Na/Cl	Mg/Cl	K/Cl	Q	Mg/Ca	Ca/Cl	Br/Cl x10 ⁴	SO ₄ /Cl	B/Clx10 ⁴	HCO ₃ /Cl	Sr/Cax10 ⁴	Sr/Clx10 ⁴
S1	1.51	0.78	0.32	0.19	1.23	0.64	*	0.11	63.4	3.21	24.6	15.6
S2	1.45	0.58	0.24	0.18	1.35	0.43	*	0.11	57.2	2.33	23.1	9.9
S3	1.48	0.58	0.25	0.18	1.37	0.43	*	0.11	54.6	2.23	25.7	10.9
S4-1	0.90	0.13	0.03	0.30	2.20	0.06	15.2	0.06	12.2	0.13	42.5	2.4
S4-2	0.82	0.11	0.02	0.37	4.39	0.03	15.7	0.06	5.8	0.01	68.5	1.7
S5-1	0.81	0.18	0.04	0.35	2.08	0.08	15.7	0.06	11.9	0.18	37.7	3.2
S5-2	0.92	0.11	0.02	0.31	4.91	0.02	16.9	0.07	8.9	0.01	68.2	1.5
S6	0.83	0.12	0.03	0.54	1.51	0.08	15.0	0.06	8.2	0.09	38.3	3.0
S7	1.54	0.04	0.01	0.11	0.55	0.07	11.0	0.11	34.4	0.57	80.8	6.4
S8	0.49	0.17	0.04	0.76	0.59	0.29	14.7	0.05	5.1	0.34	11.8	3.5
S9	0.80	0.12	0.02	0.41	2.43	0.05	14.0	0.06	6.3	0.07	45.2	2.3
S10	1.24	0.70	0.19	0.17	1.53	0.45	24.0	0.08	25.6	2.58	26.9	12.2
S11	0.71	0.24	0.05	0.36	1.64	0.15	16.2	0.07	6.3	0.34	40.4	5.9
12	0.86	0.16	0.03	0.16	4.41	0.04	15.7	0.06	8.6	0.16	98.0	3.6
S13-1	0.82	0.10	0.02	0.32	4.99	0.02	16.8	0.06	6.8	0.00	73.2	1.4
S13-2	0.84	0.10	0.02	0.33	4.88	0.02	15.8	0.06	7.3	0.00	69.0	1.4

*Q=Ca/(SO₄+HCO₃)

4.3. Ionic and molar ratios

Table 1 shows the concentrations of Na, K, Ca, Mg, Sr, Cl, Br, SO₄ and B in groundwater, spring water and seawater. They had significant correlations with the values of ECs, which suggests, tentatively, the possibility of simple mixing with seawater in the process of salinisation of local groundwater. Molar ratios of Na/Cl, Mg/Ca, Mg/Cl, Q(=Ca/HCO₃+SO₄), K/Cl, SO₄/Cl, Br/Cl and B/Cl of the Mediterranean Sea are known to be 0.86, 4.5 ~ 5.2, 0.08, 0.4, 0.02, 0.05, 15 x 10⁻⁴, 7.5 x 10⁻⁴, respectively [15]. Molar ratios of chemical composition of seawater in the eastern part of Jeju island were similar with those of the Mediterranean Sea.

The Na/Cl ratios of very fresh groundwaters (S1, S2, S3 and S4) ranged from 1.24 to 1.51, whereas those of groundwaters (S4-1/2, S5-1/2, S8, S9, S11 and S12) with the higher salinity were close to marine ratios.

Mg/Ca ratios of S4-2, S5-2 and S12 groundwaters were similar to the marine ratio. The Mg/Ca ratio of other groundwaters were between 1.23 and 2.43. Q(Ca/SO₄+HCO₃) values of S6 and S8 groundwaters

were higher than the marine, ratio whereas S12 shows a lower ratio than the marine one. The relative decrease/increase of Ca or Na content as compared with theoretical mixing fractions of seawater in groundwater reflects that the ionic exchange reaction between Na and Ca occurs in the aquifer. S8, S9 and S11 groundwaters showed the reverse ionic exchange reaction appearing when the seawater intrudes into the fresh groundwater ($2 \text{Na}^+ + \text{Ca-Clay} \rightarrow \text{Na}^2\text{-Clay} + \text{Ca}^{2+}$) [25]. Generally Br concentrations in the fresh water is very low. Br is a conservative element that does not take part in the secondary reactions with rock. Therefore, the Br/Cl ratio can be a reliable parameter for the delineation of the salinization origin. Besides the very fresh groundwaters (S1, S2, S3, S10), in which Br concentrations could not be detected because of the analytical detection limit, Br concentrations in most groundwaters were well correlated with Cl and the resultant Br/Cl ratios showed $14 \times 10^{-4} \sim 15 \times 10^{-4}$ which are close to the seawater ratio. The ratios of SO_4/Cl and B/Cl also represented the marine ones (Figure. 3). In addition, there were two main water types of groundwaters in the study area on the expanded Durov diagram (Figure 3). The lower end member of groundwater should a NaHCO_3 facies, while high salty groundwater had a NaCl facies.

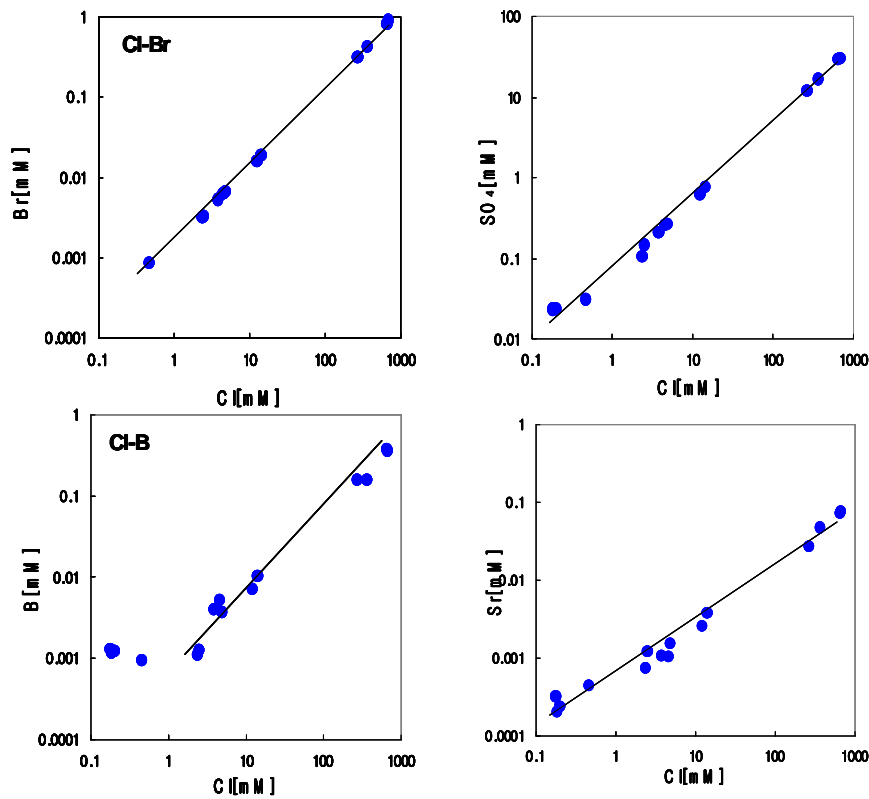


Fig. 3. Plots of Cl-Br, Cl-SO₄, Cl-B and Cl-Sr

4.4. Isotopic composition

4.4.1. ¹⁸O and D

$\delta^{18}\text{O}$ and δD in seawater and groundwater sampled in April are shown in Table 3. $\delta^{18}\text{O}$ in seawater was about +2 ‰, while groundwaters ranged from -3.05 to -6.80 ‰, respectively.

Table 3. Isotopic composition of groundwater samples collected from the study area.

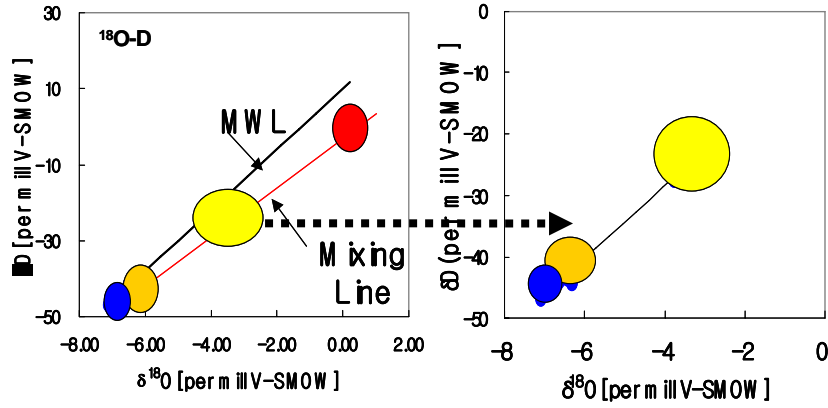
Sample No.	$\delta^{18}\text{O} \text{ ‰}$ (V-SMOW)	$\delta \text{D} \text{ ‰}$ (V-SMOW)	$\delta^{13}\text{C} \text{ ‰}$ (PDB)	$\delta^{34}\text{S} \text{ ‰}$ (CDT)	$\delta^{18}\text{O}_{\text{SO}_4} \text{ ‰}$ (V-SMOW)	$\delta^{11}\text{B} \text{ ‰}$ (NBS951)	$^{86}\text{Sr}/^{87}\text{Sr}$
S 1	-6.80	-43.29	-15.23	12.37	10.09	*	*
S 2	-7.09	-46.85	-12.05	11.43	10.46	*	*
S 3	-6.86	-45.89	-10.92	11.25	11.32	33.97	0.70523
S 4 -1	-6.73	-44.37	-11.10	18.74	10.79	40.46	0.70807
S 4 -2	-3.05	-22.40	-2.83	18.58	9.34	42.96	0.70904
S 5 -1	-6.64	-44.27	-11.90	18.13	9.60	42.21	0.70776
S 5 -2	-3.77	-27.31	-3.59	19.99	10.49	40.96	0.70909
S 6	-6.32	-44.47	-12.48	18.39	*	43.21	0.70871
S7	-8.03	-51.43	-4.76	19.74	9.53	*	0.70914
S 8	-6.48	-41.77	-10.47	18.22	9.93	36.96	0.70594
S 9	-6.47	-42.67	-9.80	18.92	12.05	45.95	0.70810
S 10	-6.55	-42.85	-9.50	13.58	10.83	35.21	0.70577
S 11	-6.22	-41.09	-10.02	18.06	10.16	50.70	0.70689
S 12	-6.43	-43.59	-10.41	18.22	8.18	47.70	0.70753
S 13 -1	0.20	-1.14	-0.87	19.57	10.58	*	*
S 13 -2	0.22	-1.09	-0.91	18.34	11.03	*	*

*: not determined

δD in seawater was close to -1.1 ‰ , whereas δD those in groundwaters ranged from -22.4 to 46.8 ‰ . The results of water samples analysed in August and November had the same trends as those on April. However, $\delta^{18}\text{O}$ and δD in August were more depleted than those April and November. $\delta^{18}\text{O}$ and δD values in groundwaters were near the global MWL. High salinity groundwaters were placed on the mixing line between two end-members (Figure 5). This indicates that the salinisation of groundwater is due to the simple mixing between seawater and groundwater. $\delta^{18}\text{O}$ and δD values of S7 geothermal groundwater were much more depleted than other groundwaters, reflecting the contribution of the depleted precipitation from the more distant mountain area.

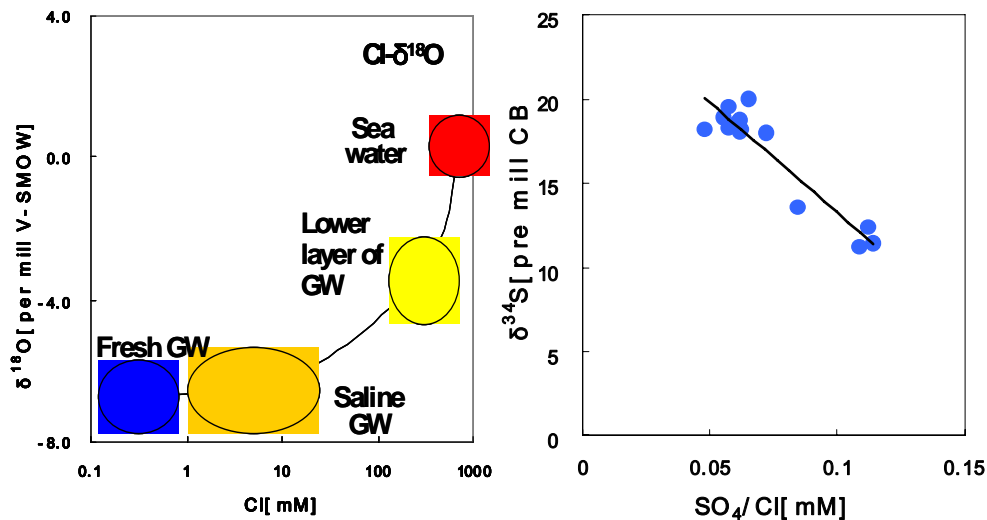
4.4.2. $^{34}\text{S}_{\text{SO}_4}$ and $^{18}\text{O}_{\text{SO}_4}$

$\delta^{34}\text{S}$ of SO_4 dissolved in groundwater shows various ranges depending their origin. In particular, their values in the modern seawater are $+20 \text{ ‰}$ [8]. $\delta^{34}\text{S}$ in the fresh groundwater ranged from $11.3 - 14.0 \text{ ‰}$ whereas those in the salty groundwater from 18 to 20 ‰ . $\delta^{34}\text{S}$ of SO_4 in groundwater may be changed by redox process. However, Cl and SO_4 in the groundwaters were on the straight line between those for the fresh and marine end members. This indicates that the local aquifer is not under reducing conditions. It is also reported that the redox potentials (EHs) of groundwater in the island ranges from $+100$ to $+200 \text{ mV}$ [10]. Therefore, SO_4 reduction by bacteria in groundwater the study area can not happen. $\delta^{34}\text{S}$ in the salty groundwater represented the marine origin and had a negative linear relationship with the ratio of SO_4/Cl , indicating that groundwater salinization is due to the simple mixing with seawater. On the other hand, $\delta^{18}\text{O}$ of SO_4 ranged from 9 to 10 ‰ representing the mixing with modern seawater (10 ‰) [8].

Fig. 4. Plot of ^{18}O and D

4.4.3. ^{11}B

In nature there are two boron isotopes (^{10}B and ^{11}B). ^{11}B tends to separate preferentially in the dissolved boron as $[B(OH)_3]$, whereas ^{10}B tends to be preferentially incorporated in the tetrahedral species $[B(OH)_4^-]$ in the solid phase [16][24]. As a result of this isotopic fractionation, seawater ($\delta^{11}B = +39\text{‰}$) [33] has a very different isotopic value in comparison with the terrestrial rocks ($\delta^{11}B \approx 0 \sim \pm 5\text{‰}$), terrestrial-derived groundwater ($\delta^{11}B = -16 \sim 2\text{‰}$, in the Great Artesian Basin, Australia) and non-marine brines ($\delta^{11}B = 0 \sim 15\text{‰}$, Qaidam Basin, China) [24][28][29]. The volcanic rock hosted end-member water was also characterized by $\delta^{11}B \leq -5\text{‰}$. $\delta^{11}B$ of S4-1/2, S5-1/2, S6, S9, S11 and S12 groundwaters were in the ranges of $40.46 \sim 50.70\text{‰}$ and it was over 40‰ . This is due to that ^{11}B in seawater intruded in the aquifer is more enriched, by preferentially elimination of ^{10}B in the liquid phase. However, $\delta^{11}B$ of S3 and S10 fresh groundwater showed values on the range $33.91 \sim 35.21\text{‰}$, groundwater also showed $33.91 \sim 35.21\text{‰}$, which represents the isotopic signature of the typical coastal fresh end member [33].

FIG. 5. Plot of $Cl-^{18}O$ and $^{34}S-SO_4/Cl$

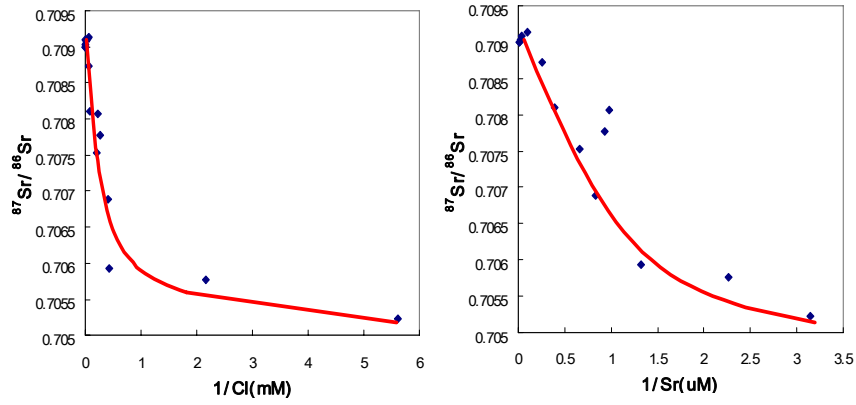


FIG. 6. Plot of $1/Cl$ - $^{87}Sr/^{86}Sr$ and $1/Sr$ - $^{87}Sr/^{86}Sr$

4.4.4. $^{87}Sr/^{86}Sr$

There are four Sr isotopes in nature [^{84}Sr (0.56%), ^{86}Sr (9.87%), ^{87}Sr (7.04%), ^{88}Sr (82.53%)]. ^{87}Sr is formed from the β decay of the long-lived ^{87}Rb (half life: 4.88×10^9 a). Hence, the ratio of $^{87}Sr/^{86}Sr$ is governed by ^{87}Rb content in the geochemical materials [4]. Since there is also no natural isotopic fractionation in Sr species of which their masses are heavy, the ratio of $^{87}Sr/^{86}Sr$ has been used for tracing Sr of different origin, evaluating the mixing of groundwater and the interaction of between and rocks [3][8][9][17][22]. It is reported that its ratio for basalt is 0.704 -0.705 [18] and for seawater is 0.70915. The ratio of $^{87}Sr/^{86}Sr$ for fresh groundwater was same as basalt ratio and those for the salty groundwaters ranged from 0.706 to 0.709, increasing depending on the salt content in groundwater (Figure 6). This reflects that the increased salty contents in the groundwater originates from mixing with seawater.

4.4.5. ^{13}C

Although ^{13}C is an excellent tracer of carbonate evolution in groundwaters because of the large variations in the various carbon reservoirs, ^{13}C values gave no satisfactory isotopic signature for the simple mixing with seawater in this study.

4.5. Geochemical and isotopic properties along a groundwater profile

Since most of the existing groundwaters on the Jeju island are pumped out near the averaged sea level, we do not have much information on the geochemical and isotopic properties of groundwater depending on its water depth. Therefore, water sampling at different depths were taken from the research wells at the different elevations. As shown in Figure 7, the contents of Cl and SO_4 at the deeper parts of the wells, H1 that is 0.9 km away (altitude: 14 m), H2, 2.5 km (altitude: 44 m) as well as H3 5.2 km (altitude: 114 m) away from the seashore were very high and in fact were similar to those of seawater. In particular, the molar ratio of Cl/SO_4 , $\delta^{34}S_{SO_4}$ and $\delta^{18}O_{SO_4}$ of those groundwaters also represent their marine values (Figures 8 and 9). The existence of an interface between the fresh and the salty water also explains the evidence of typical coastal aquifers. Considering that those wells are not equipped a the pumping device and not disturbed, the chemical compositions of groundwater profiles could be attributed to the naturally occurring seawater intrusion.

5. Conclusion

From these results, we tentatively suggest that the salinization of groundwater in the eastern part of Jeju-do island was neither due to the over-exploitation of groundwater resources nor to the dissolution of salts in the bedrock but due to the simple mixing with modern seawater resulted from the geological

structure. It is considered that the mixing process on sea water does not happen in a short period of time, but in a certain time is required to reach an equilibrium in the Na-Ca ion exchange reaction in the aquifer. Thin layer formation of fresh water in the aquifer was also attributed to the geological structure (Figure 10). Especially, the analysis of ^{18}O , D, ^{11}B , $^{87}\text{Sr}/^{86}\text{Sr}$, $^{34}\text{S}_{\text{SO}_4}$ and $^{18}\text{O}_{\text{SO}_4}$ gave the direct answer on the cause of salinization of groundwater in the study area. ^{18}O and D showed the mixing of fresh ground water with sea water. ^{11}B showed that the saline component originated from the sea water. $^{34}\text{S}_{\text{SO}_4}$ and $^{18}\text{O}_{\text{SO}_4}$ gave the evidence of intrusion of modern sea water into groundwater. In addition, the value of $^{87}\text{Sr}/^{86}\text{Sr}$ indicated that the salinization was not from the dissolution of salts from the rock matrix, but due to the mixing between seawater and groundwater.

ACKNOWLEDGEMENTS

The study was carried out as part of an Atomic Energy Research & Development Project of the Korean Ministry of Science and Technology, and an IAEA Co-ordinated Research Programme on “Origin of Salinity and Impacts on Fresh Groundwater Resources” (Contract Number: 11323/R1). We deeply thank Dr. T. D. Bullen at U. S. Geological Survey for analyzing boron and strontium isotopes in our water samples.

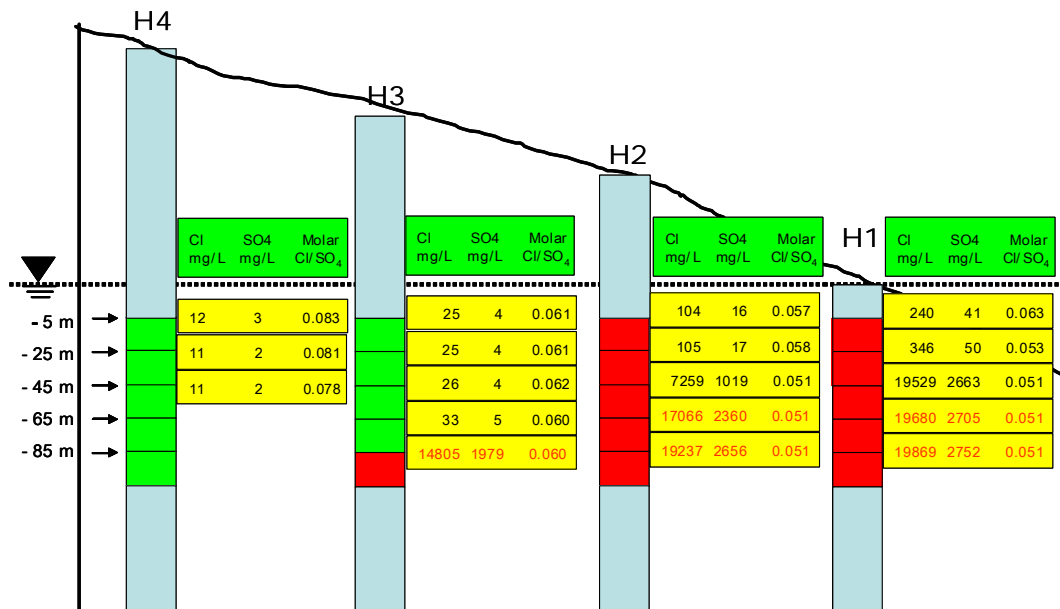


FIG. 7. The concentrations of Cl, SO₄ and molar ratio of Cl/SO₄ of the groundwater depth profile in the aquifer

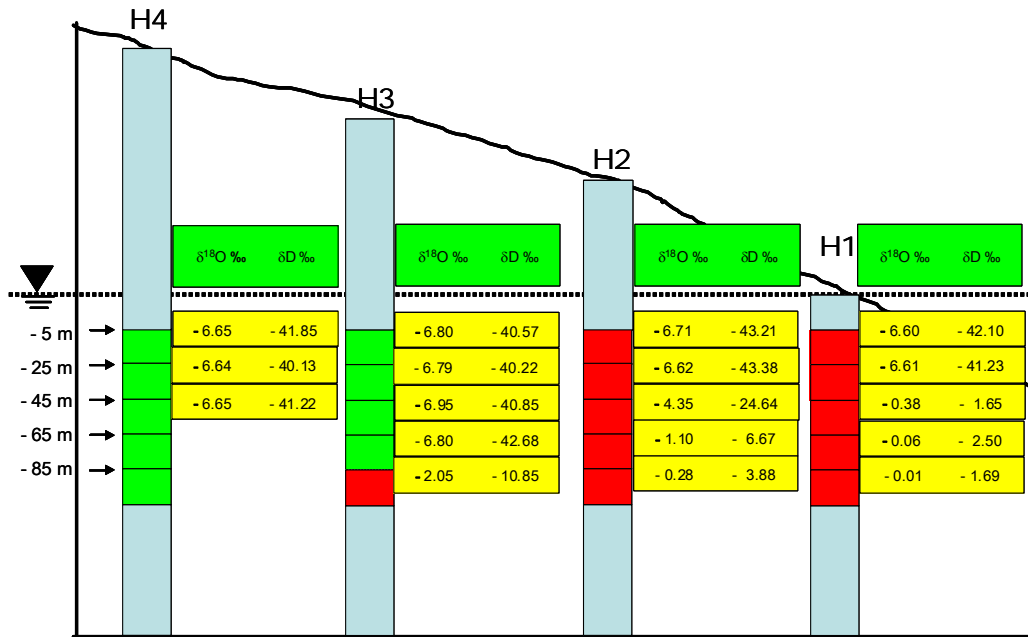


FIG. 8. $\delta^{18}O$ and δD values along a groundwater depth profile in the aquifer

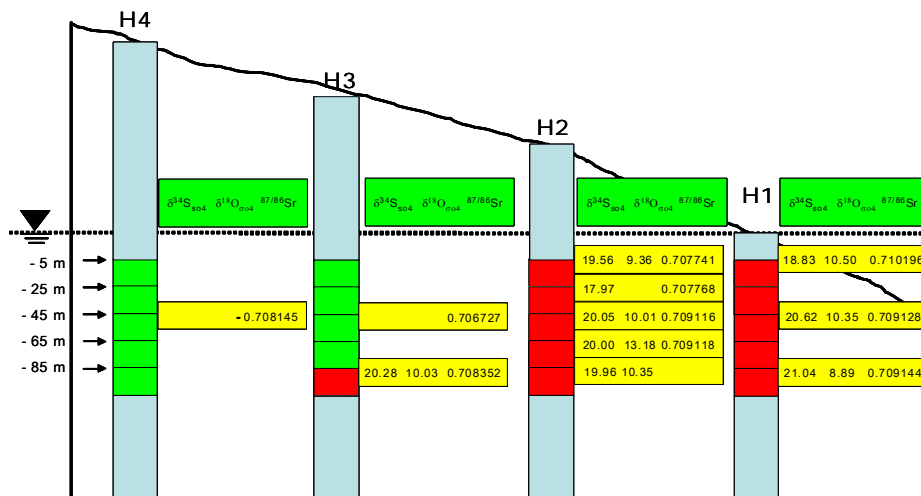


FIG. 9. The concentrations of $\delta^{34}S_{SO_4}$, $\delta^{18}O_{SO_4}$ and $^{87}Sr/^{86}Sr$ of the groundwater depth profile in the aquifer

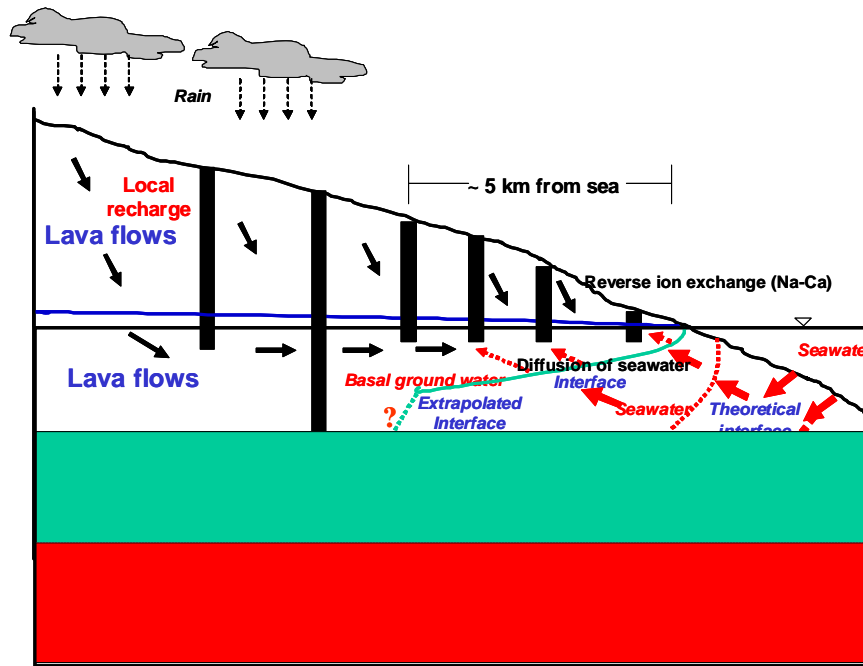


FIG. 10. The conceptual model suggested by this study

REFERENCES

- [1] AGGARWAL, J., SHEPPARD, D.S, ROBINSON, B. W., Analytical developments in the measurements of boron, nitrate, phosphate and sulfate isotopes and case examples of discrimination of nitrogen and sulfur sources in pollution studies In"Application of Isotope Techniques to Investigate Groundwater Pollution, IAEA-TECDOC-1046, (1998) 17-37.
- [2] BARTH, S. R., Geochemical and boron, oxygen and hydrogen isotopic constraints on the origin of salinity in groundwaters from the crystalline basement of the Alpine Foreland. Applied Geochemistry 15, (2000) 937-952.
- [3] BOHLKE, J. K., HORAN, M., Strontium isotope geochemistry of groundwaters and streams affected by agriculture, Locust Grove, MD. Applied Geochemistry 15, (2000) 599-609.
- [4] CAPO, R. C., STEWART, B. W., CHADWICK, O. A., Strontium isotopes as tracers ecosystem processes: theory and methods. Geoderma 82, (1998) 197-225.
- [5] CHOI, S. H., Jeju island formation and groundwater characteristics, Jejudo Res., (1988) 5:59-77.(in Korean).
- [6] CHOI, S. H., KIM, Y. K., Characterization of groundwater quality in Jeju Island. J. Geol. Soc., (1989) 25: 230-238. (in Korean with English abstract).
- [7] CHOI, S. H., KIM, Y. K., LEE, D. D., Seawater intrusion in the coastal area of Cheju volcanic island, Korea, J. Inst. Mining Geol., (1991) 24: 319-327 (In Korean with English abstract).
- [8] CLARK, I. D., FRITZ, P., Environmental isotopes in hydrogeology, Lewis Publishers, New York, (1997) 111-122.
- [9] GROBE, M., MACHEL, H. G., HEUSER, H., Origin and evolution of saline groundwater in the Munsterland cretaceous basin, Germany: Oxygen, hydrogen, and strontium isotope evidence. Journal of Geochemical Exploration (2000) 69-70. 5-9.
- [10] JEJU-DO., A survey on the groundwater recharge and discharge system in Jeju island.(In Korean) (1999).
- [11] JEJU-DO., The integrated report on the hydrogeology and groundwater resources on Jeju island(I).(In Korean) (2001).

- [12] JEJU-DO., The integrated survey of hydrogeology and groundwater resources on Jeju island(II).(In Korean) (2000).
- [13] JEJU-DO., A report of groundwater conservation and management plans in Jeju island.(In Korean) (2003).
- [14] JEJU-DO., KOREA WATER RESOURCES CORPORATION, The integrated survey of hydrogeology and groundwater resources in Jeju island(III).(In Korean) (2003).
- [15] JONES, B. F., VENGOSH, A., ROSENTHAL, E., YECHIELI, Y., Geochemical investigation In: Sea water intrusion in coastal aquifers- concepts, method and practice, J. Bear, A. H.-D. Cheng, S. Sorek, D. Quazar and I. Herrera(eds.), Kluwer Academic Publishers, (1999) pp. 51-71.
- [16] KAKIHANA, H., KOTAKA, M., SATOH, S., OKAMOTO, N., OKAMOTO, M., Fundamental studies on the ion exchange separation of boron isotopes, Bull. Chem. Soc. Jap. 50 (1977) 158-163.
- [17] KATZ, B. G., BULLEN, T. D., The combined use of $^{87}\text{Sr}/^{86}\text{Sr}$ and carbon and water to study the hydrochemical interaction between groundwater and lakewater in mantled karst. *Geochimica et Cosmochimica Acta*. Vol 60, No 24. (1996) 5075-5087.
- [18] KIM, B. K., WOO, K. S., SOHN, Y. K., Sr isotopes of the Seoguipo Formation(Korea) and their application to geologic age, *J. of Asian Earth Sci.* 19, (2001) 701-711.
- [19] KOH, K. W., Characteristics of the groundwater and hydrogeologic implications of the Seoguipo formation in Cheju Island. PhD dissertation, Pusan University(in Korean with English abstract) (1997).
- [20] KOH, K. W., The hydrogeology and groundwater management of Hawaii. Jeju Provincial Water Resources Management Office. (in Korean) (2001).
- [21] LAUVAT, D. J., MICHELOT, L., ARANYOSSY, J. F., Origin and residence time of salinity in the Aspo groundwater system. *Applied Geochemistry* 14, (1999) 917-925.
- [22] LYONS, W. B., TYLER, S. W., GAUDETTE, H. E., LONG, D. T., The use of strontium isotopes in determining groundwater mixing and brine fingering in a playa spring zone, lake tyrrell, Australia. *Journal of Hydrology* 167, (1995) 225-239.
- [23] PENNISI, M. W., LEEMAN, P., TONARINI, S., PENNISI, A., NABEL, P., Boron, Sr, O, and H isotope geochemistry of groundwaters from Mt. Etna(Sicily)-hydrologic implications. *Geochimica et Cosmochimica Acta*. Vol 64. (2000) 961-974.
- [24] SPIVADS, A. J. EDMOND, J. M., Boron isotope exchange between seawater and the oceanic crust, *Geochim. Cosmochim Acta* 51, (1987) 1033-1047.
- [25] STUMM, W., MORGAN, J. J., Aquatic chemistry, Chemical equilibrium and rates in natural waters(3rd edition), John Wiley & Sons, Inc. New York (1996) 586-590.
- [26] U. Z. K., AHN, J. S., CHOUNG, C. C., SONG, S. J., Environmental isotope –aided study on Cheju groundwater resources (□)KAERI/RR-527/86. (in Korean with English abstract) (1986).
- [27] U. Z. K., AHN, J. S., CHOUNG, C. C., SONG, S. J., Environmental isotope –aided study on Cheju groundwater resources (□) KAERI/RR-1036/86. (in Korean with English abstract) (1991).
- [28] VENGOSH, A., CHIVAS, A. R., McCULLOCH, M. T., STARINSKY, A., KOLODNT, Y., Boron isotope geochemistry of Australian salt lakes. *Geochimica et Cosmochimica Acta*. Vol. 55. (1991) 2591-2606.
- [29] VENGOSH, A., CHIAS, A. R., STARINGSKY, A., KOLODNY, Y., BAOZHEN, Z., PENGXI, Z., Chemical and boron isotope composition of non-marine brines from the Qaidam Basin(China). *Chem. Geol.* 120 (1995) 135-154.
- [30] VENGOSH, A. A., STARINSKY, Y. ,CHIVAS, A. R., Boron isotope geochemistry as a tracer for the evolution of brines and associated hot springs from the dead sea, Israel. *Geochimica Cosmochimica Acta*. Vol. 55. (1991) 1689-1695.
- [31] VENGOSH, A., GILL, J., DAVISSION, M. L., HUDSON, G. B., A muti-isotope(B, Sr, O, H, and C) and age dating(^3H - ^3He and ^{14}C) study of groundwater from Salinas Valley, California: hydrochemistry, dynamics, and contamination processes, *Water Resour. Res.* 38(1) (2002) 9-1 - 9-17.

- [32] VENGOSH, A., HEUMANN, K. G., JURASKE, S., KASHER, R., Boron isotope application for tracing sources of contamination in groundwater. *Environ. Sci. Technol.* 28, (1994) 1968-1974.
- [33] VENGOSH, A., KOLODNY, Y., SPIVACK, A.J., Ground-water pollution determined by boron isotope systematics; In "Application of Isotope Techniques to Investigate Groundwater Pollution, IAEA-TECDOC-1046, (1998) 17-37.
- [34] YOON, J. S., Study on the occurrence of high saline groundwater in the eastern area of Cheju island, Cheju-do Res. 3 (1986) 43-53. (in Korean).
- [35] WENTWORTH, The specific gravity of sea water and the Ghyben- Herzberg ratio at Honolulu, Univ. of Hawaii, Occas. Paper 39 (1939).

Isotopic techniques as a tool to investigate salinization problems in the Souss Massa coastal plain (South West Morocco)

L. Bouchaoua^a, M. Qurtobib^b, Y. Hsissoua^a, M. Ibn Majahb^b, H. Marahb^b

^aLaboratoire de Géologie Appliquée, Faculté des Sciences, Agadir, Morocco, Kingdom of

^bCentre National de l'Energie des Sciences et des Techniques Nucléaires (CNESTEN), Rabat, Morocco, Kingdom of

Abstract. The principal water resource in the Souss-Massa coastal plain is provided by the Souss-Massa Plio-Quaternary aquifer and several reservoirs. The sand and gravel aquifer, which was mainly exploited for irrigation, is becoming a source of increasing importance for the domestic supply of the Souss-Massa region. The over-pumping of this aquifer has resulted in water level declines ranging from 0.5 to 2.5 meters per year during the past three decades. The water quality is very variable and in some areas, it presents a high salinity, exceeding 4 g.l⁻¹, that constitutes a major problem for irrigation and domestic water supply. In order to improve the management of these precious resources, a hydrogeologic investigation using several chemical and isotopic tracers such as ¹⁸O, ²H, ³H, ⁸⁷Sr, ¹¹B, ¹⁴C, ⁴He, bromide and chloride, was carried out to determine the sources and mechanisms of recharge to the aquifer and to investigate the origin of salinity. Seawater intrusion and other processes that contribute dissolved solids to groundwater are a major threat to water quality in the heavily exploited Souss-Massa aquifer. The information gathered on the hydrology and the relative importance of various sources of salinity will be used to make decisions about water resource allocation and possible remediation strategies. Stable isotope data indicate that the Atlas Mountain, with high rainfall and depleted values (-6 to -7.5 ‰ δ¹⁸O), constitute the main source of recharge to the Souss-Massa shallow aquifer. Deuterium and oxygen-18 values show a westward gradient with more depleted values, particularly the occurrence of more enriched values areas of the irrigated perimeters is an indicator of induced recharge by irrigation return. The results of this multi isotope study from few groundwater samples collected on the middle and downstream (coastal area) part of the basin suggest that relatively old water is mined at some wells, and seawater intrusion is just one of the multiple sources of salinity present in these waters. Some of the waters ages show as old as several thousands of years. It allows to differentiate between modern seawater intrusion, ancient seawater, agricultural water, and evaporate-derived water. The relative abundances of some anions along with bromide indicate that dilution of intruded seawater from west to east is taking place. Another significant source of salinity is water/rock interaction, indicated by the isotopic strontium that indicates also mixing of groundwater from a different origin in this area.

1. Introduction

In the Souss-Massa basin (Figure 1), situated in the southern part of Morocco, agriculture, tourism and sea fishing are the primary economic activities. These various activities require significant water resources. The Souss-Massa River Basin, covers approximately 27,000 square kilometres. With a year-round growing season, irrigated agriculture in the river basin produces more than half of Morocco's exported citrus and vegetables. Total water use in the basin is about 965 million cubic meters per year; approximately 94 per cent of the water use is for irrigation. Although water used for irrigation is obtained from surface water and groundwater sources, these sources are not sufficient to sustain current agricultural practices, and groundwater resources are being depleted. The area is characterized by a semi-arid climate and by marked seasonal contrasting climate variables. The rainfall average amounts to 250 mm/yr in the plain area and 500 mm/yr in the mountains. Every river of the region, called "oued", has an intermittent flow regime, because the dry season is very long (6 to 8 months) every year. The principal water resource is provided by the Souss-Massa Plio-Quaternary

plain aquifer and by the reservoirs (Figure 1). The sand and gravel aquifer, which was previously mainly exploited for irrigation, is becoming a source of increasing importance for the domestic supply of the Souss-Massa region. The transmissivity of the aquifer is variable, and ranges from 2×10^{-4} to $6 \times 10^{-3} \text{ m}^2 \text{ s}^{-1}$ while the flow direction is from east to west, towards the sea. The aridity of the climate, the drought in these last years, the overexploitation and the deterioration of the water quality, induce serious problems for a sustainable water management in the area. On average, groundwater extraction in the basin exceeds recharge by an estimated 260 million cubic meters annually. This over-pumping of the alluvial aquifer has resulted in water level declines ranging from 0.5 to 2.5 meters per year during the past three decades. The water quality is very variable and in some areas, it presents a high salinity exceeding 4 g l^{-1} [1][2][3][4]. The first chemical and isotopic data [1][5][6] gave indications on the possible sources for the groundwater salinity that included the following processes: (1) present day marine intrusion, (2) old marine intrusion, (3) water rock interaction and dissolution process of evaporites, (4) concentration by evaporation, (5) anthropogenic pollution. The Souss-Massa coastal plain was selected to be the flagship site for the CRP, where a multiple isotope approach study using several isotopes such ^{18}O , ^2H , ^3H , ^87Sr , ^{36}Cl , ^{11}B , ^{129}I , ^{14}C , and ^4He was performed by an international team, as it offered scope for the study of both coastal (saline intrusion) and inland basin problems.

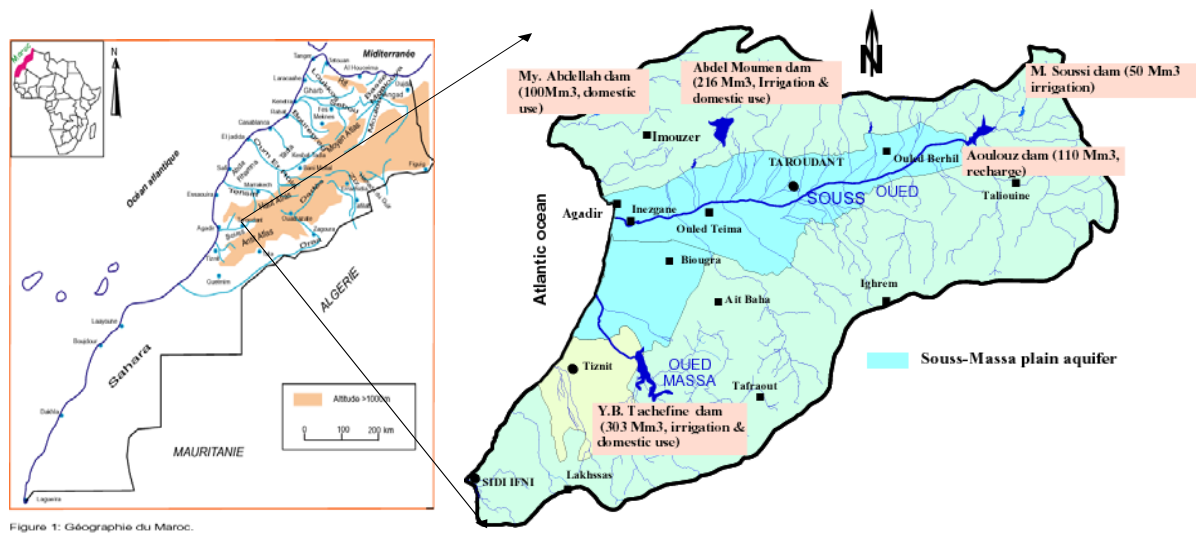


FIG. 1. Souss-Massa basin southern part of Morocco

2. Geology and hydrogeology

The Souss-Massa plain is a narrow depression between the High-Atlas to the north and the Anti-Atlas to the south. The age of the geological formations ranges from Paleozoic to Quaternary (Figure 2).

The plain corresponds to a Plio-Quaternary filling which covers a Cretaceous syncline in the north of the basin, and a schists Paleozoic basement to the south. The syncline axis is oriented east-west (Figure 3). Its northern flank outcrops vertically in the High-Atlas and marks a vertical fault which is well-known as the South-Atlas fault. Its southern short flank outcrops slightly in the centre of the basin. The layers of the High-Atlas go deep under the plain. This is confirmed by boreholes through alluvium to the Turonian rocks. Other boreholes and geophysical measurements showed variability in the substratum.

The presence of evaporitic layers in the Mesozoic formations of the southern side of the High-Atlas is likely to influence the water quality of the wadis (temporary rivers) that drain this side of the Atlas aquifers and those of the plain. The faulted structure of the Cretaceous-Eocene syncline can also favour hydrodynamic relations between the different aquifers of the plain (Figure 3).

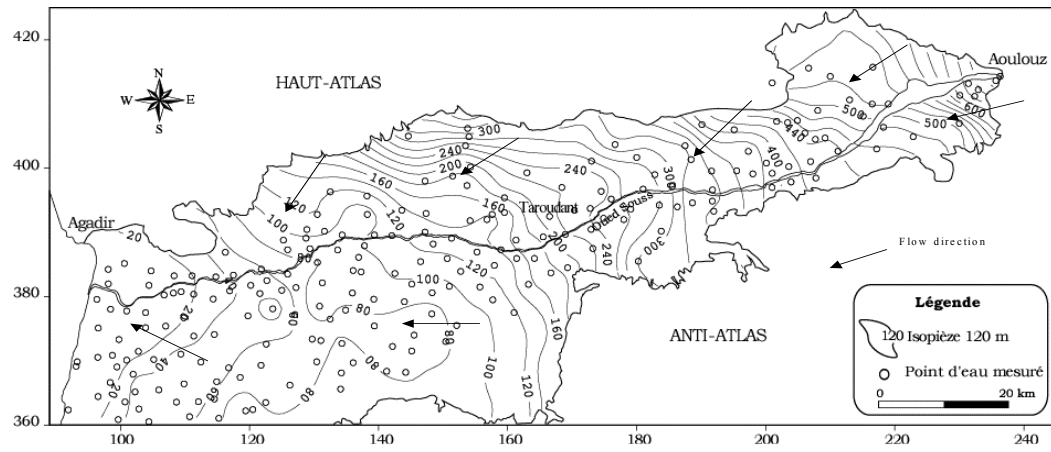


FIG. 3. Piezometric map of Souss aquifer [4]

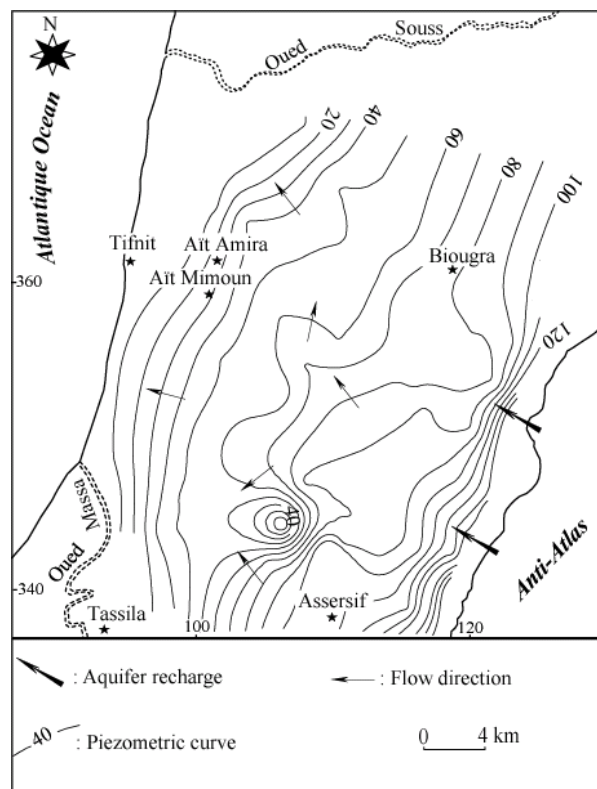


FIG. 4. Piezometric map of Massa-Chtouka aquifer [9]

3. Sampling and analyses

About 70 water samples were collected during two sampling campaigns over a two-year period from surface water bodies (dams and oueds), dug wells, boreholes and springs in various parts of the basin (Figure 6 and Table 1) and analyzed for their chemical and isotopic compositions.

Temperature, pH, EC, and total alkalinity were measured in the field. Chemical analyses of major elements were carried out at the “Laboratoire de Géologie appliqué”, University of Agadir, the analytical laboratories of the Department of Geological and Environmental Sciences, Ben Gurion University of the Negev and, the IAEA laboratories in Vienna respectively. Trace elements (B, Sr) were measured at the analytical laboratories of the Department of Geological and Environmental Sciences, Ben Gurion University of the Negev and at the Department of Geology and Geochemistry, Stockholm University. Cations and boron were determined by ICP and anions by IC. Analytical error did not exceed 5%. The oxygen-18, deuterium and tritium analyses were done at the Isotope Laboratory of the Centre National des Sciences et Technologies Nucléaires (CNESTEN), Rabat, Morocco. Tritium concentrations are expressed in Tritium Units with a precision of ± 0.5 . Deuterium and oxygen-18 were measured by mass spectrometer, reported relative to Vienna-Standard Mean Ocean Water (VSMOW) and expressed in δ values with a reproducibility of $\pm 1\text{‰}$ for D and $\pm 0.1\text{‰}$ for O-18 respectively. Boron isotopes were measured by a negative thermal ionization mass spectrometry technique. The NIST SRM-951 standard was used and isotope ratios are reported as $\delta^{11}\text{B}$ values. Strontium was separated by cation-exchange chromatography using standard techniques at BGU. Isotope ratios were determined using a MAT-261 261 solid-source mass spectrometer at the U.S. Geological Survey, Menlo Park, California.

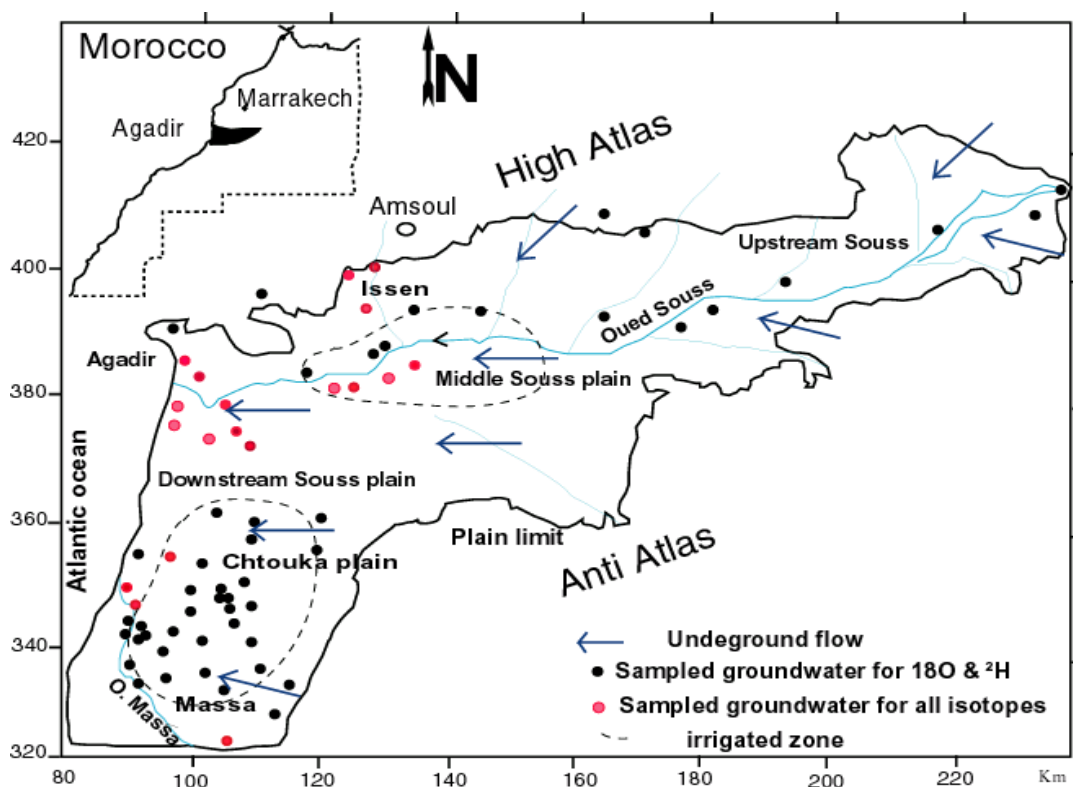


FIG. 5. Situation map of Souss Massa plain, and sampled points in the studied area [10]

Table 1. Sampling water points in the second campaign (* points sampled for the first campaign).

Name	Key	Total depth (m)
*Source Ameskrout	AC 1	Bound spring (Lias)
Puits n° 59	AC 2	100 m
*Bou El Baz	AC 3	surface water
118 Briqueterie	AC 6	40 m
*Puits pour l'AEP (120)	AC 7	80 m
Douar Bouzoug	AC 8	60 m
*Ferme de Ami (Puits n°2)	AC 9	100 m
Puits de Qsebt	AC 24	30
*Puits Ait Oumribt	AC 27	30
Source Aghbalou	AC 33	Spring emerging in the Massa lacustrine limestone
*Jardin Ibn Zaidoun	AC 43	120 m
*Puits n°51	AC 44	120 m
*N°8 Petromin Al Hana (Ait Melloul)	AC 46	110 m
*Forage Ferrugineux Kléa	AC 47	300 m
*Puits ONEP Club Med	AC 48	
*Petromin oil Al Farah (Ait Melloul)	AC 49	100 m
ONEP Ait Melloul	AC 50	
Forage réserve royal	AC 51	60 m (inshore dunes)
Forage Lamzar n°8	AC 58	inshore dunes
Forage Lamzar n°10	AC 59	inshore dunes
Forage ONEP Massa	AC 60	80 m
Station Belfâa	AC 61	70 m

4. Results and interpretation

The overall results are considered in relation to the conceptual cross section and the regional map with all sampled sites [12][13][14] and summarized in Table 2.

4.1. Origin of water

In spite of the scarcity of the measurements of the rain in the Souss-Massa area, it could be noted, that the few more or less dispersed values, show enriched values in the plain, and relatively depleted values towards the mountain ranges (-7.5% in the Amsoul rain gauge, Figure 2). The $\delta^{18}\text{O}$ and $\delta^2\text{H}$ values of water from wells, surface water and springs sampled in 1998 campaign are plotted and compared with this Meteoric World Line in the following sections (Figure 7). The values of the oxygen-18 contents vary respectively between -2.3 and -7.64% , and deuterium between -13.6 to -51.6% . This range displays a high variability of the isotopic input in the area. This figure shows a close similarity between the data of Souss-Massa and the World Meteoric Line, but the slope of the experimental line (6.7) is lower than the World Meteoric Line (8), which seems to demonstrate the relevance of water evaporated from the aquifer system.

In groundwater, the oxygen-18 and deuterium values are related to the precipitation values in the Atlas Mountain (>700 m above sea level (a.s.l.)). The apparently atlantic isotope signature in many groundwater samples from wells is attributed to the contrasted change of the local climate between the plain and the mountain range, but may also be attributed to an increasing evaporative isotope enrichment from irrigation return water. We notice a very clear differentiation between the depleted rains of the rain gauges -4% in the Agadir station (50 m a.s.l) in the west and $>-7\%$ in the mountain station (>700 m a.s.l.) in the east. The increase of isotope values from the east to the west of the region is attributed to the altitude and the continental effect. In addition, the regional distribution of the stable isotopes may be controlled by isotopic enrichment due to the partial evaporation of water; the effect of

an admixture of irrigation return flow is noticed in the irrigated perimeter (middle Souss plain, Chtouka and Massa part) and during flood irrigation, water is submitted to evaporation and becomes isotopically enriched.

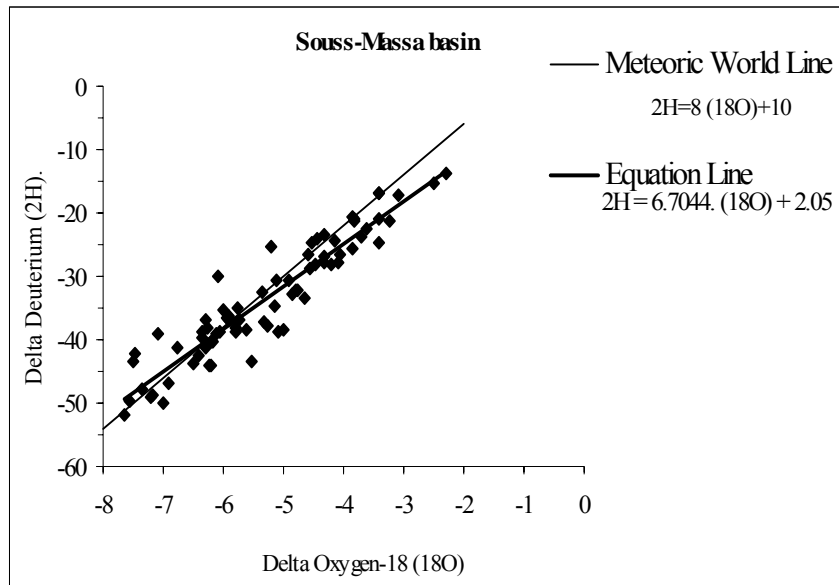


FIG. 6. Isotopic composition of several types of waters in the Souss-Massa watershed [10]

1. On the figure 8 showing the last sampling data, evaporated waters indicate a direct contribution of river coming from dams (Cl < 500 mg/l) or the presence of sea water intrusion or irrigated water return (Cl > 500 mg/l).

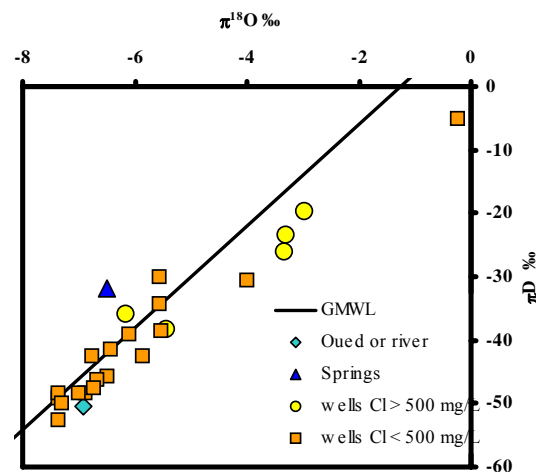


FIG. 7. Deuterium –oxygen-18 in relationship for different types of waters

4.2. Groundwater residence time and origin of salinity

During this project reference was made to the latest studies [2][6][8][9], where electrical conductivity and some chemical tracers (chloride, bromide, nitrate, Ca/Mg, strontium) were measured. These studies show some anomalies related to salinity in the Souss-Massa. Salinity can be explained by several origins: present salt encroachment, palaeosalinity, sea intrusion and wastewaters, particularly in the downstream part. The water-rock interaction is a main source of salinity in the region. The dissolution of Triassic evaporites constitute the main origin of the high salinity in this part of the basin.

The groundwaters are oxidizing and contain quite high nitrate contents (up to 150 mg/l). The Piper diagram (Figure 8) shows a high variability in the salinity levels in some zones (i.e., Massa). So far only reconnaissance results are available for trace elements (ICP-MS). Most waters shows saturation with barite, calcite, dolomite and chalcedony. The Br/Cl ratio is a particularly valuable indicator of different salinity sources.

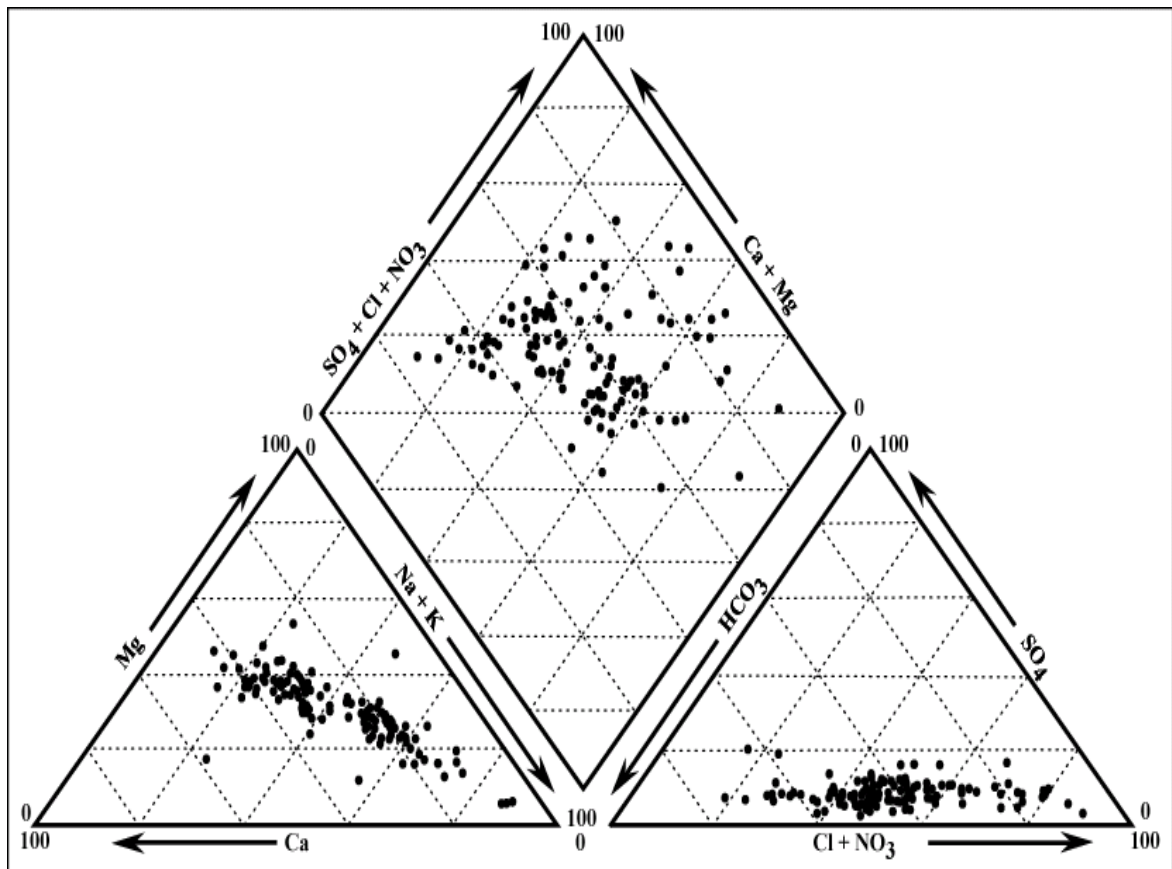


FIG. 8. Piper diagram for groundwaters in Chtouka-Massa [9]

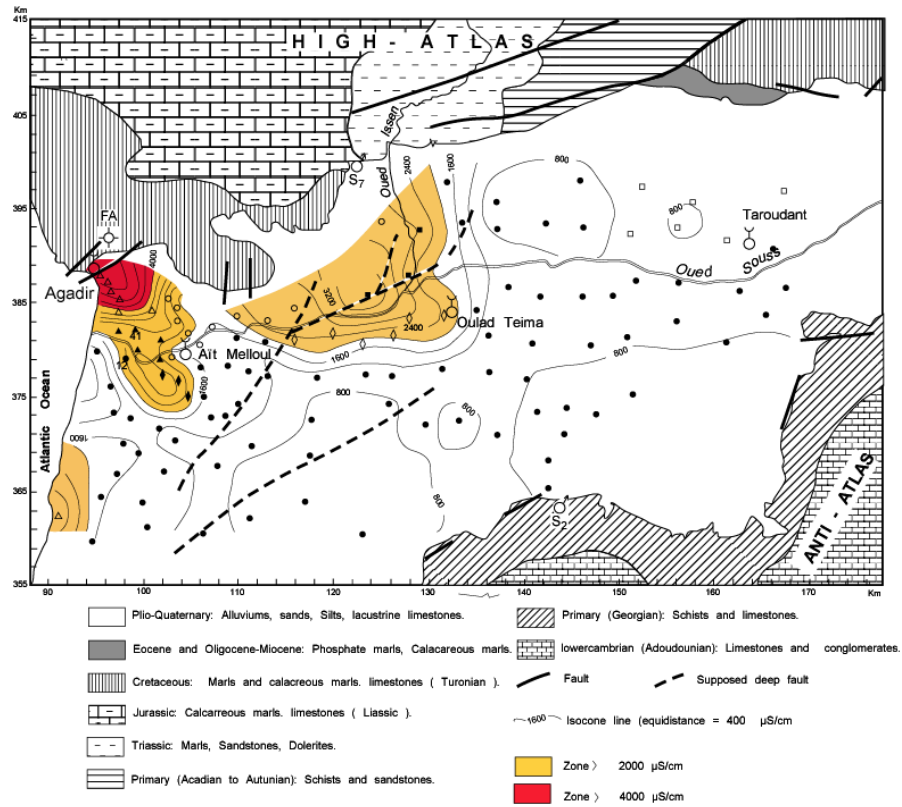


FIG. 9. Salinity anomaly in Souss basin ([11], modified)

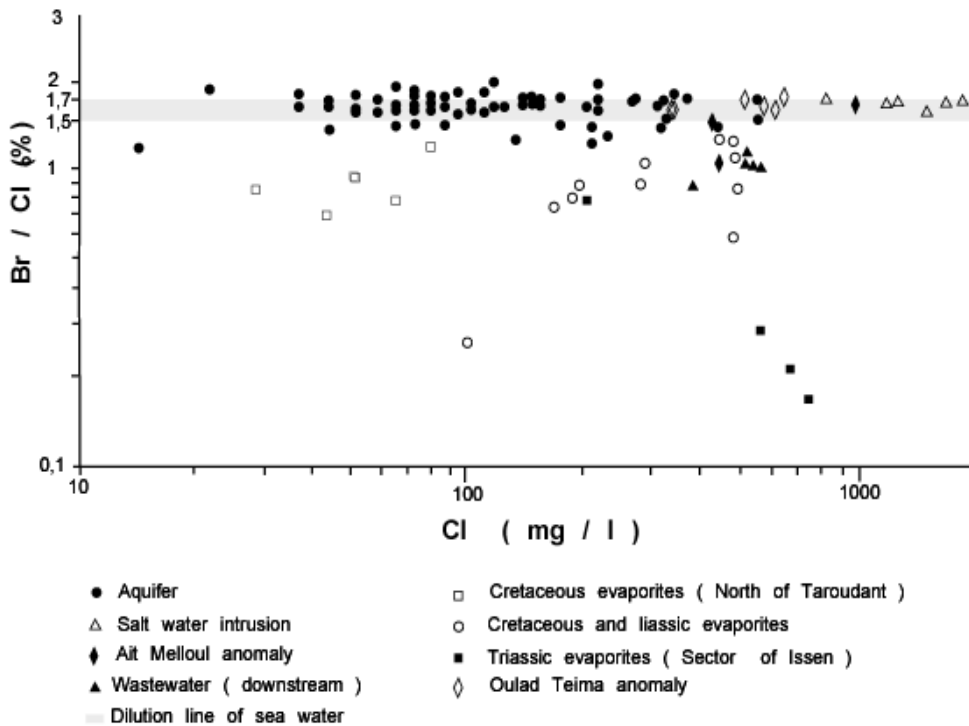


FIG. 10. Relationship between bromide and chloride in Souss groundwaters, according to Figure 10 in [1]

The origin of salinity anomalies in Souss groundwater can be distinguished through analysis of bromide contents. Br/Cl molar ratio thus distinguishes marine influenced areas (recent and palaeo salt intrusion, precipitation and aerosols coming directly from the ocean), from evaporitic influence areas (otcrops of salty formations) or anthropic (wastewaters), depleted versus the oceanic domain. This result enables to assign the downstream conductivity anomalies (Figure 2) to the existence of a present marine intrusion, to sedimentary palaeosalinity and wastewaters, those of the main Souss to evaporites and recycling of irrigation waters.

In order to confirm or to clarify these salinity sources, a multi-isotope tracing was tried in this CRP (Figure 12).

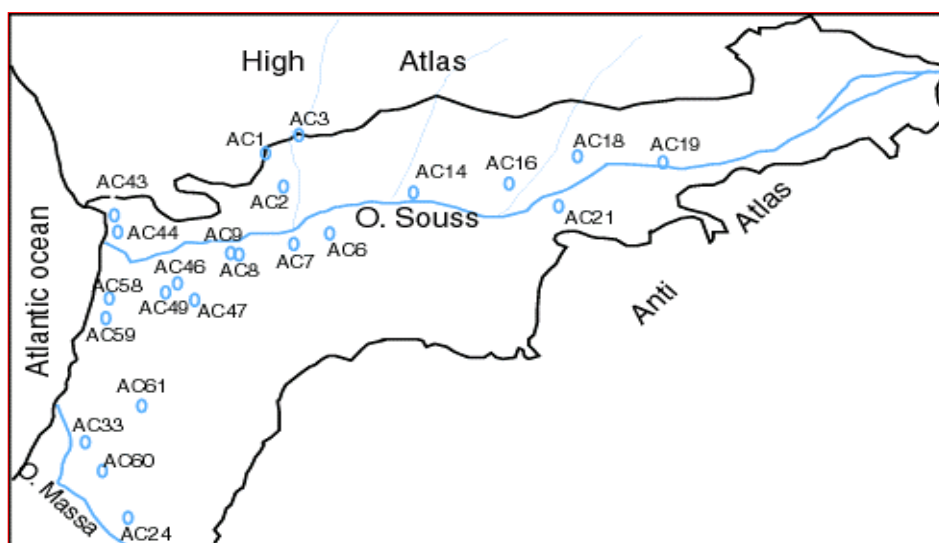


FIG. 11. Situation of wells sampled for radioactive isotope measurements

The results of this study from nineteen groundwater samples from the middle part of Souss-Massa basin (Figures 2 and 10), and the coastal part suggested that relatively old water is mined at some wells, and seawater intrusion is just one component of the dissolved solids present in these waters.

4.2.1. Tritium

The tritium contents are very low (Figure 13). This variation of the tritium contents in the aquifer shows two types of groundwater: (i) an old deep groundwater circulating and not influenced by the modern recharge and; (ii) a water mixing near the surface including a modern water contribution. However, considering that significant mixing may occur within the groundwater system, water having measurable tritium is interpreted as recharged after 1952. Furthermore, since the rainfall is low in the plain, the lack of tritium suggests that the aquifer in this area did not receive water through vertical infiltration. Therefore, the very low tritium values suggests that groundwater recharge follows a long path, as also indicated by oxygen and deuterium isotopes and by a long residence time required by saturation or supersaturation with respect to some minerals. The fact that some samples do not contain tritium suggests that they do not contain modern components and are thus not susceptible to contamination from the surface in deep wells are not connected to modern recharge, indicating that water followed a long flow path. The slight evaporation recorded by stable isotopes in water from the

southern margin close to the Anti-Atlas Mountains indicates that groundwaters are subject to a drier climate, marking the Anti-Atlas Mountains, which form a barrier against the influence of the Saharan climate.

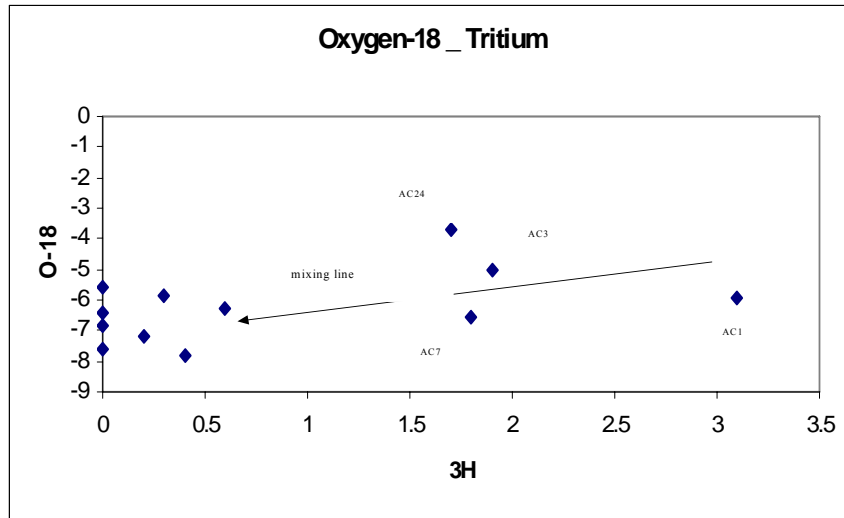


FIG. 12. Relationship between O-18 and Tritium

4.2.2. Strontium isotopes

The isotopic composition of dissolved strontium also indicates mixing of groundwater from several origins (Figure 14).

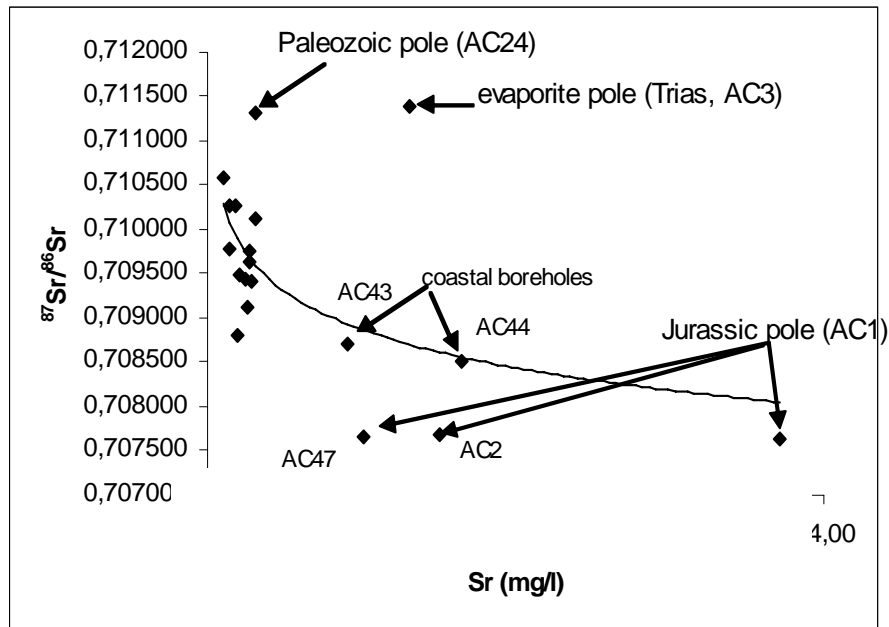


FIG. 13. Differentiation of 3 groups showing a mixture with recent waters from the recharge area

The plot in Figure 13 showss three characteristic ratios: (i) 0.707 to 0.7075 (AC1, AC2 & AC47) which characterize the gypsum-containing formations in the mountain range and the deep aquifer; ≥ 0.71 (AC3, AC24) which can be explained by leaching of schists and crystalline rocks; 0.708 characterizing sea intrusion in some deep coastal wells (AC43, AC44, AC49 & AC46). This is in agreement with the geologic formations in the basin which are constituted by several facies (evaporites, limestones, crystalline rocks).

Figure 14 shows the relationship between nitrate and strontium isotope ratios, which confirm the anthropogenic influence (fertilizers and wastewaters) on groundwater quality in the aquifers. This hypothesis is in agreement with the very developed agricultural activity in the Plain (example AC6, AC9).

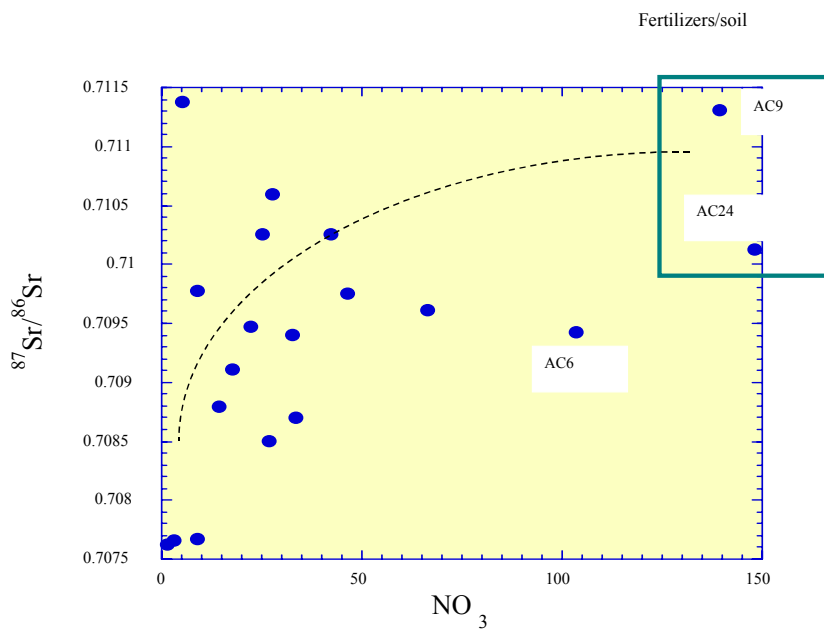


FIG. 14. Relationship $^{87}\text{Sr}/^{86}\text{Sr}$ vs NO_3

4.2.3. Boron isotopes

Some samples are analyzed for boron isotopic results and show a wide isotopic range (Figure 15)

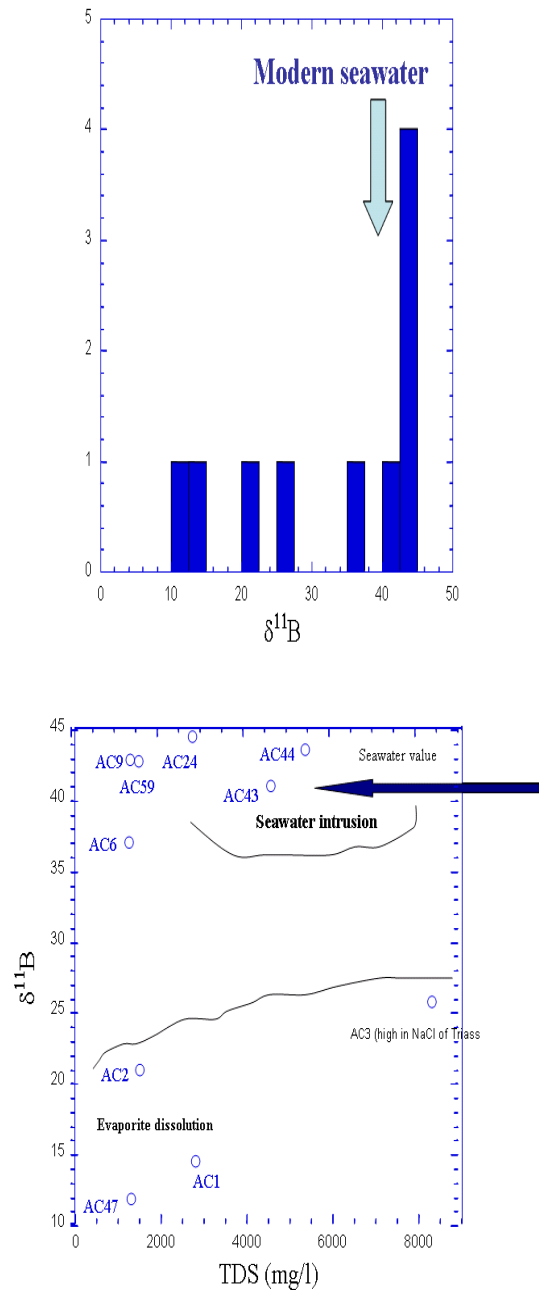


FIG. 15. Results of boron isotopic analysis

The figure above shows clearly the presence of seawater intrusion in AC43 (n°51) and AC44 (Ibn zaidoun) situated near the coast. Also, evaporite dissolution (AC47, AC1, AC3, AC2), in agreement with the geological context. Boul Baz sample (AC3) represents surface water which dissolves Triassic evaporites (NaCl).

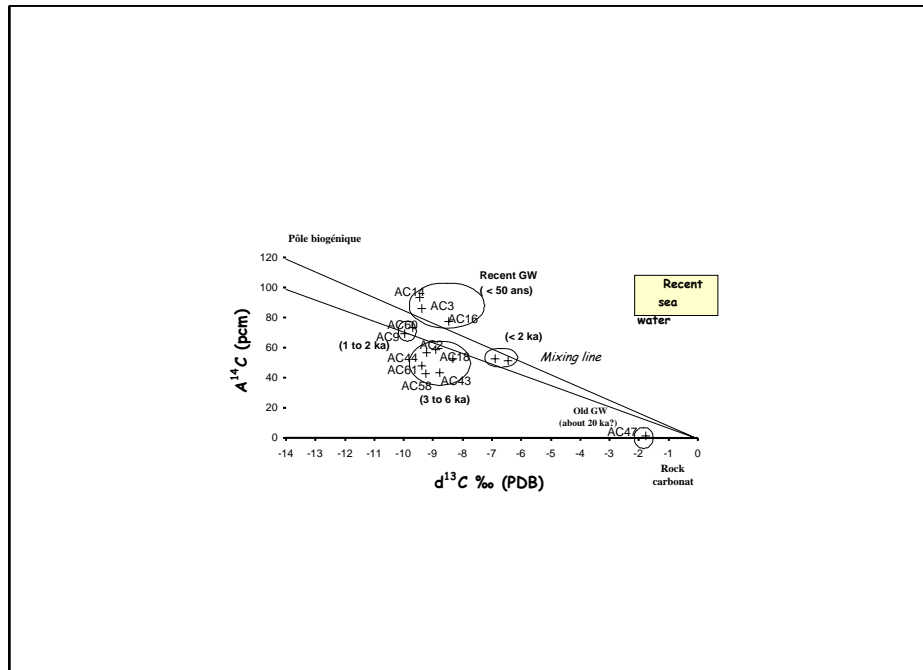
4.2.4. Radiocarbon

The radiocarbon results in the Souss-Massa aquifer vary between 42 and 93 pmc, indicating (Pearson corrected) ages up to 6000 years with an average of 3000 years BP (Table 3 and Figure 16). In the Turonian aquifer a value of 1.35 pmc indicates age of ca 20 kyr.

Table 3. Carbon isotope data.

<i>Code</i>	$\delta^{13}\text{C}$ (‰ PDB)	Activity ^{14}C (pCM)	Corrected age (Pearson model) years BP
AC2	-8.92	58.9	2850 ± 100
AC3	-9.39	85.98	Recent
AC6	-6.44	51.24	1300 ± 50
AC9	-9.96	69.17	2400 ± 100
AC14	-9.46	93.3	Recent
AC16	-8.47	77.04	Recent
AC18	-8.34	52.4	3250 ± 100
AC21	-6.9	52.94	1600 ± 50
AC43	-8.76	43.39	5200 ± 100
AC44	-9.23	56.77	3400 ± 100
AC47	-1.76	1.35	20600 ± 100
AC58	-9.25	42.5	5900 ± 100
AC60	-9.71	73.35	1700 ± 50
AC61	-9.39	47.77	5000 ± 100

The most recent groundwaters are found in the middle part of the basin and along the Souss wadi which indicate the influence of the recent recharge from the High Atlas Mountain. A recent recharge component can be also assumed from the Turonian outcrop near high Atlas mountain or by circulation along the faults.

FIG. 16. Relationship between $\delta^{13}\text{C}$ vs $A^{14}\text{C}$

4.2.5. Others age tracers

The radioactive isotopes of chlorine and iodine, with their very long half-lives, cannot be used for dating, but their concentrations may help to characterize the sources of groundwater salinity, which are multiple: intrusion of modern seawater, but also ancient seawater, irrigation return, and dissolution of evaporites. This is confirmed by the Br/Cl⁻ and I/Cl⁻ ratios in groundwater: intrusion of seawater is identified in the coastal part of the aquifer, but water/rock interaction is another significant source of salinity.

Dissolved ⁴He concentration ranges up to 2×10^{-7} cm³ STPg⁻¹, sometimes suggesting very long residence times as great as several tens of thousands of years.

Boron and strontium isotope results are in good agreement and confirm at least 3 salinity sources: marine intrusion (present day and/or Pliocene sea water); Jurassic and Cretaceous evaporates; local contribution from the unsaturated zone; anthropogenic pollution.

This is confirmed by the distribution of Br/Cl ratio in groundwater: intrusion of seawater is identified in the coastal part of the aquifer (Figures 10 and 11), but water/rock interaction is another significant source of salinity. The isotopic composition of dissolved strontium also indicates mixing of solutions from several origins.

5. Conclusions

The aim of this work is to determine the acquisition modes of the water mineralization of the Souss unconfined groundwater to understand its hydrodynamical behavior and to define a way of studying alluvial groundwaters in semi-arid zones, taking into consideration the geological and hydrogeological conditions, and looking for appropriate hydrochemical traces.

Stable isotope ratios indicate how the Souss-Massa shallow aquifer is highly influenced by the contribution of the Atlas Mountain, which has a high rainfall, particularly in its upstream part. Data indicate that the Atlas Mountain with its depleted isotope values (-6 to -8 ‰ $\delta^{18}\text{O}$), constitutes the main recharge area of the Souss-Massa shallow aquifer (Figure 17).

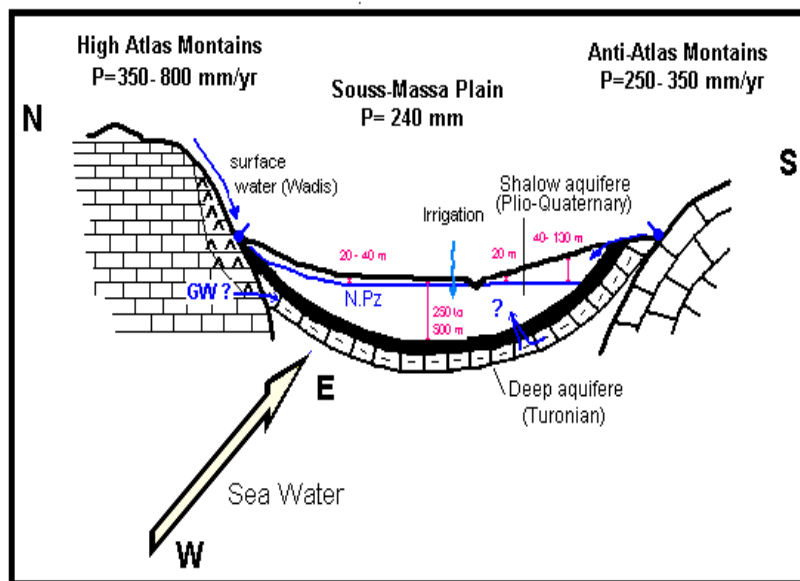


FIG. 17. Schematic view of groundwater circulation in the Souss-Masse Plain

Taking into account the hydrogeological and climatic contexts of the region, several potential sources of groundwater salinity can be mentioned:

- 1 Sea-water intrusion: low Na/Cl, marine Br/Cl, low SO₄/Cl, marine $\delta^{11}\text{B}$ (~40‰), and low $^{87}\text{Sr}/^{86}\text{Sr} \sim 0.7085$.
- 2 Dissolution of evaporites: high SO₄/Cl, low $\delta^{11}\text{B}$ (12-21‰) and very low $^{87}\text{Sr}/^{86}\text{Sr}$ (~0.7076);
- 3 Agriculture return flows : characterized by high nitrate, high $\delta^{11}\text{B}$ (45 ‰), and high $^{87}\text{Sr}/^{86}\text{Sr} \sim 0.711$ (fertilizers). This composition suggests interaction of seawater/brine with silicate rocks (crystalline and schist) for obtaining a non-marine signature.
- 4 The radiocarbon groundwaters "ages" range from 0 to about 6 ka, with one exception (AC47: ferruginous borehole). This result of radiocarbon does not confirm the hypotheses based on high ^4He concentrations. Also, no detectable effect of recent seawater intrusion.
- 5 Radiogenic excess ^4He ranges up to $2 \times 10^{-7} \text{ cm}^3 \text{ STP.g}^{-1}$ indicating ages as great as several tens of thousands of years.

These conclusions are in agreement with the very variable lithology and tectonic and high agricultural activity of the region. All the aquifers are very vulnerable, particularly in Souss-Massa plain.

The diagram below (Figure 18) schematizes these conclusions indicating the different components of salinity origins and groundwater circulation.

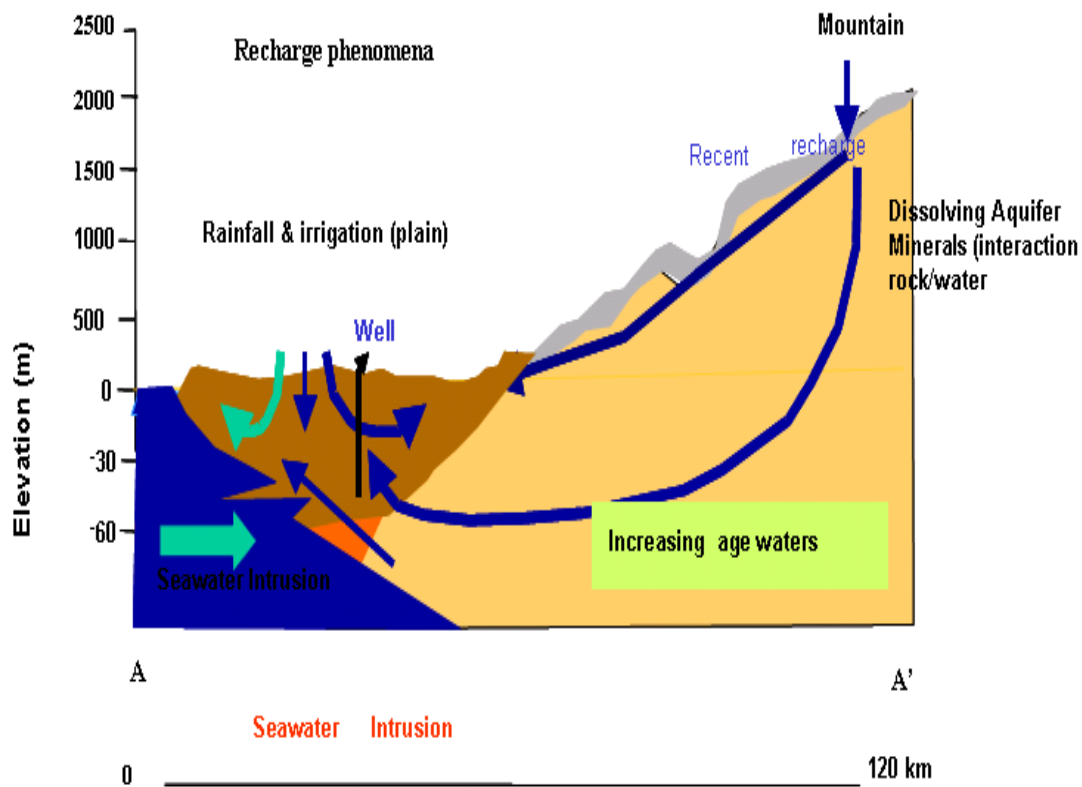


FIG. 18. . Sources of groundwater salinity are multiple: intrusion of modern seawater, ancient seawater, irrigation return and dissolution of evaporites [15]

6. Recommendations and Problems

The following measurements are still required and recommended in a further round of sampling;

- 1 TOC.
- 2 CFC's.
- 3 Quantitative analyses for trace elements, including F, I, U (trace element analyses on the existing water samples are also still to be completed).
- 4 Complete database for reactive isotopes (B, S, Sr, C).
- 5 ^{15}N to distinguish origins of nitrate.

The following questions remain;

- 1 Clear definition of the modern component and the contribution of pollution.
- 2 Lateral recharge contributions to the alluvial aquifer.
- 3 Feedback to hydrogeological and management model and recommendations.
- 4 Recommendation to establish a scientific local committee to ensure progress in the interpretation of information and identification of future analytical requirements – and to work closely with the Moroccan national coordination.

Acknowledgements

We are grateful for the help provided by all Laboratories where the analyses have been made. Furthermore, we thank the Hydraulic Agency of Souss-Massa Basin. We also would like to thank Drs. J.L. Michelot, M. Edmunds, G.M. Zuppi and A. Vengosh, for their help at various stages.

REFERENCES

- [1] HSISSOU, Y., BOUCHAOU, L., MUDRY, J., MANIA, P., CHAUVE Use of chemical tracing to study acquisition modalities of the mineralization and behaviour of unconfined groundwaters under a semi-arid climate: the case of the Souss plain (Morocco). *Env Geol* (2002) 42: 672-680
- [2] BOUTALEB, S. (2000) Influence de la géologie et du climat des bassins versants sur la qualité des eaux d'une grande nappe alluviale en climat semi-aride: Application aux relations hydrologiques entre le Haut atlas et la plaine du Souss; PhD, Université Ibn Zohr, Faculté des Sciences, Agadir, Maroc.
- [3] KRIMISSA, S., MICHELOT, J.L., BOUCHAOU, L., MUDRY, J., HSISSOU, Y., Sur l'origine par altération du substratum schisteux de la minéralisation chlorurée des eaux d'une nappe côtière sous climat semi-aride (Chtouka-Massa, Maroc) *Comptes rendus Geoscience*. (2004) Volume 336 Numéro 15, 1363-1369.
- [4] HSISSOU, Y., (1999) Impact de l'environnement naturel et anthropique sur la qualité des eaux alluviales en zone semi-aride: cas de la plaine du Souss (Maroc). Thèse d'état, Université Ibn Zohr, Faculté des Sciences, Agadir Maroc.
- [5] EKWURZEL B., MORAN JE., HUDSON G.B., BISSANI M., BLAKE R., KRIMISSA M., MOSLEH N., MARAH H., SASAF N., HSISSOU Y., BOUCHAOU L., (2001). An isotopic investigation of salinity and water sources in the Souss-Massa basin, Morocco. *Cyber Proc Salt Water intrusion and Coastal Aquifers First Intern Conf*.
- [6] BOUTALEB, S. L., BOUCHAOU, J., MUDRY, Y., HSISSOU, J., MANIA, ET, CHAUVE, P., Acquisition of salt mineralisation in semi-arid watershed. The case of oued Issen (Western Upper Atlas, Morocco). (2000) *Hydrogeology Journal* (2000) Vol. 8, pp. 230-238.

- [7] EL MORJANI ZINE ELABIDINE, Conception d'un système d'information à référence spatiale pour la gestion environnementale; application à la sélection de sites potentiels de stockage de déchets ménagers et industriels en région semi-aride (Souss, Maroc). (2003) Vol. 42, Section des Sciences de la Terre, Université de Genève, Suisse.
- [8] DINDANE, K., BOUCHAOU, L., HSISSOU, Y., KRIMISSA, M., Groundwater in the Souss upstream basin, southwestern Morocco: evidences to its chemical evolution and origin. (2003) JAES, 36, pp. 315-327
- [9] AHKOUK, HSISSOU, BOUCHAOU, KRIMISSA, MANIA– Impact des fertilisants agricoles et du mode d'irrigation sur la qualité des eaux souterraines (cas de la nappe des Chtoukas, bassin du Souss-Massa). (2003) Africa Geoscience Review, Vol. 3, n°4.
- [10] BOUCHAOU, L., HSISSOU, Y., KRIMISSA, M., KRIMISSA, S., MUDRY, J., (2005) ^2H and ^{18}O isotopic study of ground waters under a semi-arid climate. Environmental Geochemistry, pp. 57-64, Green Chemistry and Pollutants in Ecosystems, E. Lichtfouse, J. Schwarzbauer, D. Robert (Eds.) XXVI, 780 p. 289 illus. ISBN: 3-540-22860-8 Springer.
- [11] HSISSOU Y., MUDRY J., MANIA J., BOUCHAOU, L., CHAUVE, P., Utilisation du rapport Br/Cl pour déterminer l'origine de la salinité des eaux souterraines: exemple de la plaine du Souss (Maroc). (1999) C. R. Acad. Sci. Paris, 1999. 328, 381-386.
- [12] AHKOUK, S. (2004) Contribution à l'étude de la contamination des eaux souterraines par les Nitrates: cas des Chtouka et du Souss, PhD, Université Ibn zohr, Faculté des Sciences, Agadir, Maroc.
- [13] KRIMISSA, S., (2005) Nappes superficielles en zone semi-aride: origine des eaux et de la salinité, renouvellement: exemple des nappes Massa et Souss, Maroc). Thèse PhD soutenue à l'Université de Franche Comté, Besançon, France.
- [14] DINDANE Kh.(2005) Apports des techniques hydrogéochimiques et isotopiques a la compréhension des systèmes aquifères des régions arides et semi arides : application a la nappe du Souss amont, (sud-ouest du Maroc). Soutenue en mars 2005.
- [15] BOUCHAOU, L., QURTOBI, M., GAYE, C.B., HSISSOU, Y., IBN MAJAH, M., MICHELOT, J.L., MARAH, H., SAFSAF, N., EL HAMDAOUI, A. Isotopic investigation of salinity and water resources in the souss-Massa basin (Morocco). (2003) International Symposium on isotope hydrology and integrated water resources management 19- 23 May, 2003, Vienna, Austria.

Table 2. Sampling results.

						contents in mg/l									
Code	X	Y	T °C	pH	EC. µs/cm	HCO3	Cl	SO4	NO3	Na	K	Ca	Mg	B	⁸⁰ Br
AC1	122.75	399.52	24.1	6.5	2776.5	251.7	60	1745	8.6	41.3	31.9	482.4	160.8	0.125	0.09
AC2	125.39	393.33	24.5	6.6	1932	313.9	86.2	691.4	16.3	60.9	6.0	201.6	104.8	0.075	0.173
AC3	126.077	402.75	14.2	7.9	6504.5	199.2	2501.6	734.8	3.8	1107.9	21.3	268.7	76.1	0.509	1.663
AC6	133.42	402.834	22.7	7.4	1885.5	334.9	346.1	167.6	59.6	138.9	11.7	88.0	97.0	0.140	0.977
AC7	128.43	382.91	22.4	7.4	1947	381.8	359.2	74.5	29.9	134.4	3.2	95.9	102.8	0.137	1.853
AC8	116.66	380.82	24.1	7.0	947	284.3	90.1	111.2	11.4	44.6	5.3	62.3	58.8	0.052	0.204
AC9	116.245	380.991	21.7	6.8	1957.5	406.0	247.0	755.0	50.2	84.6	3.6	275.4	83.6	0.131	1.478
AC24	99.77	330.66	24.6	6.8	4267	789.0	1951.0	289.2	92.1	1217.5	16.5	232.9	93.8	0.562	12.21
AC33	91.47	344.82	25.1	7.7	1163.5	325.5	173.0	43.9	20.9	81.1	2.8	57.6	60.6	0.057	0.62
AC43	96.93	387.28	24	6.6	4118	453.7	1280.1	223.0	17.0	455.7	10.9	141.8	134.4	2.571	6.677
AC44	97.37	385.879	29.1	6.7	8425.5	313.4	1897.9	301.5	14.6	477.4	15.0	288.8	217.4	0.323	6.264
AC46	105.09	376.23	24.9	7.3	1030.5	402.2	132.6	240.9	42.0	113.0	4.3	80.6	68.1	0.072	2.695
AC47	107.74	375.74	31	6.8	2039	365.2	298.2	388.7	6.8	174.0	27.9	119.5	102.5	0.364	0.566
AC49	105.45	376.226	25.6	7.2	1644.5	360.4	200.0	395.6	11.5	106.1	4.5	96.9	76.2	0.096	0.709
AC50	105.01	379.26	24.8	6.5	1665.5	499.0	458.3	33.2	33.5	266.7	5.7	87.9	42.6	0.109	1.093
AC58	99.25	383.9	24.4	6.9	1549	382.4	201.2	140	10.2	230.3	4.5	94.3	70.3	0.248	
AC59	96.32	370.98	24.9	7.0	1388	411.3	322.4	102.6	16.4	174.6	7.3	76.9	69.8	0.136	
AC60	90.87	335.32	25	7.0	986.5	496.7	91.3	44.1	16.1	78.5	3.7	66.2	50.4	0.049	
AC61	96.42	346.25	23.7	6.9	817.5	403.8	252.4	235.3	9.9	178.6	24.1	101.9	75.4	0.205	
AC14	162.153	391.542	22.7	7.2	975										
AC16	187.762	401.016													
AC18	213.257	415.11													
AC21	191.322	393.926													
AC31	91.077	341.539													

Table 2. Sampling results. (continuation)

Code	X	Y	$^{87}\text{Sr}/^{86}\text{Sr}$	1/Sr	^{18}O	^2H	^3H	^{129}I mg/l	$^{129}\text{I}/\text{I}$ (e-15)	^4He cm ³ STP/g H ₂ O	^4He eq_div_ ^4He meas	Ar cm ³ STP/g H ₂ O	$^{36}\text{Cl}/\text{Cl}^*(1\text{e}-15)$
AC1	122.75	399.52	0.7076	0.077	-5.93	-32.05	3.1	0.056					28
AC2	125.39	393.33	0.7077	0.190	-5.58	-29.75	0						
AC3	126.077	402.75	0.7114	0.218	-5.02	-31.05	1.9	0.168					0
AC6	133.42	402.834	0.7094	1.145	-6.27	-37.95	0.6						
AC7	128.43	382.91	0.7098	1.027	-6.56	-38.9	1.8	0.035					58
AC8	116.66	380.82	0.7098	1.916	-7.63	-46.85	0						
AC9	116.245	380.991	0.7101	0.935	-6.18	-38.65		0.027		4,8635 E-08	0.936000255	0.00031748	59
AC24	99.77	330.66	0.7113	0.909	-3.71	-20.3	1.7	0.92	16000				
AC33	91.47	344.82	0.7103	2.024	-6.45	-37.35	0	0.001					18
AC43	96.93	387.28	0.7087	0.316	-4.71	-24.6		0.541	18000	4,8522 E-08	0.938168188	0.00034494	5
AC44	97.37	385.879	0.7085	0.173	-5.84	-29	0.3	0.063		1,107 E-07	0.411210622	0.00030788	0
AC46	105.09	376.23	0.7088	1.477	-7.81	-47.75	0.4	0.116		2,4392 E-07	0.18662434	0.00034565	36
AC47	107.74	375.74	0.7077	0.281			0						
AC49	105.45	376.226	0.7091	1.114	-7.19	-47.9	0.2	0.041	16000				31
AC50	105.01	379.26	0.7096	1.056	-6.82	-45.45	0	0.012		1,0923 E-07	0.416742615	0.00034352	
AC58	99.25	383.9	0.7094	0.980	-6.56	-46.3							
AC59	96.32	370.98	0.7095	1.372	-6.4	-45.75							
AC60	90.87	335.32	0.7106	2.740	-6.05	-43.15							
AC61	96.42	346.25	0.7103	1.621	-5.4	-38.85							
AC14	162.153	391.542			-7.35	-24.05	1.3						
AC16	187.762	401.016			-7.79	-46.45	1.3						
AC18	213.257	415.11			-7.26	-42.45	0						
AC21	191.322	393.926			-6.9	-43.4	0.9						
AC31	91.077	341.539			-6.28	-37.75	0						
					-5.38	-38.3							

Isotopic investigation of saline water intrusion and related impacts on potable water quality in the coastal aquifer of Karachi, Pakistan

A. Mashiatullah^a, R. M. Qureshi^a, T. Javed^a, M. A. Tasneem^a, M. Fazil^a, N. Ahmad^b, E. Ahmad^c

^aPakistan Institute of Nuclear Science and Technology, Islamabad, Pakistan, Islamic Republic of

^bCenter for Advance Studies in Earth Sciences - University of the Punjab Lahore, Pakistan, Islamic Republic of

^cWorld Wide Fund for Nature (WWF), Karachi, Pakistan, Islamic Republic of

Abstract. Environmental isotopes such as $\delta^2\text{H}$, $\delta^{18}\text{O}$, $\delta^{13}\text{C}$, $\delta^{34}\text{S}$ and physico-chemical techniques are used for the investigation of the origin of groundwater salinity in the potable shallow and deep groundwater in the coastal aquifer of Karachi Pakistan. Water samples from seawater, surface/groundwater were collected from various locations along polluted streams/rivers namely: Layari River and Malir River, Hub Dam, Hub River and local sea shallow seawater off Karachi coast during period of 2001 to 2003 for in-situ chemical and stable isotope analyses. Physico-chemical parameters such as pH, electrical and conductivity (E.C.) and salinity were measured in-situ. The hydro-chemical and stable isotope results indicate that the shallow/phreatic aquifers are recharged by a mixture of fresh waters of Indus River and Hub River as well as polluted Layari and Malir rivers and their feeding drains both under natural infiltration conditions and artificially induced infiltration conditions and to a much smaller extent from direct recharge of local precipitation. As far as deep groundwater is concerned, the confined aquifer hosts a mixture of rainwater infiltrating around hinterlands and surrounding regions including coastal Karachi as well as from sea seawater intrusion under natural infiltration conditions or under induced recharge conditions.

1. Introduction

Pakistan bears a 960 km long coastline along the northern boundary of Arabian Sea in Indian Ocean. It consists of the Sindh Coast (215 km long) and the Baluchistan/Makran Coast (745 km long). The coastal belt of Pakistan is one of the eight ecological zones, which are the most under developed and non-productive areas in the world. The entire coastal strip is arid with less than 20 mm precipitation per year. Salt tolerant, xerophytic species are common vegetation type. Shallow aquifers along the coastline mostly host saline groundwater due to intrusion of seawater and there is an acute shortage of fresh water resources for drinking and agricultural purposes. The most important coastal dwellings are Karachi, Ormara, Pasni, Gwadar, and Jiwani. Among these, Karachi is the largest coastal city, which lies on the extreme side of Sindh Coast towards the Indus River Delta.

Coastal Karachi is by far, the most populous (~10 million inhabitants as per 1998 census) and the largest industrial (more than 1000 large industrial units) base of Pakistan with a coastline extending up to about 80 km (Figure 1). The major industries in Karachi include: tanneries, textile, chemical, iron and steel, pharmaceutical, metallurgical, vegetable oil, power plants, oil refineries and a large number of cottage industries. According to an estimate, the Metropolis Karachi generates approximately 262 million gallons per day of domestic and industrial wastes, out of which approximately 40% is

generated by municipal sources while 60% is generated by industry. Approximately 80% of the untreated sewage which also includes untreated industrial effluents from industrial units located at Sindh Industrial Trade Estate (SITE), Longhi Industrial Estate (LITE) and Korangi Industrial Area of Karachi is discharged into the sea mainly through public sewers, and natural water courses such as nullahs, Layari River, Malir River as well as Ghizri Creek and Korangi Creek. Discharge of raw sewage into the natural water resources is not only affecting the quality of surface water resources but is also a potential threat in expectedly deteriorating the quality of shallow potable groundwater through seepage of polluted stream waters under natural conditions as well as under artificially induced recharge conditions caused by heavy pumping of the local aquifer.

In Karachi freshwater resources are very limited. The available shallow groundwater and deep groundwater is exploited for certain domestic and industrial uses. Prolonged over-pumping of groundwater or other alterations of the natural equilibrium between recharge and discharge regimes of coastal aquifer system in Karachi can lead to an encroachment of the interface between seawater and freshwater, through intrusion and/or up-coning. Contamination by salty seawater can further elevate deterioration of groundwater quality in the coastal aquifer. A two to three percent mixing of coastal aquifer water with seawater makes freshwater unsuitable for human consumption. A five percent mixing makes it unusable for irrigation [1].

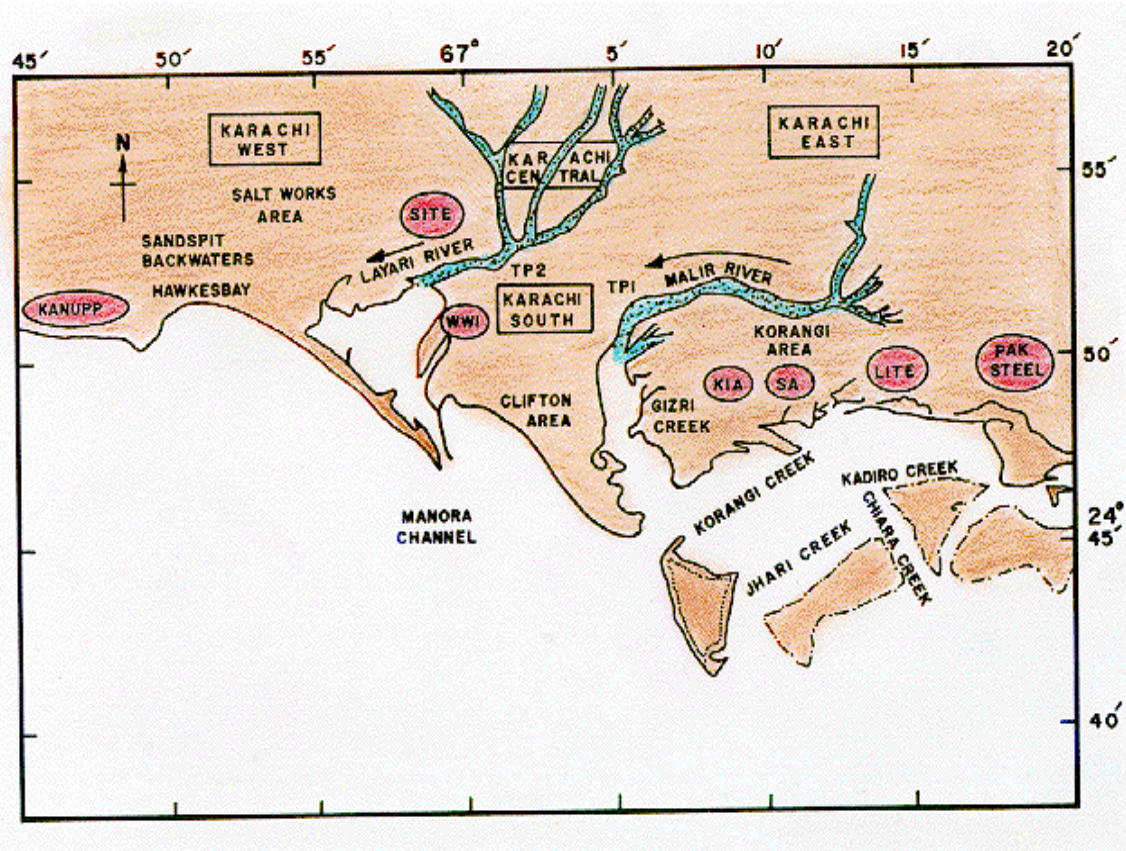


FIG. 1. Karachi map showing the location of industrial areas

2. Description of Study Area

The city of Karachi lies in the Hub River Basin and the Malir River Basin. The Malir River Basin is drained by the Malir River and the Layari River. The coastal aquifer of Karachi is, mainly recharged by seepage from the Hub River, the Hub Dam as well as the Malir and the Layari Rivers. The Hub River lies on the western frontier of Sindh and for some distance the boundary between Sindh and the Baluchistan provinces. It flows about 30 kms to the west of Karachi along the Karachi-Lasbela boundary. It falls into the Arabian Sea near Cape Monze, with a total drainage course length of

336 km. Its principal tributaries are the Saruna, the Samotri and the Wira Hub. Hub River gradually widens and for some 80 kms from its mouth, is bordered by fine pastureland. Water is always found in pools, but the river is being utilized for irrigation and drinking purposes after building of the Hub Dam in the north-west of Karachi in the year 1980. The Hub Dam is 46 meters above the downstream riverbed. The dam has a gross storage of 1000 million cubic meters submerging about 8,000 ha of barren land. Its live storage is 920 million cubic meters with a life of ~75 years. The canal system is 32 km of main canal, 35 km of branch canal and 40 km of minors. The main canal capacity is 370 m³/s. A canal of 200 m³/s capacity is designed to supply 89 MGD to the city of Karachi, 15 MGD to the city of Lasbela and 167 m³/s to irrigate 8400 ha of land in the Bela District. The Malir River Basin hosts the Malir River and the Layari River and lies in the coastal belt. The Malir River flows in the east of Karachi while the Layari River flows through the heart of Karachi city. In the up-stream region, these rivers have important streams that drain the hinterlands of Karachi. These rivers have been the source of fresh water supply for the Karachi metropolis for quite some time. However, both the watercourses are polluted with the passage of time due to input of vast quantities of untreated industrial and domestic wastes.

3. Water Supply Scenario for Coastal Karachi

Karachi has a complex water supply system that developed over a period of more than 100 years. The shallow groundwater near the coastal belt is moderately saline. The drinking water supply to most of the population in Karachi is provided through three schemes:

- i) reserves in the nearby Hub Dam;
- ii) exploitation of relatively adequate quality potable water in selective zones within the city by pumping wells and dug wells;
- iii) pumping of piped water from the Indus River near Thatta City about 160 km away from Karachi;

The Hub Dam reservoir capacity is insufficient to maintain long-term supplies of drinking water to the population of Karachi. During the past 15 years, the Karachi Development Authority (KDA) has installed a large number of pumping and open wells into the Malir Basin to withdraw shallow and deep groundwater to meet requirements for the irrigation water supply (to raise vegetables, fruits, dairy and poultry) and drinking water supply for the ~10 million inhabitants of Karachi. Excessive pumping of groundwater and continuous depletion of water table is likely to result in seawater intrusion into the Malir Basin under natural seepage conditions and under artificially induced conditions of recharge of saline seawater in the coastal aquifer(s) of Karachi. It is feared that any further depletion of water table in coastal aquifer of Karachi will enhance seawater intrusion, thereby, affecting the drinking water quality of potable water in the coastal aquifer system. Ultimately, the whole aquifer water will be unfit for use not only for drinking purposes but also for domestic, industrial and irrigation purposes. It is, therefore, necessary to encourage groundwater recharge in the Malir River Basin on one hand and on the other hand define the existing water quality scenario of coastal aquifers of Karachi using modern & relatively precise techniques such as nuclear techniques so as to evaluate possibilities and impacts of seawater intrusion under heavy pumping of the Malir Basin.

4. Objectives

The growing concerns on deterioration of groundwater systems due to disposal of untreated domestic sewage and industrial effluents into surface water courses (mainly: Malir River, Layari River etc.) and its partial recharge under natural infiltration conditions and possibly under artificially induced infiltration conditions as well as saline sea water intrusion in coastal aquifers of Karachi are of great significance from hydrological, environmental and public health view point. Conjunctive use of hydro-chemical, biological and nuclear techniques can provide reliable information on dynamics of groundwater flow, origin and mechanism of groundwater salinity. Nuclear techniques can be used as reliable supplementary tools to conventional non-nuclear techniques to address these issues. As a first step, it was considered necessary to initiate primary studies to:

- i) develop a general understanding about the isotopic, chemical and biological labeling of various recharge sources (rain, polluted streams/rivers, lakes, seawater) and the potable shallow and deep groundwater in coastal aquifer of Karachi;
- ii) determine surface water and potable groundwater pollution characteristics;
- iii) delineate spatial extent of saline groundwater and
- iv) evaluate the possible role of seawater intrusion in the coastal belt of Karachi.

This study focusses on the evaluation of stable isotope composition ($\delta^{18}\text{O}$ and δD) of water molecule, stable isotopes of carbon (^{13}C) in dissolved inorganic carbon and the physiochemical and chemical characteristics as well as coliform bacterial content of the water. The information will be quite helpful in better planning and assessment of:

- a) mechanisms of salinity build-up;
- b) deterioration of surface and groundwater quality, for a better understanding of the hydrological characteristics of the coastal aquifer in the coastal zone of Karachi.

5. Present investigations

5.1. Field sampling

Field sampling was performed in Karachi Metropolis from November 2001 to December 2003. Figure 2 shows the location of various sampling points. Surface water samples were collected from various locations along streams/rivers namely: Layari River and Malir River, Hub Dam, Hub River and local sea (shallow seawater off Karachi coast). Groundwater samples were collected from shallow (depths 8-30 meters), intermediate (up to 50 m) and deep (depths 70-100 meters) aquifers. All water samples were collected in leak-tight /lined cap plastic bottles or in glass bottles. Sterile bottles were used for collection of water for coliform bacterial analysis. Standard field sample preservation methods were used for subsequent chemical, biological and isotopic analysis in the laboratory [2]. In the field, all samples were stored under cool conditions ($<12^\circ\text{C}$). Table-1 shows the list of collected water samples.

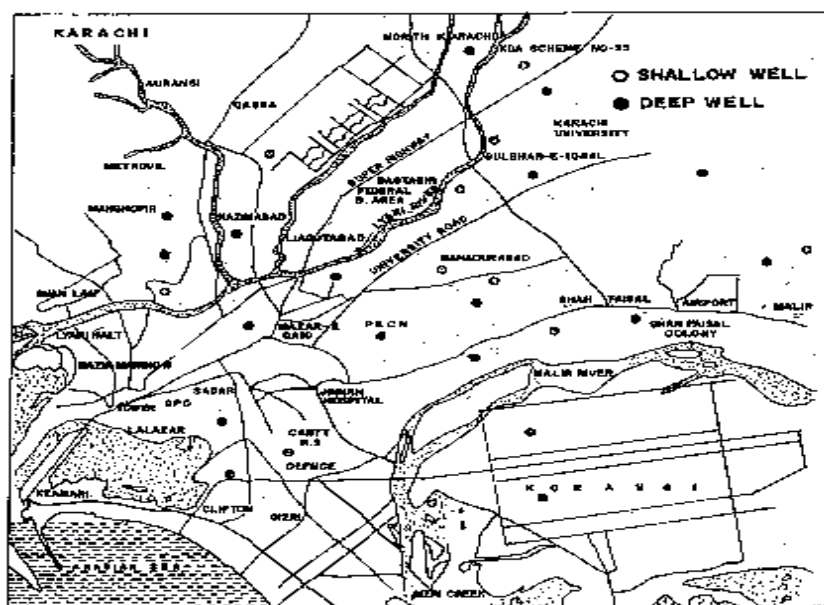


FIG. 2. Map of Karachi showing sampling location.

The rivers were accessible by road. In the down stream zone, the rivers were tapped during the low tide period and at a point much beyond the influence of high tide so as to collect representative municipal waste waters and industrial effluents from the rivers.

Table 1. Inventory of collected water samples.

Source of Water	Locations	1 st Sampling	2 nd Sampling	3 rd Sampling
Input Water Sources	Indus River (near Thatha)	2	1	
	Hub River	4	1	1
	Pollutant Rivers			
	❖ Layari River	5	5	5
	❖ Malir River	3	2	2
	Seawater (Karachi Coast:	6	6	6
	Precipitation (Rain)*	+		
Shallow Groundwater	Hand-pumps, Dug Wells. Shallow bore-holes/ pumping wells	8	28	12
Deep Groundwater	Pumping wells/ Tube-wells	10	25	16

* No rain during the sampling year

+ No determined/samples/samples no collected

5.2. Field in-situ analysis

Electrical conductivity, pH, turbidity and salinity were measured in-situ. Turbidity was measured with a portable turbidity meter (Model 6035, JENWAY). Electrical conductivity and temperature were measured with portable conductivity meter (Model HI 8633, M/S HANNA Instruments). Salinity was measured with a portable Salinometer (refractometer).

5.3. Laboratory analysis

5.3.1. Coliform bacterial analysis

For the measurement of Total Coliform Bacterial population and Faecal Coliform Bacterial population, accurately, 100 ml aliquots of a water sample were poured in two sterilized glass bottles. These were filtered separately to collect the Coliform bacteria onto 0.45 µm nitrocellulose membrane filter papers (Gelman Sciences, USA). Thereafter, the membrane filter papers were carefully put onto pads soaked in Membrane Lauryle Sulphate bacterial broth (ELE International Limited, U.K.) and placed in pre-labeled aluminum petri dishes. The dishes were placed in PaqualabTM incubator (Paqualab Standard System 50, ELE International Limited, U.K.) for 16- 24 hours. One set of dishes was incubated at 44 °C for determination of the Faecal Coliform bacterial population, while the other set of dishes of same sample was incubated at 37 °C for determination of the Total Coliform bacterial population. Afterwards, the dishes were removed and the membrane filters were studied with a magnifying glass for presence of yellow spot colonies that confirm presence of Coliform bacteria in water samples [3].

5.3.2. Chemical analysis of water samples

Major ion analysis of HCO_3^- , Cl^- and SO_4^{2-} on selective surface water and groundwater samples was carried out using UV-visible spectrometer for SO_4^{2-} , ion selective electrode for Cl^- and titration for HCO_3^- .

5.3.3. Stable isotope analysis

Oxygen and hydrogen isotope data are reported in the standard delta (δ) notation in parts per thousands (‰) to Vienna Standard Mean Ocean Water (VSMOW) [4]. The $\delta^{18}\text{O}$ values of the water samples were determined by the $\text{CO}_2\text{-H}_2\text{O}$ equilibrated method [5] and measured using GD-150 Gas

Source Ratio Mass Spectrometer. The δD values of water samples were obtained by reduction to hydrogen over hot metallic zinc [6] and measured using GD-150 Gas Source Ratio Mass Spectrometer. The reproducibility was better than ± 0.1 ‰ (oxygen) and ± 1 ‰ (hydrogen). Stable carbon isotope analysis of Total Dissolved Inorganic Carbon ($\delta^{13}C_{TDIC}$) in water samples was converted to CO_2 gas using routine sample preparation methods for mass spectrometric analysis by using 85% H_3PO_4 [7]. The measurement was made on modified GD-150 Mass Spectrometer (Varian MAT, Germany). The results are expressed as $\delta^{13}C$ values relative to the international carbonate standard namely: PDB (Pee Dee Belemnite). The reproducibility of $\delta^{13}C_{TDIC}$ measurements was better than 0.05 ‰. Barium chloride was used for the precipitation of Sulphate into $BaSO_4$. The conversion of $BaSO_4$ to SO_2 for the measurement of $\delta^{34}S$ was carried out using V_2O_5 as catalyst. The $\delta^{34}S$ are expressed CDT [8].

6. Results and discussion

Five possible water sources are contributing to the groundwater storage in Karachi. The first possible source is the rainfall. As the city of Karachi suffers from deficit of precipitation (only rainfall), the contribution to shallow groundwater storage from rain is very little. However, rainfall in the hinterlands and other areas surrounding Karachi may significantly contribute to the confined groundwater flow system. The two freshwater sources are the Hub Lake/Hub Dam and the Indus River. Water from Hub Dam and the Indus River is piped to various residential zones in Karachi for drinking water and irrigation purposes. The spring water discharges into Malir River and Layari River and the municipal/industrial waste effluents added to these rivers are also contributing to groundwater storage as a fourth recharge source. Seawater intrusion along Karachi coast is the fifth possible source. Keeping in view this recharge scenario of surface water sources, we submit the following results/discussions with respect to our field and laboratory physico-chemical (pH, electrical conductivity, salinity and concentrations of major ion viz. HCO_3^{-1} , Cl^- , SO_4^{-2}), biological (Total and Fecal Coliform counts/100 ml) and isotopic (δ^2H , $\delta^{18}O$, $\delta^{13}C$, and $\delta^{34}S$) investigations of surface water and groundwater in Coastal Karachi-Pakistan. Tables 2-4 through present ranges of analyzed parameter for three year sampling.

6.1. Surface water sources

6.1.1. Local precipitation (Rain)

During the sampling period, no rainfall events occurred in coastal Karachi. Therefore, it was not possible to collect and analyze local rain for chemical and isotopic information. However, stable isotope data on precipitation for the period from 1961 to 1975 is available from the IAEA Precipitation Network for the Karachi Station (IAEA Precipitation Network Code: 41780000, Lat. 24.90N Long. 67.13E, Alt. 23 meters above mean sea level) [9]. The following stable isotope indices of precipitation in Karachi were, therefore, used for interpretation purposes:

Long Term Weighted Means:

$$\begin{aligned}\delta^{18}O \text{ (water):} & \quad - 3.93 \pm 1.94 \text{ ‰ V-SMOW} \\ \delta^2H \text{ (water):} & \quad - 23.5 \pm 18.1 \text{ ‰ V-SMOW}\end{aligned}$$

Long Term Monthly Correlation between $\delta^{18}O$ and δ^2H (LSF):

$$\delta^2H = [7.56 \delta^{18}O \pm 0.34] + [3.41 \pm 1.50] \\ (r = 0.965)$$

6.1.2. Indus River

Physico-chemical, bacteriological and environmental stable isotope analysis was performed on water samples collected from the Indus River near Thatta city during three sampling periods (2001 to 2003).

A. Mashiattullah et al.

Table 2 to 4 present the physico-chemical, bacteriological and stable isotope analysis of Indus River water. The physico-chemical parameters indicate that there is no significant changes in these values during three years of sampling from 2001 to 2003. However, there are certain variations in the values of the stable isotopes of water. Slightly depleted values are observed during the sampling period in December 2003. This is probably due to the seasonal effect. Significant counts of total and fecal coliform bacteria are observed in 2001 and 2002 (Tables 2-3). This is because, the Indus River also taps sewage mixed water flow from three other major rivers (Ravi, Chenab and Jhelum) of Pakistan. The SO_4^{2-} concentrations in the river water are ranges from 13-86 ppm. There is no change in the concentration of chloride contents during the sampling periods. The stable isotope indices of total dissolved inorganic carbon (TDIC) in water, and of oxygen and hydrogen in water molecule, and stable sulfur isotope of sulfate are as following:

$\delta^{13}\text{C}$ (TDIC):	-1.66 to + 1.7 ‰ PDB	(n=3)
$\delta^{18}\text{O}$ (water):	-8.2 to - 5.9 ‰ V-SMOW	(n=3)
$\delta^2\text{H}$ (water):	- 62.8 to - 48.12 ‰ V-SMOW	(n=3)
$\delta^{34}\text{S}_{\text{SO}_4}$:	6.28 ‰ CDT	(n=1)

Table 2. Physico-chemical and isotopic analysis of Indus River, Hub Dam, Layari River, Malir River, Karachi Sea, Shallow ground-water and Deep Water Samples (2001).

Parameters (Units)	Indus River (n=1)	Hub River (n=4)	Layari River (n=5)	Malir River (n=3)	Karachi Sea (n=5)	Shallow Ground- water (n=8)	Deep Groundwater (n=10)
pH	7.6	8.3 – 8.8	7.2 - 8.4	6.9 - 7.9	7.7 - 8.5	6.3-7.9	6.5 - 8.6
E.C. (mS/cm)	0.48	1.42 – 1.50	1.3 - 9.0	1.6 - 3.4	49.3 - 53.7	1.1-1.9	1.9 - 19.1
Salinity (ppt)	<1	<1	<1 - 5.0	1 - 5	32 - 39	0.8-1	1.7 - 7.4
Turbidity (NTU)	36	27 – 79	54 - 89	75 - 98	52.6 -195.5	3.6-95	2.7 - 41
HCO ₃ ⁻¹ (ppm)	ND	98 to 128	364 - 660	201 - 971	145-196	356-514	144 - 886
Cl ⁻¹ (ppm)	ND	34 – 320	233 - 3296	201- 970	21578 - 25230	82-169	402 - 6034
SO ₄ ⁻² (ppm)	86	272 – 326	52 - 525	65 - 235	2076 - 2323	38-117	102 - 2221
Total Coliform (counts/100 ml)	150	240 – 600	560 – 1080	900 - 1116	350 - 650	0-492	0 -112
Fecal Coliform (counts/100 ml)	98	124-347	540 - 920	860 - 940	215 - 418	0-120	0 - 60
SO ₄ ⁻² /Cl ⁻¹	ND	0.65 –0.67	0.12 – 0.17	0.18 – 0.24	0.064 - 0.082	0.22 – 0.52	0.05 – 0.27
Cl ⁻¹ /HCO ₃ ⁻¹	ND	4.18 – 5.35	1.07 – 8.35	0.73 – 3.34	183.7 – 190.0	0.32 - 0.66	11.0 - 165
δ ¹⁸ O (‰ V-SMOW)	-8.2	+2.8 to +2.9	-5.4 to –2.7	-4.9 to +1.0	+0.27 to +1.1	-5.8 to –6.2	–6.2 to -4.2
δ ² H (‰ V-SMOW)	-62.8	+8.9 to +11.8	-45 to -31	-44.7 to –6.0	- 0.7 to +3.0	-54.0 to –29.0	–62.8 to -37.9
δ ³⁴ S _{SO4} (‰ CDT)	ND	ND	ND	ND	ND	ND	ND
δ ¹³ C (‰ PDB)	1.7	+1 to +6.3	-7.2 to –0.2	-8.7 to –1.4	-3.9 to +0.8	-6.6 to –16.5	-13.2 to -0.3

ND Not determined

Table 3. Physico-chemical and isotopic analysis of Indus River, Hub Dam, Layari River, Malir River, Karachi Sea, Shallow ground-water and Deep Water Samples (2002).

Parameters (Units)	Indus River (n=1)	Hub River (n=1)	Layari River (n=5)	Malir River (n=2)	Karachi Sea (n=5)	Shallow Ground-water (n=28)	Deep Groundwater (n=24)
pH	7.2	8.2	7.7 - 8.1	7.7 - 7.9	7.7 - 8.5	7.1 - 8.3	6.5-7.8
E.C. (mS/cm)	0.3	1.01	28.1 - 28.2	1.7 - 5.7	49.3 - 53.7	0.4 - 21.4	2.1- 32.5
Salinity (ppt)	<1	<1	1.92 - 2.7	1- 2.3	31 - 39	1 - 5.1	1 - 6.1
Turbidity (NTU)	135.1	2.9	81- 187	191 - 192	52.6 - 195.5	5.6 - 142	2.6 - 79
HCO ₃ ⁻¹ (ppm)	108	13	477 - 794	538 - 589	145 - 196	164 - 630	102 - 764
Cl ⁻¹ (ppm)	14	225	431 - 1304	288 - 2024	21578 - 25230	56 - 9031	170 - 12766
SO ₄ ⁻² (ppm)	13	108	31- 195	31 - 33	2076 - 2323	25 - 968	36 - 2413
SO ₄ ⁻² /Cl ⁻¹	0.69	0.36	1.48 - 2.82	0.92 - 5.9	0.06 4 - 0.068	0.08 - 0.81	0.05 - 11.3
Cl ⁻¹ /HCO ₃ ⁻¹	0.22	3.02	0.05 - 0.11	0.04 - 0.1	189.17 - 299.34	0.38 - 24.6	0.08 - 215.06
Total Coliform (counts/100 ml)	356	452	2.15 x 0 ⁴ to 2.65x10 ⁴	4.5 x 10 ³ to 5.9 x 10 ³	80 - 390	0 - 74	0 - 105
Fecal Coliform (counts/100 ml)	250	228	1.76x10 ⁴ to 4.79x10 ⁴	1.9 x 10 ³ to 2.1 x1 0 ³	30 - 226	0- 39	0 - 63
δ ¹⁸ O (‰ V-SMOW)	-8.2	+1.7	-4.6 to -1.6	-4.7 to -3.3	+0.27 to +1.1	-7.2 to -3.0	-7..2 to -3.6
δ ² H (‰ V-SMOW)	-57.4	+0.9	-35 to -19	-36.0 to -28.0	+3.0 to + 4.9	-53 to -27	-72 to -33
δ ³⁴ S _{SO4} (‰ CDT)	ND	ND	ND	ND	ND	ND	ND
δ ¹³ C (‰ PDB)	ND	ND	-9.6 to -6.7	-7.52 to -3.2	-3.9 to +0.8	-13.1 to -1.7	-11.4 to -1.2

ND Not determined

Table 4. Physico-chemical and isotopic analysis of Indus River, Layari River, Malir River, Karachi Sea, Shallow groundwater and Deep Water Samples (2003).

Parameter (Units)	Indus River (n=1)	Layari River (n=3)	Malir River (n=2)	Arabian Sea / Karachi Sea (n=5)	Shallow Groundwater (n=12)	Deep Groundwater (n=16)
pH	7.56	7.46 – 8.40	7.7 – 7.9	7.7 – 8.5	6.75 – 8.3	6.94 – 7.94
E.C (mS/cm)	0.483	1.5 – 9.02	3.2 – 3.4	49.3 – 53.7	0.9 - 12.5	1.9 – 32.5
Salinity (ppt)	< 1	>1 – 5.0	1 - 5	31 – 39	<1 – 5.1	1.3 – 7.4
Turbidity (NTU)	36	54 - 76	97- 98	52.6 – 195.5	13.9 - 95	2.7 – 59.6
HCO ₃ ⁻¹ (ppm)	108	502 - 660	486	145 - 196	246 – 520	102 – 764
Cl ⁻¹ (ppm)	14	431 - 1304	2024	21578 - 25230	58 - 1419	501 - 12766
SO ₄ ⁻² (ppm)	13	33-195	271	2076 - 2323	26 - 220	61 - 2221
SO ₄ ⁻² /Cl ⁻¹	0.69	0.06 - 0.11	0.10	0.064 - 0.06	0.10 - 0.79	0.04 - 0.87
Cl ⁻¹ / HCO ₃ ⁻¹	0.22	1.48 - 3.39	6.52	189.7 - 299.3	0.33 - 6.35	1.8 - 215
δ ¹⁸ O(‰ V-SMOW)	- 5.9	-5.4 to - 2.7	-0.95 to - 0.66	+ 0.27 to + 1.1	-6.74 to -4.41	-6.07 to -3.56
δ ² H(‰ V-SMOW)	-48.12	-44.4 to -31	-27.5 to -35.91	+ 4.9 to + 8.6	-53.89 to - 33.06	-72.59 to - 26.7
δ ³⁴ S _{SO4} (‰ CDT)	6.28	7.2 – 8.9	11.6 to 14.2	17.6 to +19.5	2.69 to 8.7	-12.04 to -2.47
δ ¹³ C _{TDIC} (‰ PDB)	-1.66	- 7.2 to -0.2	- 4.5 to - 2.4	- 3.9 to 0.8	-11.23 to -1.72	1.5 to 17.9

6.1.3. Hub river

The water storage in the Hub Lake was very little because the Hub River was dry due to drought conditions in and around the study area over the past several years. Thus, most of the Hub Lake had patches of stagnant water. Hub Dam water was collected during sampling periods of 2001 and 2002. Results of physico-chemical, bacteriological and stable isotopic analyses on Hub Dam water are presented in Tables 2 and 3. Except in Coliform bacterial population, different sectors the ratio in the water show similar values of pH (~8.2-8.8) E.C (~1.1 to 1.5 mS/cm). The electrical conductivity values were three times higher than the Indus river water supply. Significant population of Total Coliform bacteria and fecal Coliform populations are observed during first and second sampling periods. This indicates that sewage/domestic waste is being continuously added into the dam waters. This is well indicated by the following enriched values of ¹⁸O and ²H contents of the lake water:

δ ¹⁸ O (Hub Lake water):	+ 1.7 to + 2.9 ‰ V-SMOW	(n=5)
δ ² H (Hub Lake water):	+ 0.9 to + 11.8 ‰ V-SMOW	(n=5)
δ ¹³ C (Hub Lake water):	+ 1.0 to + 6.3 ‰ PDB	(n=5)

The stable carbon isotope index (δ¹³C_{TDIC}) of total dissolved inorganic carbon in lake water varies in the range of +1‰ PDB to + 6.3 ‰ PDB in different sectors of stagnant lake water. This is indicative

of different sources of dissolved inorganic carbon in the lake (TDIC) into other carbon containing compounds over the drought regime.

6.1.4. Polluted rivers

Table 4 summarizes the ranges of physico-chemical, bacteriological and stable isotope analysis of oxygen and hydrogen in water collected from polluted Layari and Malir Rivers. Results are discussed in the following section.

6.1.4.1. Layari river

The Layari River was monitored at locations along its flow from North Karachi (upstream region) to Sher-Shah Bridge (downstream region) near Keamari/Sea. The range of variation in the stable isotope content of total dissolved inorganic carbon (TDIC) and of oxygen and hydrogen in Layari River water are the following:

$\delta^{18}\text{O}$ (Layari River Water):	-5.4 to -1.6 ‰ V-SMOW	(n=15)
$\delta^2\text{H}$ (Layari River Water):	-45.0 to -19.0 ‰ V-SMOW	(n=15)
$\delta^{13}\text{C}$ (TDIC-Layari River Water):	- 9.6 to -0.2 ‰ PDB	(n=15)
$\delta^{34}\text{S}_{\text{SO}_4}$:	7.2 to 8.9 ‰ CDT	(n=5)

There is a good covariation between electrical conductivity and salinity along the flow in the river. Generally, the E.C. and salinity values tend to decrease downstream. Maximum values of EC (28.2 mS/cm) and Salinity (5 ppt) were observed at the origin of the Layari stream near Yousuf Goth (shown in the map) area. In this zone, the Layari stream receives minor spring water, domestic wastewater from small isolated dwellings and wastewater from industries (flour mills, electronic industry etc.) which host deep tube-wells with quite high salinity values. Downstream, the Layari River receives highly reducing municipal sewage of the Karachi city that comprises of relatively low electrical conductivity water that is a mixture of the Indus River water and the local shallow groundwater supplied to the city for domestic use. Turbidity levels in the river water also fluctuate depending upon the concentration of inputs from industrial and domestic sector. Total Coliform and Fecal Coliform bacterial population in the Layari River water increased along the flow. The Total Coliform population ranges between 560 to 2.65×10^4 per 100 ml water whereas, the Fecal Coliform population ranges between 540- 4.79×10^4 per 100 ml water. Fecal Coliform population is quite dominant and of immense concern for health. High concentrations of Cl^- (233-3,296 ppm) and SO_4^{2-} (33-525 ppm) coupled with mildly alkaline pH values are found in the upstream regions of the river. However, these values decrease significantly along the flow downstream whereby, the pH values remain slightly above neutral values. This indicates that the source of water in the upstream regions of Layari River is quite different than the downstream regions. Significantly, high values of Cl^- and SO_4^{2-} in the upstream region indicate that the source of water in the river is the saline water discharged from deep tube-wells installed in the nearby industrial complexes. The $\delta^{13}\text{C}_{\text{TDIC}}$ and $\delta^{18}\text{O}$ (water) values are also quite enriched at the starting Point of Layari River as compared to local shallow groundwater and are in fact, relatively closer to the sea values. Downstream, as the Layari River receives sewage water of the city, which is a mixture of the Indus River water, and the local shallow groundwater supplied to the city for domestic use, the values of $\delta^{18}\text{O}$ are consistently around -5‰ V-SMOW. It is thus, speculated that the water in the extreme up-stream region of Layari River is a mixture of deep groundwater which is partly trapped seawater (or geothermal water as there are geothermal springs nearby) and the local shallow groundwater.

6.1.4.2. Malir river

The Malir River was monitored three locations along its flow from Karachi East to the Sea before Ghizri Creek during three sampling phase. The range of variation in stable isotope content of total dissolved inorganic carbon (TDIC) in water and of oxygen and hydrogen in Malir River water are the following:

A. Mashiattullah et al.

$\delta^{18}\text{O}$ (Malir River Water):	-4.9 to +1.0 ‰ V-SMOW	(n=8)
$\delta^2\text{H}$ (Malir River Water):	-44.7 to -6.0 ‰ V-SMOW	(n=8)
$\delta^{13}\text{C}$ (TDIC - Malir River Water):	-8.7 to -1.4 ‰ PDB	(n=2)
$\delta^{34}\text{S}_{\text{SO}_4}$	11.6 to 14.2 ‰ CDT	(n=2)

Like Layari River, there is good covariation between electrical conductivity and salinity along the flow in Malir River. However, in contrast to Layari River, the concentrations of these parameters increase downstream. Lowest values of EC and Salinity were observed at the source of the River behind Shah (shown on the map) Faisal Colony. In this zone, the River receives minor spring water, minor domestic wastewater from small isolated dwellings and seepage from agricultural fields/vegetable farms that use the low E.C Indus River water supply for irrigation. Turbidity of the river increases along flow as it receives more and more water of industrial origin (mainly tannery wastes). Total Coliform and Fecal Coliform bacterial population in the river water increased along the flow. The Total Coliform population ranges between 4.5×10^3 to 5.9×10^3 per 100 ml water whereas, the Fecal Coliform population ranges between 1.9×10^3 to 2.1×10^3 per 100 ml water. This shows that the Fecal Coliform population which are indicators of sewage inputs, is quite dominant and of immense concern from health view point. The pH of the river water increases by one unit as it receives domestic and industrial alkaline effluents. High concentrations of Cl^- (2024 ppm) and SO_4^{2-} (271 ppm) are found in the downstream region of the river. This is perhaps due to the effect of sea tides in the Qayyum Abad area near Ghizri Creek.

6.1.5. Karachi Sea

Table 2-3 presents the summary of physiochemical, bacteriological and stable isotope analysis of shallow seawater collected at six representative locations along Karachi coast. The pH values of ~8.5 for open seawater off Karachi Coast generally conform to those for normal ocean waters. However, pH values decrease to levels of ~7.7 near the Ghizri Creek and the Korangi Creek which receive significant quantities of industrial acidic wastewaters. Similarly, the pH values of seawater increase to ~8.5 in the backwaters of Manora Channel near Village Shamas-pir. This increase is perhaps due to input of alkaline waters from local industry, such as the tanning industry. Electrical Conductivity values for Karachi seawater range between 49.3 mS/cm to 53.7 mS/cm while the salinity values are ~39 ppt. The electrical conductivity values higher than 53 mS/cm correspond to relatively non-polluted open seawaters on northwest and southeast sides of Karachi coast. The E.C values of open seawater drop due to input of wastewaters from Malir River via Ghizri Creek and polluted drains about Korangi Creek. The lowest E.C. values of 49.3 mS/cm and salinity value of 32 ppt correspond to mixing of mainly domestic and partly industrial wastewater from Layari River in Manora Channel backwaters near village Shamas-pir. The measured temperature of seawater off Karachi coast is fairly constant about 25.5 °C. Slightly higher temperature is observed near Ghizri Coast, which is attributed to input of relatively warmer wastewaters of industrial and domestic origin. Like Hub Lake waters, the seawaters are also quite oxidizing. Turbidity values of open seawater are quite higher than the on-shore surface water sources (polluted Layari and Malir Rivers, Indus River and the Hub Lake). This is attributed to much higher contents of particulate matter in seawater as compared to on-shore surface water sources. The lowest values of turbidity are observed along Clifton coast, as this coast is relatively free of pollution along southeast side of Karachi coast. Coliform bacterial population is lower along non-polluted Clifton coast and the northwest coast. However, significantly higher Coliform counts are observed along polluted coastal spots along Karachi coast. Highest Coliform counts are observed along Ibrahim Haideri Fish Harbour zone along southeast coast of Karachi and the Manora Channel backwaters. Cl^- contents of seawater off Karachi coast are in the range of 21,578 to 25,230 ppm while the SO_4^{2-} concentrations are in the range of 2076 to 2323 ppm. The stable carbon isotope contents ($\delta^{13}\text{C}_{\text{TDIC}}$) of total dissolved inorganic carbon (TDIC) vary in the range of -3.9 ‰ PDB to + 0.8 ‰ PDB in different zones off Karachi coast. This is indicative of different levels and sources of dissolved inorganic carbon in seawater due to input of domestic and industrial wastewater into the sea from key industrial trading estates (LITE, KITE, SITE etc.) via polluted drains. The highest $\delta^{13}\text{C}_{\text{TDIC}}$ value of + 0.8 ‰ PDB corresponds to relatively non-polluted seawater along northwest coast of Karachi. The lowest $\delta^{13}\text{C}_{\text{TDIC}}$ value of -3.9 ‰ PDB corresponds to highly polluted

seawater in Korangi Creek which receives industrial and domestic waste drains from Korangi Industrial Trading Estate (KITE). The high tide (HT) stable isotope content of oxygen and hydrogen in relatively non-polluted seawater along Karachi coast falls in the following range:

$\delta^{18}\text{O}$ (seawater) _{HT} :	+ 0.27 to + 1.1	‰ V-SMOW	(n=15)
$\delta^2\text{H}$ (seawater) _{HT} :	- 0.7 to + 8.6	‰ V-SMOW	(n=15)
$\delta^{13}\text{C}$ (TDIC - seawater):	- 3.9 to +0.8	‰ PDB	(n=15)

The low tide (LT) stable isotope content of oxygen in relatively polluted seawater along Karachi coast falls in the following range:

$\delta^{18}\text{O}$ (seawater) _{LT} :	- 1.3 to + 0.1	‰ V-SMOW	(n =15)
--------------------------------------------------	----------------	----------	---------

6.2. Potable Groundwater in the Coastal Aquifer

Shallow groundwater samples were obtained from hand pumps (n=1), dug wells (n=1) and shallow bores with centrifugal pumps (n=8) installed at depths less than 50 meters (mainly between 8-50 meters); and (b) relatively deep groundwater obtained from pumping wells (cased wells/Tube-wells) installed at depths greater than 50 meters in the coastal aquifer of Karachi. These cased wells also tap various proportions of shallow groundwater in addition to deep groundwater. Tables 2-4 present the ranges of physico-chemical, bacteriological and stable isotope data of shallow and deep groundwater of three sampling (2001-2003). The following section presents discussion on these data elements.

6.2.1. Shallow groundwater

Physico-chemical data of shallow groundwater (depth less than 50 meters) shows that the shallow wells located in the vicinity of coast and in the proximity of polluted rivers have relatively higher values of electrical conductivity, salinity and population of Coliform bacteria. Selective borehole/well samples in the vicinity of Layari River and Malir River have extremely high values of total coliform and fecal coliform bacteria. In general, the bacteriological quality of shallow groundwater is quite poor and renders the water unfit for drinking purposes without prior treatment. The shallow groundwater is moderately saline representing electrical conductivity values. However, some located near coastal belt have very high electrical conductivity values (0.4 to 21.4 mS/cm). The pH of shallow groundwater varies from mildly acidic (~6.3) to mildly alkaline values (~8.3). Turbidity of shallow groundwater varies between 3.6 NTU to 142 NTU. The concentration of HCO_3^- (164 - 630 ppm, n=48), Cl^- (56-9031 ppm, n=48) and SO_4^{2-} (25-968 ppm, n=48) in general except for few samples is very reasonable.

The range of variation in stable isotope content of total dissolved inorganic carbon (TDIC) and oxygen and hydrogen in Layari River water is as following:

$\delta^{18}\text{O}$ (shallow groundwater):	- 7.2 to -3.0	‰ V-SMOW	(n=48)
$\delta^2\text{H}$ (shallow groundwater):	- 54.0 to -27.0	‰ V-SMOW	(n=48)
$\delta^{13}\text{C}$ (TDIC - shallow groundwater):	-16.1 to -1.7	‰ PDB	(n=48)
$\delta^{34}\text{S}_{\text{SO}_4}$ of water:	2.7 to 8.7	‰ CDT	(n=48)

The mean stable isotope content of $\delta^{18}\text{O}$ and $\delta^2\text{H}$ in shallow groundwater is as following:

Mean $\delta^{18}\text{O}$ (shallow groundwater):	-5.68 ± 1.84	‰ V-SMOW	(n=48)
Mean $\delta^2\text{H}$ (shallow groundwater):	-46.5 ± 6.2	‰ V-SMOW	(n=48)
Mean $\delta^{13}\text{C}$ (TDIC-shallow groundwater):	-8.13 ± 3.1	‰ PDB	(n=48)

The correlation between $\delta^{18}\text{O}$ and $\delta^2\text{H}$ (LSF) for shallow groundwater is as following:

$$\delta^2\text{H} = 6.4 \delta^{18}\text{O} - 10.2 \quad (r = 0.61, n=48)$$

The stable isotope results indicate that the shallow /phreatic aquifers are recharged by a mixture of fresh waters of Indus River and Hub River (draining spring water and flooded rainwater) as well as polluted Layari and Malir rivers and their feeding drains (both under natural infiltration conditions and artificially induced infiltration conditions) and to a much smaller extent from direct recharge of local precipitation.

6.2.2. Deep Groundwater

In general, deep groundwater is mostly saline and has high electrical conductivity and salinity as compared to shallow groundwater. The sampled deep groundwater from pumping wells is in fact a mixture of various proportions of shallow groundwater from freshwater phreatic/unconfined aquifer and actual deep groundwater from the confined aquifer. In the absence of well logs of sampled tube-wells/pumping wells, it is not possible to estimate the proportions of inputs of shallow groundwater in the discharge of these wells. Based on hydro-chemical data, it is assumed that the shallow mixed deep groundwater discharged by large scale pumping wells mainly represents the deep groundwater from confined aquifer. The more representative deep groundwater wells are those that have relatively higher values of electrical conductivity (range: 1.9-32.5 mS/cm), salinity (range: 1.0-7.4 ppt) as well as concentrations of Cl^- (range: 170-12,766 ppm) and SO_4^{2-} (range: 36-2,413 ppm). The deep wells located close to the coast/shoreline also have relatively higher values of electrical conductivity, salinity, Cl^- and SO_4^{2-} . High counts of Total Coliform and Fecal Coliform bacteria was found in relatively less deep shallow wells installed in the Layari River belt. High counts of Total Coliform and Fecal Coliform bacteria was also found in relatively less deep shallow wells installed in poorly drained and poorly managed sanitary conditions.

The range of variation in stable isotope content of total dissolved inorganic carbon (TDIC) and oxygen and hydrogen in shallow mixed deep groundwater is as following:

$\delta^{18}\text{O}$ (deep groundwater):	-7.22 to -3.56 ‰ V-SMOW	(n=51)
$\delta^2\text{H}$ (deep groundwater):	-72.59 to -26.7 ‰ V-SMOW	(n=51)
$\delta^{13}\text{C}$ (TDIC - deep groundwater):	-13.2 to -0.3 ‰ PDB	(n=51)
$\delta^{34}\text{S}_{\text{SO}_4}$ (deep groundwater):	-12.04 to +17.9 ‰ CDT	(n=51)

The mean stable isotope content of ^{18}O and ^2H in shallow mixed deep groundwater is as following:

Mean $\delta^{18}\text{O}$ (deep groundwater):	-5.6 ± 1.3 ‰ V-SMOW	(n=51)
Mean $\delta^2\text{H}$ (deep groundwater):	-43.9 ± 2.4 ‰ V-SMOW	(n=51)
Mean $\delta^{13}\text{C}$ (TDIC- deep groundwater):	-7.9 ± 3.4 ‰ PDB	(n=51)

The correlation between $\delta^{18}\text{O}$ and $\delta^2\text{H}$ (LSF) for shallow mixed deep groundwater is as following:

$$\delta^2\text{H} = 9.32 \delta^{18}\text{O} + 7.0 \quad (r = 0.95, n=51)$$

The hydro-chemical and stable isotope results indicates that the confined aquifer hosts a mixture of rainwater from hinterlands and surrounding regions around coastal Karachi as well as sea trapped water/seawater through intrusion under natural infiltration conditions or under induced recharge conditions.

6.3. Groundwater Recharge Characteristics/ Sea water Intrusion

Presently, coastal Karachi is known to have five sources of recharge to its groundwater reserves. These are:

- i) rainfall,
- ii) Indus River water supply,
- iii) Hub-River and Hub Lake water supply;

- iv) polluted Layari and Malir rivers/contributory channels draining mixtures of domestic, industrial and agricultural wastewater composed of pre-said three sources; and
- v) seawater.

The possibilities of major contribution to groundwater recharge of shallow/phreatic aquifer directly by local rainfall seems very small due to very poor frequency of rainfall events and rainfall intensities in the Karachi and high evaporation rates. The long term (15 years annual record) mean monthly average precipitation for Karachi is between 0-15 mm during the months of January to June, 23 - 91 mm during the months of July to September and 0-7 mm during the months of October to December [3]. The remaining four sources can play a significant role in recharge of the shallow aquifer system and deep groundwater system (confined aquifer) in coastal Karachi.

In order to postulate the origin of shallow and deep groundwater and related salinity in the shallow aquifer system and the confined deep aquifer system, the stable isotope composition of oxygen and hydrogen and hydro-chemical data of groundwater samples collected in present investigation is statistically evaluated.

Figure 3 shows the $\delta^{18}\text{O}$ versus $\delta^2\text{H}$ plot of groundwater in coastal Karachi vis-à-vis isotopic indices of local rainwater, Indus River water and local seawater. The large term mean stable isotope composition of ^{18}O and ^2H in precipitation falls on the Local Meteoric Water Line (LMWL), while the surface water samples (Hub Lake water and the river water, local seawater) and the groundwater samples fall below the local meteoric water line. Further, the large shift in $\delta^{18}\text{O}$ values of shallow and less deep groundwater towards right of Local Meteoric Water Line (LMWL) must be result of various possible process such as recharge of local precipitation, Indus River water and Hub River water used for domestic and agricultural irrigation purposes, followed by evaporation prior to recharge and recharge of mixed waters from polluted rivers.

The representative deep groundwater samples fall relatively closer to the LMWL in the vicinity of long term mean of precipitation in Karachi. There is a distinctly large spread of data for shallow groundwater samples and representative deep groundwater samples, thereby indicating distinct sources of recharge to the shallow aquifer system and the deep confined aquifer system. The shallow groundwater samples cluster around a mean $\delta^{18}\text{O}$ values of $-5.6 \pm 1.8\text{‰}$ V-SMOW and clearly indicate strong effect of mixing of local precipitation recharge ($\delta^{18}\text{O} = -3.9 \pm 1.94\text{‰}$ V-SMOW) with water from the Indus River ($\delta^{18}\text{O} = -8.2\text{‰}$ V-SMOW).

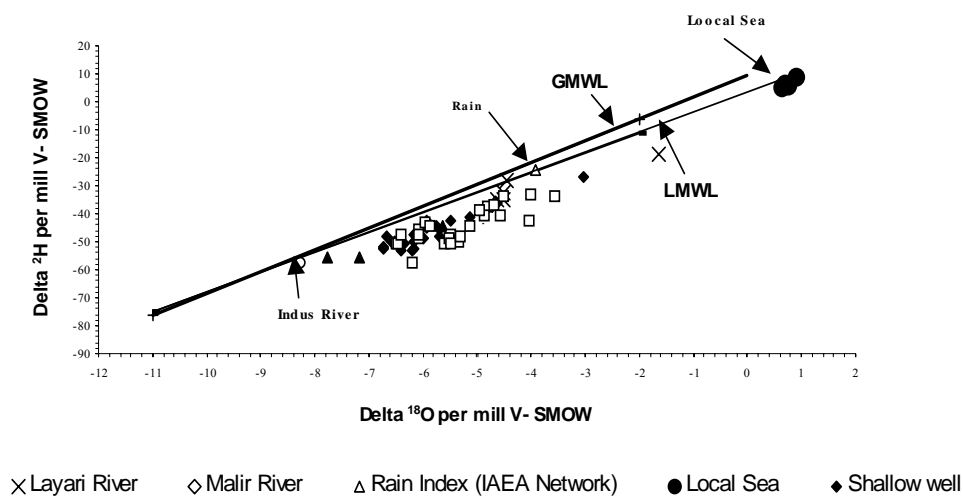


FIG. 3. $\delta^{18}\text{O}$ versus $\delta^2\text{H}$ plot for groundwater, Coastal Karachi, Pakistan

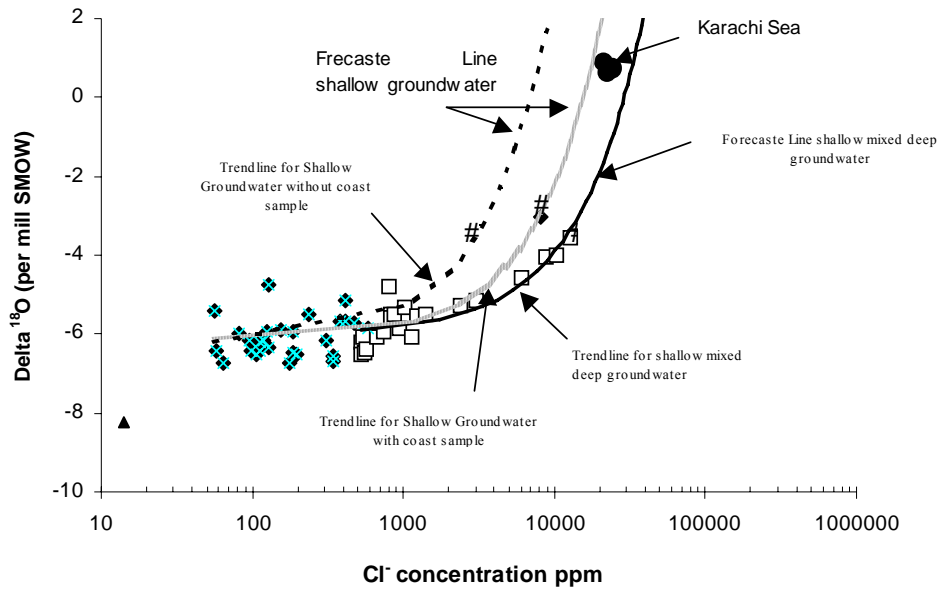


FIG. 4. Trend lines of Cl^- versus $\delta^{18}\text{O}$ for shallow groundwater and shallow mixed deep groundwater in coastal Karachi, Pakistan.

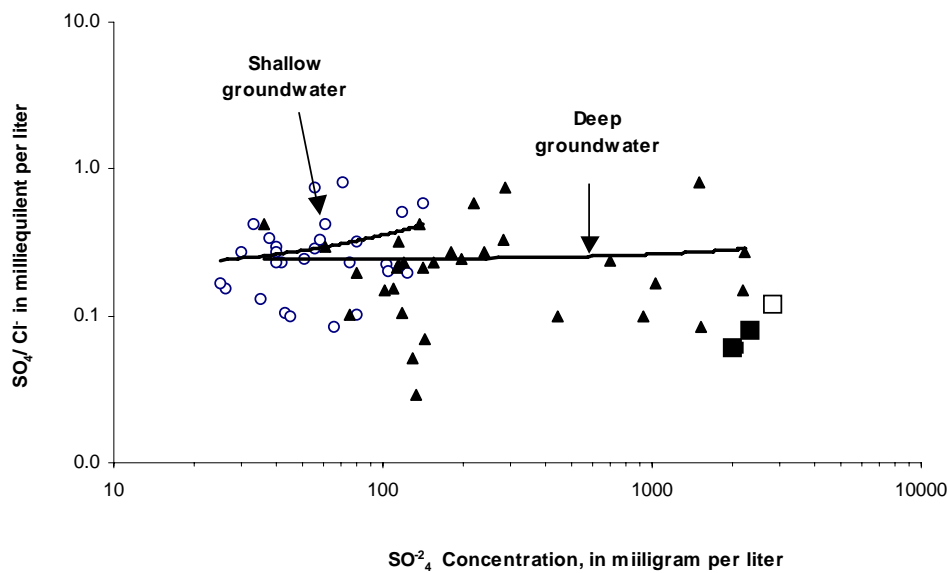


FIG. 5. Graph of $\text{SO}_4^{2-}/\text{Cl}^-$ ratio and SO_4^{2-} concentration in shallow and deep groundwater, coastal Karachi (Pakistan)

Keeping in view the mean stable isotope indices of oxygen in local rainwater ($\delta^{18}\text{O} = -3.93 \pm 1.94$ ‰ V-SMOW) and local seawater ($\delta^{18}\text{O}$: +0.1 to +1.1 ‰ V-SMOW) as a major recharge source the shallow and deep groundwaters, it may be realized that a strong impact of seawater intrusion in coastal aquifer system will shift the ^{18}O isotopic composition the groundwater and towards the seawater $\delta^{18}\text{O}$ index. Nevertheless, $\delta^{18}\text{O}$ versus $\delta^2\text{H}$ plot of groundwater in coastal Karachi shows that the shallow groundwater trends in the direction of stable isotope index of ^{18}O and ^2H of the Indus River water. It is therefore, believed that under the present water supply practices and drought conditions, the stable isotope index of ^{18}O and ^2H in shallow and intermedia depth groundwater will ultimately shift from local precipitation index to the direction of isotopic composition of the Indus River.

Unpolluted seawater off Karachi coast is characterized by a $\delta^{18}\text{O}$ value of $\sim +1$ ‰ V-SMOW and a chloride content of $\sim 23,000$ ppm. Both the Layari River and Malir River waters as well as the Indus River water and the Hub Lake water have extremely very low contents of chloride and sulfate ions as compared to seawater. The average mean value of $\delta^{18}\text{O}$ in polluted river waters is ~ 5 ‰ V-SMOW and in shallow groundwater is -5.9 ‰ V-SMOW. Therefore, those pumping wells that are located near the coastline/shore line (where seawater intrusion could be expected) and have high chloride and sulfate values should represent seawater intrusion and relatively enriched ^{18}O values. However, for pumping wells located comparatively far away from the coast and representing high salinity (chloride and sulfate concentrations), the contribution of saline water may be derived from upward diffusion from the freshwater- seawater interface possibly as a result of local fluctuation of water table due to pumping. In present investigations, the wells tapping the intermediate aquifer along the coast have significantly high values of chloride and sulfate but have $\delta^{18}\text{O}$ values closer to polluted river water and shallow groundwater. This suggests that this coastal pumping wells are withdrawing significant quantities of water from shallow aquifer that also hosts recharge of seawater pushed into the coastal zone during summer monsoon period. However, possibilities of direct seawater intrusion in these wells under prolonged pumping conditions is yet to be verified. Noteworthy are the pumping wells with significantly high chloride content and relatively lower sulfate content. It is speculated that the lower sulfate contents are due to biological reduction of sulfate. Sulfur isotopic analysis ($\delta^{34}\text{S}$) of aqueous sulfate indicates that the well situated close to the coast host the recharge of seawater. These wells have values of $\delta^{34}\text{S}$ close to sea water.

The relatively deeper groundwaters representing confined aquifer have enriched $\delta^{18}\text{O}$ and excessively high values of aqueous chloride and sulfate. Some deep groundwater samples have $\delta^{13}\text{C}$ (TDIC) value very close to the $\delta^{13}\text{C}$ (TDIC) value for seawater. Some deep wells have depleted $\delta^{13}\text{C}$ (TDIC) values up to -13.2 ‰ PDB. Similar depleted $\delta^{13}\text{C}$ values have been reported for deep saline groundwater tapped from confined aquifer in the coastal zone of Orissa- India [10]. It is believed that the groundwater tapped by these wells mainly represents a mixture of recharge from rainfall in the hinterlands, floodwater and spring water drained by the Malir River Basin and the Hub River Basin around coastal Karachi as well as seawater. For some wells located in Clifton areas, we speculate direct seawater intrusion by excessive pumping. However, incase of pumping wells with excessively high values of chloride and sulfate in deep groundwater away from the coast suggest possibilities of trapped seawater. To verify possibilities of seawater intrusion in shallow groundwater and mixed deep groundwater and/or existence of trapped seawater in deep groundwater, the concentrations of SO_4^{2-} (in milligrams per liter, log scale) are plotted against $\text{SO}_4^{2-}/\text{Cl}^-$ ratios (in milliequivalents per liter, log scale) for all analyzed water samples (Figure 4). It is obvious that shallow groundwater and deep groundwater plot along two distinct lines. This is further justified by demonstrating the trend of Cl^- concentrations versus $\delta^{18}\text{O}$ values (in ‰ V-SMOW, linear scale) in shallow and deep groundwater and the local seawater as well as seawater from Doha-Qatar in Gulph Area [11]. It may be realized from Figure 5 that the extrapolated or forecast trend for shallow groundwater samples (with low SO_4^{2-} content) do not fall on the data points for local seawater (or other tropical seawater from Doha/Qatar). However, the extrapolated or forecast trend for deep groundwater samples (with high SO_4^{2-} and Cl^- contents and enriched $\delta^{18}\text{O}$ values) falls in the vicinity of the data points for local seawater (or other tropical seawater from Doha/Qatar). This observation strengthens the possibilities of seawater intrusion in the coastal zone and existence of trapped seawater salinity/build-up of salt-water up-coning in the deep confined aquifer in coastal Karachi.

7. Conclusion

The study carried out during three years of the project on conjunctive use of stable isotope techniques and conventional non-nuclear techniques have successfully facilitated a general view on the stable isotope composition of oxygen, hydrogen and inorganic carbon in water and its dissolved inorganic carbon as well as hydrochemistry /salinity and biological pollution of potable groundwater system in coastal Karachi. The conclusions on possibilities of seawater and/or existence of trapped seawater salinity/build-up of salt-water up-coning in the deep confined aquifer in coastal Karachi require detail sampling.

ACKNOWLEDGEMENTS

REFERENCES

- [1] KLEIN, K., RATZLAFF, K.W., Changes in saltwater intrusion in the Biscayne aquifer, Hialeah-Miami Springs area, Dade County, Florida: U.S. Geological Survey Water-Resources Investigations Report No. 87 (1989) 4249
- [2] CLARK, I.D., FRITZ, P., Environmental Isotopes in Hydrology, Capter-1 and Chapter-10, Lewis Publishers, New York, (1997) 328.
- [3] QURESHI, R.M., MASHIATULLAH, A., JAVED, T., SHAH, Z., SAJJAD, M.I., Pollution aspect of drinking water sources in Rawalpindi City (A preliminary Investigation), J. Anal., & Envl. Chem. Vol. 4, No. 2, (1999) 7-17.
- [4] COPLEN, T.B., Reporting of stable hydrogen carbon and oxygen isotope abundance (Technical report). Pure Appl chem. 66, (1994) 273-276.
- [5] EPSTEIN, S., MAYEDA, T., Variation in $^{18}\text{O}/^{16}\text{O}$ ratio in natural waters. Geochim. Cosmochim. Acta 4, (1953) 213-224.
- [6] COLEMAN, M.I., SHEPHERD, T.J., DURHAM, J.J., ROUSE, J.E., MOORE, G.R., Reduction of water with Zinc for Hydrogen Isotope Analysis. Anal. Chem. 54, (1982) 993-995.
- [7] SAJJAD, M.I., AHMED, M., TASNEEM, M.A., KHAN, I.H. LATIF, Z., Report No PINSTECH/RIAD-118, Pakistan Institute of Nuclear Science and Technology, P.O. Nilore, Islamabad, Pakistan (1989).
- [8] SAJJAD, M.I., LATIF, Z., ALI, M. et at., Fabrication of SO_2 preparation system and Calibration of PINSTECH Sulphur Standard for $^{34}\text{S}/^{32}\text{S}$ Mass Spectrometer Analysis. PINSTECH-137 (1994).
- [9] IAEA: Statistical Treatment of Data on Environmental Isotopes in Precipitation. IAEA Technical Reports Series No. 331. STI/DOC/10/331, ISBN 92-0-100892-9, International Atomic Energy Agency, Vienna, Austria (1992), 781.
- [10] KULKARNI, K.M.; NAVADA, S.V., NAIR, A.R., RAO, S.M., SHIVANA, K., SINHA, U.K., SHARMA, S., Drinking Water Salinity Problem in Coastal Orissa-India- Identification of Past Transgression of Sea by Isotope Investigation. IAEA-SM-349/18, In: Proceedings of the International Symposium on Isotope Techniques in the Study of Past and Current Environmental Changes in the Hydrosphere and Atmosphere, Vienna, Austria, 14-18 April (1997).
- [11] YURTSEVER, Y., PAYNE, B.R., Application of Environmental Isotopes to Groundwater Investigations in Qatar. IAEA-SM-228/24, In: Proceedings of the International Symposium on Isotope Hydrology, Neuherberg, F.R. Germany, 19-23 June (1978).

LIST OF PARTICIPANTS

- AL-TARAWNEH, Z.
Ministry of Water and Irrigation
Water Authority of Jordan (WAJ)
P.O. Box 2412
Amman 11183, Jordan
Tel.: 00962 6 5864361/2
Fax: 00962 6 58
E-mail: isolab@go.com.jo
- LEANNEY, F.
CSIRO Land and Water
PMB 2
Glen Osmond, South Australia - 5064
Tel.: 61 – 883038728
Fax: 61 - 883038750
E-mail: fred.leaney@csiro.au
- QURESHI, R.
Pakistan Institute of Nuclear Science & Technology (PINSTECH)
P.O. Nilore
Islamabad, Pakistan
Tel.: 92 512207228
91 51 9290231 - Ext.: 3433
Fax: 92 51 9290275
E-mail: riffat@pinstech.org.pk
- QIN, D.
Institute of Geology and Geophysics
Chinese Academy of Sciences
P.O. Box 9825 - Qijiahuozi
Beijing 100029, China
Tel.: 86-10-62008062
Fax: 86-10-62010846
E-mail: qindj@mail.igcas.ac.cn
- QURTOBIB, M.
Centre National de l'Energie des Sciences et des techniques Nucléaires
65, Rue Tansift, Agdal Rabat, Maroc
Tel.: 0021237712023
Fax: 0021237711940
E-mail: qurtobi@cnesten.org.ma
- SONG, S.-J.
Applied Radioisotope Research Institute
Cheju National University
Ara-dong Cheju-shi
Cheju-do 690-756, Korea
Tel.: 82-64-754-2313
Fax: 82-64-755-6186
E-mail: songjs@cheju.cheju.ac.kr